Aus dem Veterinärwissenschaftlichen Department
der Tierärztlichen Fakultät der Ludwig-Maximilians-Universität
München

Arbeit angefertigt unter der Leitung von
Univ.-Prof. Dr. med. vet. Eckhard Wolf

Angefertigt an der Fakultät für Chemie und Pharmazie,
Lehrstuhl für Pharmazeutische Biotechnologie der
Ludwig-Maximilians-Universität München
(Univ.-Prof. Dr. Ernst Wagner)

siRNA Delivery with Precise and Biocompatible Polycations in Neuro2A Murine Neuroblastoma Models

Inaugural-Dissertation
zur Erlangung der tiermedizinischen Doktorwürde
der Tierärztlichen Fakultät
der Ludwig-Maximilians-Universität München

von
Raphaela Claudia Katharina Kläger
aus
Landsberg am Lech

München, 2013

Gedruckt mit der Genehmigung der Tierärztlichen Fakultät

der Ludwig-Maximilians-Universität München

Dekan:	Univ.-Prof. Dr. Joachim Braun
Berichterstatter:	Univ.-Prof. Dr. Eckhard Wolf
Korreferent:	Univ.-Prof. Dr. Dušan Palić

Tag der Promotion: 09.Februar 2013

Für meine Eltern

I Introduction

1 Nucleic Acid Based Therapy

The field of nucleic acid-based therapy holds enormous promise in the treatment of a broad range of genetic and acquired diseases by targeting their cause, at gene level. Thereby a genetic defect can be compensated or target genes, which are either pathogenic or indispensable for cell viability, can be silenced with the result of an indirectly mediated therapeutic effect.

Over 1800 clinical trials on nucleic acid-based therapeutics have been or still are conducted [1]. Whereas mostly functional genes, preferentially delivered by viral vectors, are inserted into the human genome to replace defective gene sections.

The indications cover genetic disorders like cystic fibrosis, haemophilia or severe combined immunodeficiency (SCID) [2-4] as well as acquired diseases like HIV [5, 6], neuropathological diseases [1] or DNA vaccination [7]. Although noteworthy success has been achieved, e.g. in treatment of SCID or haemophilia B, reported side effects have to be taken into account and safety concerns about intervention with the human genome remain.

The main application of gene therapy is still cancer therapy [1]. Silencing gene expression that facilitates cancer growth or introducing therapeutic genes that hamper tumor growth by inducing apoptosis of tumor cells are the main ways to accomplish therapeutic effects in cancer treatment [8, 9]. Ordinary gene therapy is based, as described above, on the integration of genetic information into target cells to mediate the expression of certain proteins. In 1998 Andrew Fire and Craig Mellow discovered in Caenorhabditis elegans that the introduction of double-stranded RNA (dsRNA), encoding for a specific gene, led to silencing of its gene product [10]. It was found that the introduction of long exogenous dsRNA into target cells, inhibits cellular protein expression, causes innate immune response by interferon activation and induces apoptosis. In 2001 Tuschel et al. published that a specific gene knockdown without significant side effects can be achieved by application of small synthetic 21-23 nucleotide interfering RNA (siRNA) duplexes [11]. When dsRNA enters the cell cytosol, it is recognized by an enzyme named Dicer [12]. This Dicer cleaves the dsRNA into siRNA duplexes. Instead of the introduction and cleavage of dsRNA, synthetically produced siRNA duplexes can be processed immediately [11]. As small

synthetic RNAs reach the cytosol of a cell, they are incorporated in a multiprotein complex named RNA induced silencing complex (RISC) (Figure 1). After the siRNA is incorporated into the RNA induced silencing complex, the enzyme Argonaute 2 unwinds the siRNA and the sense strand is cleaved [13, 14]. The antisense strand remains incorporated in the RISC and activates RISC to cleave complementary messenger RNA (mRNA) of the cell, thus avoiding translation [15]. Since the activated RISC is able to repeatedly cleave mRNA, this process effectively silences genes over a significant period of several days. Hence the system of siRNA mediated gene silencing has become an essential tool for the downregulation of single genes on post-transcriptional level as well as for studying gene function in mammalian cells.

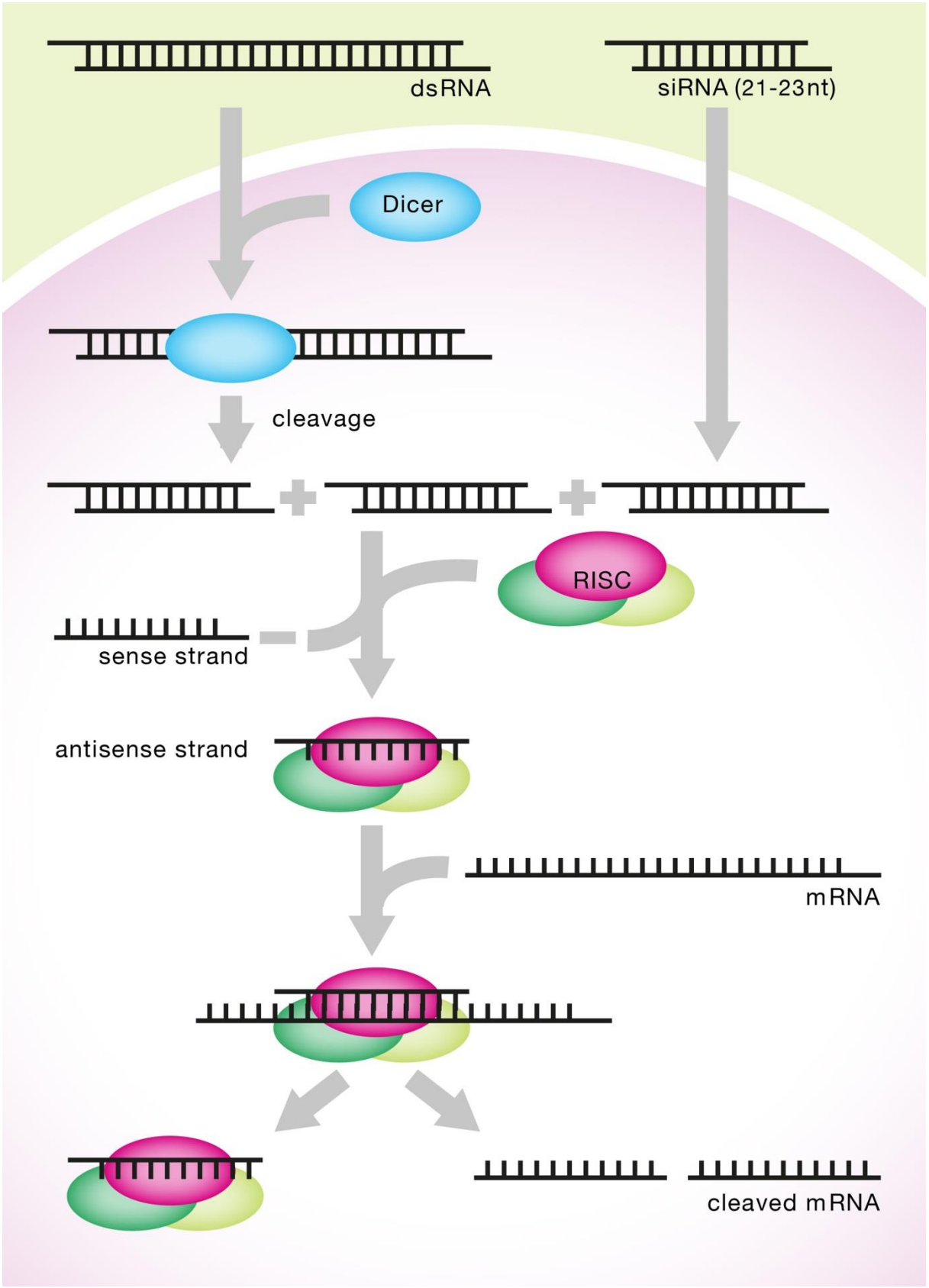

Figure 1: Mechanisms of gene silencing by introduction of siRNA and dsRNA.

RISC: RNA induced silencing complex, mRNA: messenger RNA, siRNA: small interfering RNA, dsRNA: double-stranded RNA.

Notwithstanding these promising achievements, nucleic-acid based therapy still holds a lot of challenges. Up to now naked siRNAs have only been applied successfully to tissues locally, e.g. adult late stage wet macular degeneration (AMD) was successfully treated by injections into the eye in mice and nonhuman primates [16, 17]. Also *intramuscular* injection, electroporation and hydrodynamic injections with plasmid DNA led to positive results [18-21]. Nucleic acids are highly hydrophilic, relatively large (siRNA: ~13 kDa) and can consequently not permeate the lipid layer of a cellular membrane. In addition they are, when injected *in vivo*, quickly degraded by nucleases primarily in the blood stream [22-25].

Nevertheless, for a breakthrough of this technology in the broad field of clinical utilization easy-to-handle systemic applications are obligatory.

For this intention, carrier systems have to be developed that protect siRNA from extracellular environment and efficaciously deliver it into the cytosol of target cells. Non-viral and viral delivery systems are being investigated, whereas viral gene vectors show high efficacy, but the production is quite expensive and there are safety concerns as mentioned above. Amidst the field of non-viral transfer systems, there are few approaches including lipids [26, 27], lipid-modified polymer formulations [28-31], conjugated RNAs [32] and cationic polymers [33-37].

2 Non-Viral Carrier Systems for siRNA Delivery

Up to now more than 60% of clinical gene therapy trials use viral vectors [1]. As natural gene delivery systems, viruses are highly capable to deliver their genes to their target cells. Because of the evolution process they are ideally adapted to overcome the general hurdles of delivery. In general, viruses target a distinct cell type and not a population of cells. However, domestication might cause inherent problems including immune and toxic reactions and the potential for viral recombination as mentioned above. Chemical modifications for de- or retargeting reasons are also difficult [38-40]. A dramatic disadvantage of viral gene transfer systems for siRNA delivery is the insufficient compatibility. For viral gene transfer the gene of interest is introduced into a plasmid. A special packaging cell line is transfected with this plasmid with the gene of interest, leading to the amplification of this DNA and incorporation as DNA or RNA into the intracellular produced viruses [41]. As siRNAs

are completely chemically synthesized, it is impossible to incorporate them into viruses with the virus production method described before. There are a few approaches to overcome this problem [42].

Hence a broad range of synthetic vectors have been developed. One main advantage of synthetic vectors is that they can be tailored to specific needs, including subsequent functionalizations, like shielding moieties or targeting. However, their transfection efficiency is rather low compared to viral gene vectors, which was shown by Brown et al. in 2001.

The class of liposomal siRNA formulations has become one of the most investigated of synthetic vectors [43]. Representatives for lipid based siRNA vectors are liposomes and lipoplexes. Cationic lipids are amphiphilic mainly consisting of three parts, a hydrophobic lipid tail, a linker group, such as an ester, amide or carbamate and a positively charged head-group, which condenses with negatively charged nucleic acids. These characteristics cause cationic lipids to assemble into nanospheric liposomes when put into aqueous solutions [44]. In case of liposomes nucleic acid is incorporated in the liposome and protected against endogenous nucleases and in addition liposomes are able to destabilize the endosomal membrane by lipidic interaction and release their cargo into the cellular cytosol [43]. In case of lipoplexes nucleic acid is incorporated at the outside shell of the liposome [45], thereby successful hampering of tumor progression could be shown [46, 47]. Cationic lipids are often combined with so called helper lipids e.g. dioleoylphosphatidylethanolamine (DOPE) or cholesterol [48]. A major drawback of lipidic systems is their high accumulation in the liver. As liposomes and other hydrophobic particles show remarkable liver affinity, they need a strong shielding to be efficiently directed to other tissues [49].

Cationic polymers also show high potential to condense nucleic acids. They are able to complex nucleic acids and form nanoparticles with them, through their positive charge by ionic interaction with the negatively charged phosphate groups of the nucleic acids [50]. Amongst this group, linear structures like poly-lysine (PLL) [51], linear polyethylenimine (LPEI) [52] or branched structures like polyamidoamine (PAMAM) [53], branched polyethylenimine (brPEI) [54] or polypropylenimine (PPI) [55] have been explored. In the line of polyplexes, polyethylenimine PEI is the “gold standard” for gene transfection due to its superior transfection efficacy [56, 57]. This molecule bears many advantages in the process of gene delivery. If formulated with

nucleic acids it builds stable complexes under physiological conditions. Since the polymer is highly positive charged these polyplexes in general have a positive zeta potential. This enables the attachment to cellular membranes of target cells *via* ionic interactions and thereafter results in endocytosis. Inside the endosome, PEI leads to an escape from the endosome *via* the so called “proton sponge effect” [58, 59]. As a result of its strong buffering capacity, the polycation hinders the acidification of the cellular endosome. Therefore more and more protons accumulate in the endosome, followed by chloride as counter ion. This process leads to a strong osmotic pressure, causing an influx of water. If the osmotic pressure becomes too strong, the endosomal membrane bursts and releases its payload into the cytosol of the cell [59]. In addition to the proton sponge effect, it seems to be important, too, that the polycationic charge is presented on the surface for interaction and destabilization of the endosomal membrane [34]. Standard PEI is an inefficient carrier for siRNA in vitro [60]. In spite of this, Aigner et al. demonstrated efficient siRNA delivery in a murine model [61]. Apart from this, cells cannot degrade the high molecular weight polymers, such as PEI, which results in accumulation and interactions with DNA, proteins and cellular membranes [62]. This accumulation in reticular organs, such as lung or liver, results in acute toxicity [63]. *In vivo* the highly positive charged polyplexes interact with blood components, resulting in strong aggregation, thus toxicity and undesired side effects [64, 65].

Therefore e.g. succinylation of PEI to block some of the positive polymer charges was explored and led to an efficient siRNA carrier with strongly reduced cytotoxicity [54]. Another approach is the shielding with polyethylenglycol (PEG) that prevents the polyplexes from uptake of macrophages and thus rapid removal from the blood stream as well as aggregation of positively charged polyplexes with erythrocytes causing embolism [64, 66-68]. The problem of non-biodegradability can be overcome by new biodegradable polymers that are stable in the extracellular surrounding and degrade, after having delivered their cargo into the cell, to non-toxic metabolites in the intracellular environment [55, 69]. To enhance the transfection efficacy at least two bottle necks have to be taken into account: These are endosomal escape, as mentioned above and specific uptake of the polyplexes by the targeted cells.

When polyplexes are incorporated by endosomes, they have to escape from them, otherwise the endosome gets acidified and turns into a lysosome degrading polyplex and nucleic acid. Polymers like PEI avoid degradation by the proton sponge effect

but enough polymer has to be inside one endosome to mediate this effect. Another approach is endosomolytic peptides. Those are derived e.g. from the sequence of the aminoterminus of the influenza virus haemagglutinin [70, 71]. A modification of the sequence resulted in a peptide that is only lytic at endosomal pH (pH 5.5) and not at an ordinary pH (pH 7.4) of the organism, minimizing undesired side-effects [72].
Moreover, new structures lacking a buffering capacity can be tested as feasible carrier systems [73], if combined with endosomolytic agents. A second peptide is derived from the bee venom, whose lytic activity is not pH dependent [74-77]. Artificially synthesized peptides like GALA or KALA are another solution [78-83].
The combination of polycationic backbones and fatty acids that have comparable properties has been a further reasonable approach overcoming this crucial step of endosomal escape [30, 84].
To allow specific cellular uptake, polyplexes have on the one hand to be stable in the blood stream [36, 85], on the other hand have to target distinct tissues. The field of tumor targeting can be divided into two approaches, active and passive targeting. Since a fully shielded polyplex is not able to interact with cells, an additional domain has to be incorporated to address receptors on the cell surface [86]. An enormous advantage is that almost all tissues differ in the expression level of cell surface receptors what makes them distinguishable. As endocytosis is needed for efficient gene delivery, receptors mediating endocytosis such as the transferrin receptor (Tf-R), the epidermal growth factor receptor (EGF-R), the folic acid receptor (FolA-R) or integrins (e.g. $\alpha_v\beta_3$) are mainly addressed [87-91] and, in addition, are highly upregulated in tumor tissue [92-95]. The second strategy to address tumor tissue is passive targeting. Non targeted polymers have already shown to work very efficiently in case of DNA delivery into tumor tissue. This can be explained by the enhanced permeability and retention (EPR) effect [96]. When solid tumors reach a certain size, they are limited in blood supply of the existing vessels and therefore massive angiogenesis is the result. Tumors become hypervascularized, at the same time the lymphatic drainage is hardly developed and the vessel endothelium is fenestrated and leaky [97]. When complexes are injected intravenously, they pass the leaky tumor blood vessels and diffuse through the endothelium into the tumor. When drug concentration in the blood stream decreases, small molecules are able to diffuse back into the blood stream, whereas bigger molecules can’t and accumulate in the tumor [98].

3 Assessments of Nucleic Acid Carrier Systems

Due to ethical and economic reasons, newly designed gene transfer systems need to be tested for efficacy and toxicity *in vitro* before they are applied *in vivo.* Thereafter they are, only if they have revealed high efficacy and low toxicity, tested in an *in vivo* mouse model. Efficacy measurement of siRNA delivery systems is quite a challenge *in vivo*, as it has to be geared for consecutive measurements as well as fast and easy analysis, be highly sensitive and specific, it should lead to statistically significant results and not at least be compatible with the animal welfare.
Up to now literally no *in vivo* method meets all these demands. The next chapters especially deal with *in vivo* methods focusing on methods for efficacy evaluation.

3.1 Distribution

The distribution assessment of a new siRNA carrier plays a pivotal role in gene transfer *in vivo* as by the distribution a forecast for desired as well as for undesired effects is possible. I.e. mostly whether the carrier or the siRNA is tagged with a reporter and can therefore be easily detected. Common methods to measure drug distribution *in vivo* are radioisotopes (Positron Emission Tomography (PET), Single Photon Emission Computed Tomography (SPECT) as well as quantum dots and fluorescent dyes [99-102]. Another approach is measurement of the drug concentration in body fluids e.g. urine, blood and faeces. However, carrier distribution cannot be equated with carrier efficacy. A high accumulation of e.g. a labeled polymer in the liver does not mean that the siRNA, incorporated by the time of injection, is also located in the liver or, as another possibility the polyplex is stuck in an endosome and therefore not functional. Thus it is very important to prove efficacy as well as distribution [63].

3.2 Toxicity

Toxicity is divided into acute and chronic toxicity as well as reproductive and teratogenic toxicity [103], therefore animals have to be monitored carefully during and after the experiment. However, first toxicity tests mainly focus on peracute and acute adverse reactions. In case of polycationic delivery systems those are primarily caused by interference of the polyplexes with blood components, lung or liver tissue [63, 64, 66, 67]. Before polymer/siRNA complexes are injected *in vivo* they have to pass erythrocyte leakage assays and blood aggregation assays to predict the interaction of the polymers with blood components [51, 55, 104].
Liver enzymes such as aspartate aminotransferase (AST or SGOT) and alanine aminotransferase (ALT or SGPT) are well known parameters that rise in case of liver damage [88]. Histopathological examination can also be used as a tool for visualizing liver and lung toxicity. Light and also fluorescence microscopy, in combination with distinct stains like the TUNEL stain, can reveal pathological changes such as adverse cell metabolism apoptosis or necrosis [63, 88]. Nevertheless, one of the easiest and fastest parameter in mice is body weight that increases and decreases due the general condition.

3.3 Efficacy

To evaluate the siRNA transfection efficacy of newly designed polymers a specific gene has to be silenced by interaction with the corresponding mRNA leading to a silenced protein translation. Hence transfection efficacy can be evaluated either on the nucleic acid or on the protein level. To determine efficacy on the protein level *in vivo* imaging is a very convenient method. There are many approaches such as magnetic resonance imaging (MRI), positron emission tomography (PET), computed tomography (CT), single photon emission tomography (SPECT), fluorescence and bioluminescence imaging [105, 106].
Magnetic resonance imaging relies on nuclear magnetic resonance. It reveals images with high spatial resolution, high contrasts and clear tissue delineation. CT imaging is based on absorption of X-rays by diverse tissues, hence resulting in high anatomical resolution imaging (but with relatively low contrast in soft tissue) of small animals

[107, 108]. Nevertheless, a major disadvantage lies within the relatively long acquisition and processing time and the low sensitivity (MRI) or contrast (CT). In siRNA based therapy systems CT and MRI can only be used to measure therapeutic effects, e.g. the size of a treated tumor [109]. There are new approaches to improve sensitivity and contrast [110-117]. PET imaging is based on isotopes emitting positrons (e.g. ^{11}C, ^{13}N, ^{15}O, ^{18}F), whereas for SPECT imaging isotopes emit gamma-rays (e.g. ^{99m}Tc, ^{123}I) [118-125]. The most prominent disadvantage of those imaging techniques is that mice are exposed to radiation. In contrast optical imaging is not based on radiation the acquisition and processing time is relatively short but with increasing depth the signal is attenuated. Furthermore, the usage of the same reporter gene *in vitro* and *in vivo* is possible, which is useful. Optical imaging consists of fluorescence imaging and bioluminescence imaging, whereas the light emitted is measured by a charge-coupled device (CCD) camera. In fluorescence imaging external light excitates a fluorochrome and thereby it emits light of another wavelength which is detected by the CCD camera. It is in general a very sensitive method hence autofluorescence of body tissue is very low. For this purpose there are several fluorochromes available. One of the first was green fluorescent protein (GFP), first isolated from the jellyfish Aequorea Victoria with an emission peak at 509 nm and its variations, e.g. eGFP, that has a longer emission wavelength and is also brighter than the wildtyp GFP [126, 127], red fluorescent protein (RFP) (emission peak at 574 nm) and it's variations offer a higher stability and a longer emission wavelength which is beneficial, because of low body tissue absorption, especially cyanine fluorochromes that were also used in this work [128-131].

3.3.1 *In Vivo* Bioluminescence Imaging for siRNA Efficacy Studies

Bioluminescent imaging has become an important tool for *in vivo* monitoring, mainly because almost no background signal is produced as the light is expressed by certain luciferase enzymes. Diverse luciferases serve as reporter enzymes. These enzymes catalyze the emission of photons by a reaction that is dependent on the presence of a certain substrate as well as other co-factors and/or oxygen thereby photons are emitted and detected by a CCD camera. Photons are attenuated by body tissue because of absorption and light scattering by melanin or haemoglobin

[132]. In the visible spectrum the intensity of photons, such as those produced by luciferases, is attenuated about 10-fold per cm of body tissue. Coming along with the importance of luciferases as reporter enzymes the most commonly used one is Photinus pyralis, derived from the North American firefly. Photinus pyralis oxidizes its substrate, luciferin, to oxyluciferin. Thereby light with a broad emission spectrum and a peak at approximately 560 nm, is produced [133] but the reaction is dependent on energy in the form of Adenosine-5'-triphosphate (ATP) and oxygen.

Luciferases derived from the sea pansy Renilla reniformis and Gaussia princeps, a mesopelagic copepod, react with coelenterazine independently from ATP but necessarily with oxygen. The reaction creates light with an emission peak at around 480 nm [134-138] and as the luciferase is secreted tumor sizes can indirectly be measured. Coelenterazine is applied directly into the blood stream, whether through tail vein or intracardiac injection [139, 140]. A major drawback of Renilla reniformis and Gaussia princeps is auto-oxidation of coelenterazine and a rapid kinetic peak 1 – 2 minutes after injection demanding excellent time management [135].

Click beetle red and green luciferases were isolated from Pyrophorus plagiophtalamus from the Elateridae superfamily, they are optimized for different wavelengths than Photinus pyralis (544 and 611 nm, respectively) but also rely on the same enzymatic reaction [141, 142].

Photinus pyralis luciferase has a half-life of about 3 – 4 hours, which should not limit daily performed quantitative bioluminescence imaging. Likewise the enzyme itself, biodistribution and pharmacology of the substrates are important parameters and have to be taken into consideration for reproducible quantification of bioluminescence. Increased substrate concentrations and also local application of substrate increased the signal output significantly with dependence on localization of the enzyme [143]. Another pivotal parameter is bioluminescence kinetics of the firefly luciferase that reaches its peak after approximately 10 – 20 minutes. These parameters were analyzed and optimized by Dr. Gelja Maiwald and are part of her vet MD thesis [LMU 2010].

As mentioned above successful siRNA delivery in living beings will consecutively lead to silencing of the targeted protein expression. Protein depletion can be determined directly by bioluminescence imaging, if the luciferase enzyme itself or a protein that influences the expression of luciferase is targeted. Another way leading

to an increased bioluminescent signal is the usage of cell death mediating siRNAs [88, 144-146].

4 Kinesin Spindle Protein

In this work the potential therapeutic effect of mRNA knockdown in tumor cells had to be studied. EG5 is a member of the Bim-C class of kinesin related proteins (Figure 2).

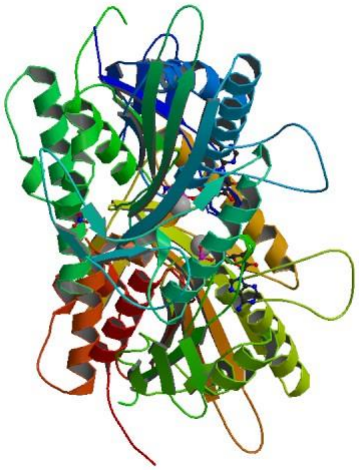

Figure 2: Crystal structure of the mitotic Kinesin Eg5 in complex with Mg-ADP [147].

The Protein influences the assembly and organization of the mitotic spindle, a self-assembled and dynamic microtubule-based structure that orchestrates chromosome segregation in dividing cells [148] (Figure 3). The EG5 protein plays a pivotal role in cell division. If there is no EG5 in the cytoplasm, abnormal monopolar spindles occur, which prevent successful cell division [149].

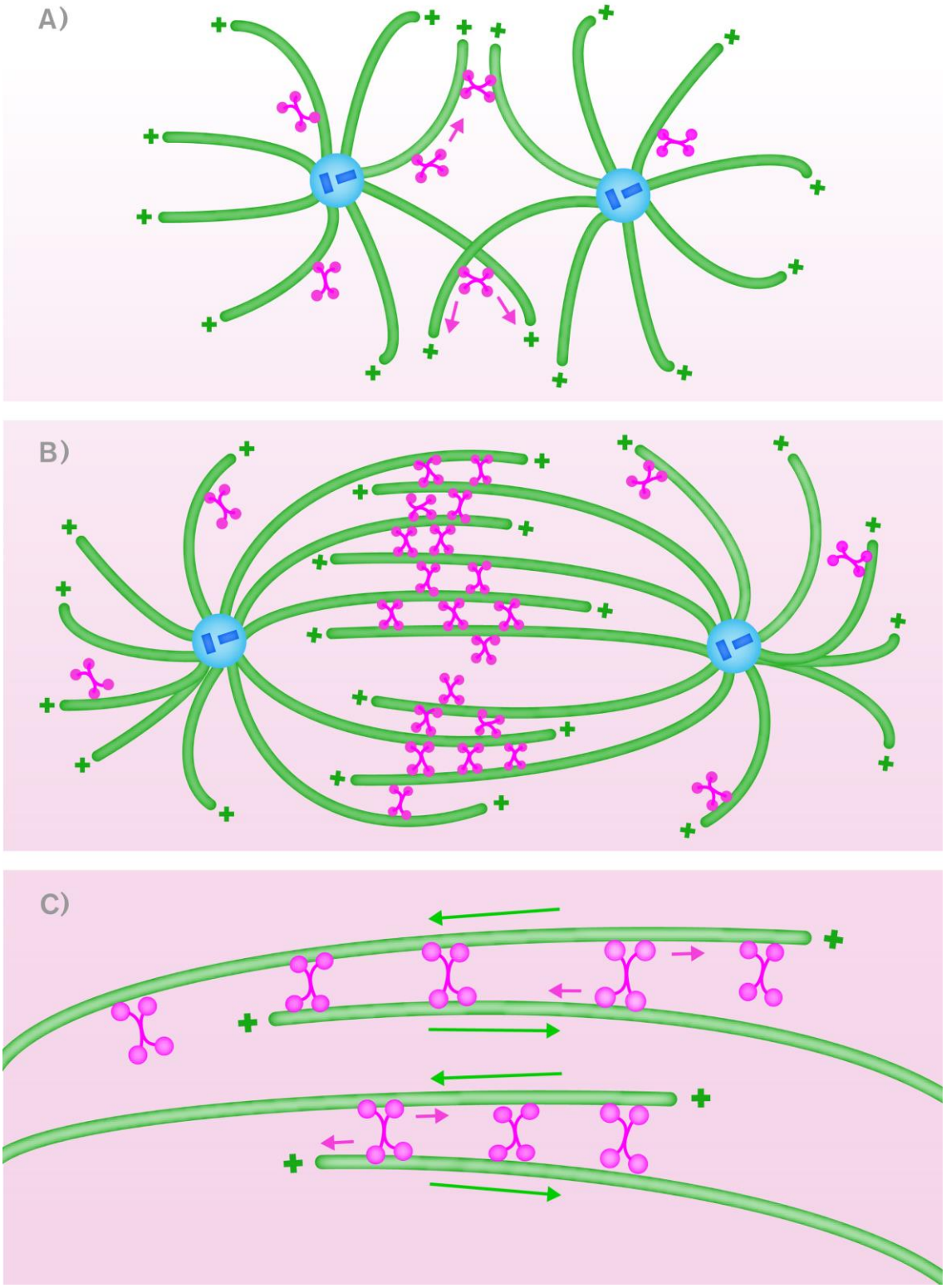

Figure 3: Schematic depicting EG5 activity in the mitotic spindle. Tetrameric EG5 motors (pink) help to organize microtubules (green) to form the mitotic spindle. (A) At the onset of mitosis, the duplicated centrosomes (light blue) separate and nucleate two microtubule asters. Processive EG5 motors may translocate to the plus-ends of microtubules, located distal to the centrosomal organizing center and by crosslinking antiparallel microtubules, may promote bipolarity. (B) By metaphase, a stable bipolar spindle has formed. EG5 motors likely provide structural integrity and also slide microtubules toward the centrosomes, contributing to the generation of poleward flux. (C) A close-up depiction of Eg5 motors walking to the plus ends of antiparallel microtubules, moving both poleward simultaneously. Figure modified from Valentin M. 2006.

Assembly, maintenance and functionality of the mitotic spindle depend on centrosome migration, organization of microtubule arrays, and force generation by microtubule motors. Therefore defects in this complex structure lead to chromosome missegregation and genomic instability. High amounts of the EG5 protein lead to disruption of the normal spindle development and hence result in tetraploid cells. Mice with this defect show higher incidences of tumor formation. EG5 overexpression disrupts the unique balance of forces associated with normal spindle assembly and function, and thereby leads to the development of spindle defects, genetic instability, and tumors [150]. We wanted to utilize a siRNA directed against the EG5 mRNA to silence protein translation. Because of its pivotal role in cell division (Figure 3), our hypothesis was that downregulation of the EG5 protein results in apoptosis of our targeted tumor cells.

5 Ran Protein

The Ran protein is a 25Kda protein and belongs to the Ras superfamily. It's a small GTPase and has been implicated in a large number of nuclear processes including formation and organization of the microtubule network and regulation of nuclear transport and formation [151-154].

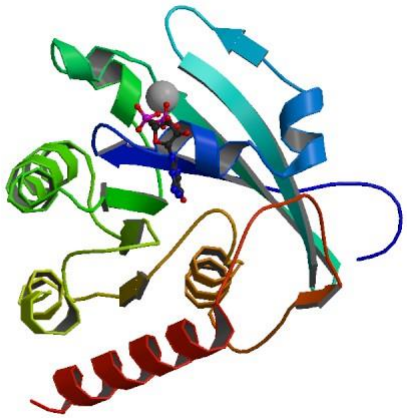

Figure 4: Ras-related nuclear protein Ran (Ran-GDP) [147].

High expression of Ran GTPase in cells is associated with appearance of cancer [155, 156]. Because it was recently identified by an RNAi based screen as possible target in cancer therapy [157], we utilized a siRNA directed against the Ran mRNA to silence protein translation. Because of its pivotal role in nuclear transport (Figure 5), our hypothesis was that downregulation of the Ran protein results in apoptosis of our targeted cells. Inside the cell Ran occurs in two nucleotide-bound forms: GDP-bound and GTP-bound. The transport into the nucleus through the nuclear pore complex is driven by a Ran/GTP concentration gradient, with a high concentration of Ran/GDP in the cytoplasm and a high concentration of Ran/GTP in the nucleus. Cargo proteins that are supposed to be transported into the nucleus contain a nuclear localization signal (NLS) that forms complexes with importin α and importin β in the cytoplasm, where Ran is in the GDP bound form. Following transport through the nuclear pore complex, Ran/GTP binds to importin β and releases importin α and the cargo protein within the nucleus. The GTPase-activation in the nucleus then leads to transportation of this Ran/GTP/importin β complex to the cytoplasm. Here hydrolysis of the bound

GTP occurs, and a Ran/GDP complex is formed, releasing importin β forming a Ran/GDP complex and releasing importin β and hence closing the Ran cycle.

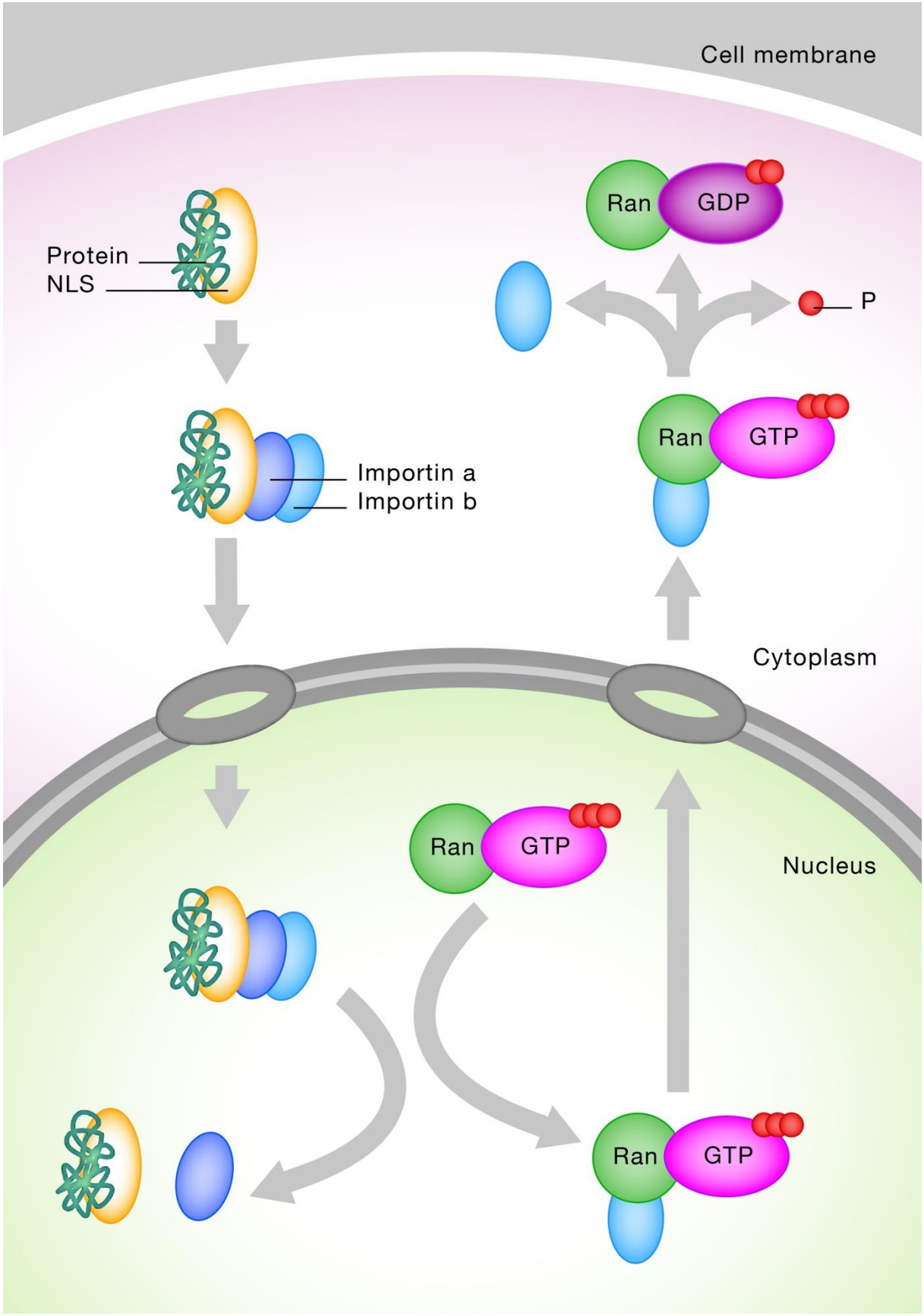

Figure 5: Role of Ran protein in nuclear transport.

6 Aims of the Thesis

In this dissertation, *in vivo* delivery of siRNAs complexed with polycationic delivery systems, systemically or intratumorally, should be analyzed.

The *in vivo* application is so far hampered by the lack of stable delivery systems that are able to protect siRNA in the blood stream and safely deliver it to the desired target cells. Nevertheless, several novel polycationic vectors that had been established in our lab, led to promising *in vitro* results for siRNA delivery.

In the actual work an *in vivo* model for the administration siRNA/polymer complexes should be established and furthermore optimized. As tumor cell line, the murine neuroblastoma cell line Neuro2A was chosen, hence a good correlation between in vitro and *in vivo* tests was expected, as these cells have been used for in vitro experiments.

In the beginning labeled siRNAs should be used to prove the transfection capability.

Thereafter, therapeutically relevant EG5 and Ran siRNAs should be utilized to prove if the transfection efficacy can be identified pathohistologically.

Furthermore, therapeutically relevant Ran siRNA should be used to try to influence the growth of subcutaneous and intrasplenic Neuro2A-eGFPLuc tumors, metastasizing to the liver, in a syngeneic mouse model as well as in a xenograft one. Size measurements of tumors were to be determined via bioluminescence as is the most advantageous *in vivo* imaging method especially for tumors inside the abdomen where caliper measurement is impossible.

Another aim was to evaluate different biodegradable polymers that had been established in our laboratory for their efficacy and safety in *in vivo* applications.

We wanted to show that our biodegradable polymers can reach a high *in vivo* efficiency with an excellent tolerability and the possibility of repeated application.

Furthermore, we were interested in clarifying the impact of the siRNA on efficiency and toxicity of the treatment. In this case, the effect of repeated systemic and intratumoral applications of siRNA/polymer formulations on the mouse organism as well as tumor tissue and skin should be investigated.

II Materials and Methods

1 Materials

1.1 Cell Culture

Murine neuroblastoma Neuro 2A cells	LGC Standards (ATCC CCI-131)
Neuro 2A-eGFP Luc cells	NeuroAa cells stably expressing a fusion protein of eGFP and Photinus pyralis luciferase
DMEM 1 g glucose	- DMEM, 4.5 g glucose/L, with L-glutamine, with NaHCO3 (Biochrom, Berlin, Germany): 10.15 g - $NaHCO_3$ p.A.: 3.7 g - ad 1 liter with aqua bidest
OptiMEM	Invitrogen (Karlsruhe, Germany)
Penicillin-Streptomycin	Biochrom (Berlin, Germany)
FBS	Invitrogen (Karlsruhe, Germany)
L-alanyl-L-glutamine	Biochrom (Berlin, Germany)
G418	Invitrogen (Karlsruhe, Germany)
Puromycin	SIGMA-Aldrich (Steinheim, Germany)
Hygromycin	SIGMA-Aldrich (Steinheim, Germany)

Cell culture plates	TPP (Trasadingen, Switzerland)
Cell culture flasks	TPP (Trasadingen, Switzerland)
TE	Biochrom (Berlin, Germany)
PBS	- Phosphate buffered saline (Biochrom, Berlin, Germany): 9.55 g - ad 1 liter with aqua bidest

1.2 In Vitro and *in Vivo* Transfection Experiments

HBS	- Hepes (Biomol, Hamburg, Germany): 2.38 g - ad 300 mL with aqua bidest - adjust with NaOH (VWR International, Darmstadt, Germany) on pH 7.1 - NaCl (VWR International, Darmstadt, Germany): 4.383 g - check pH, ad 500 mL with aqua bidest
HBG	- Hepes (Biomol, Hamburg, Germany): 2.38 g - ad 300 mL with aqua bidest - correct with NaOH (VWR International, Darmstadt, Germany) on pH 7.1 - Glucose-monohydrate (Merck, Darmstadt, Germany):27.5 g - check pH, ad 500 mL with aqua bidest
HBS	0,5 HBS/HBG: 1/1
D-luciferin sodium salt	Promega (Mannheim, Germany)

Luciferase cell culture lysis reagent Promega (Mannheim, Germany)

Luciferase assay buffer	Promega (Mannheim, Germany)
LAR	- 1 M Glycylglycin (Merck, Darmstadt, Germany): 2 mL - 100 mM MgCl (Carl Roth, Karlsruhe, Germany): 1 mL - 500 mM EDTA (SIGMA-Aldrich, Steinheim, Germany): 20 µL - DTT (SIGMA-Aldrich, Steinheim, Germany): 50.8 mg - ATP (Roche, Mannheim, Germany): 27.8 mg - Coenzym A (SIGMA-Aldrich, Steinheim, Germany): 0.5 mL - ad 100 mL with aqua bidest - adjust with NaOH (VWR International, Darmstadt, Germany) on pH 8 – 8.5
Deferoxamine	SIGMA-Aldrich (Steinheim, Germany)
Isoflurane ®	cp Pharma (Burgdorf, Germany)
Bepanthene®	Roche (Grenzach-Whylen, Germany)
Ketavet® 100 mg/mL	Pfizer, Pharmacia GmbH (Karlsruhe, Germany)
Rompun® 2%	Bayer Vital GmbH (Leverkusen, Germany)
Syringes	Heiland (Hamburg, Germany)
Needles	Heiland (Hamburg, Germany)
Isotonic sodiumchloride solution	Braun Melsungen AG (Melsungen, Germany)

1.2.1 Polymers

Polymers were synthesized by Christina Troiber, Irene Martin and Dr. Naresh Badgujar.

Polymer ID	Topology	Polymer Sequence
229	i-shape	LinA2K-C-Stp-Stp-Stp-C
386	three-arm	(C-Stp-Stp-Stp)2]K-Stp-Stp-Stp-C
49	T-shape	C-Stp-Stp-K(K-OleA2) Stp-Stp-C
332	T-shape	Y3-Stp-Stp-K(K-OleA2) Stp-Stp-Y3
454	T-shape	C-Y3-Stp-Stp-K(K-OleA2) Stp-Stp-Y3-C

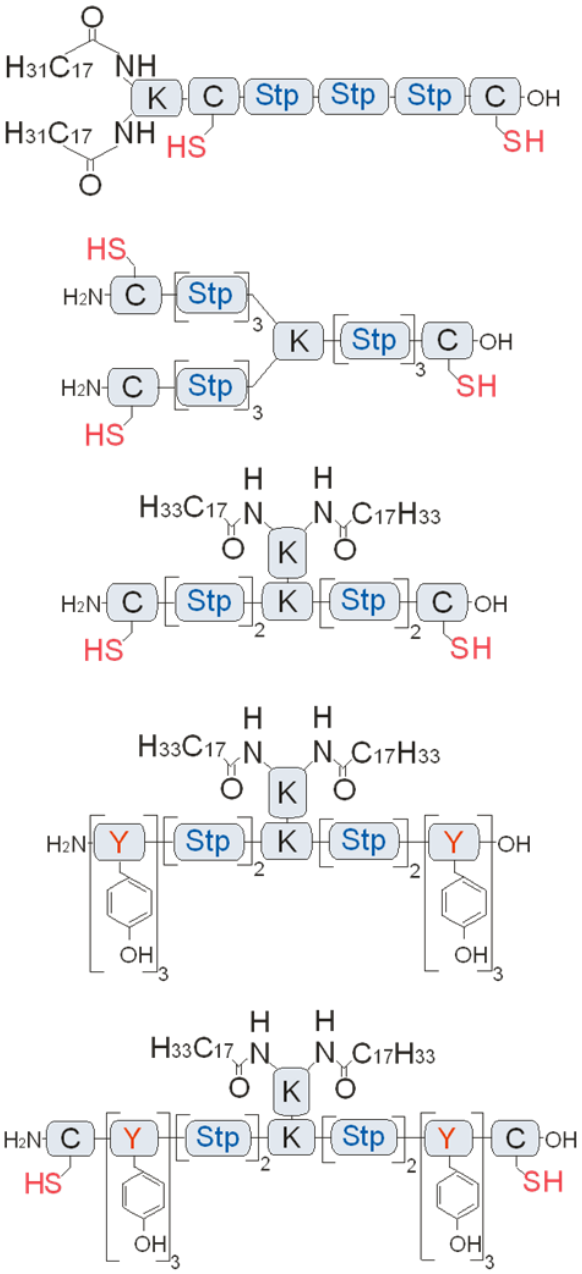

1.2.2 siRNAs

Axolabs (formerly Roche) Kulmbach:

GFP-siRNA: 5'-AuAucAuGGccGAcAAGcAdTsdT-3' (sense)
5'-UGCUUGUCGGCcAUGAuAUdTsdT-3' (antisense)
(small letters: 2'methoxy-RNA; s: phosphorothioate)

Control-siRNA: 5'-AuGuAuuGGccuGuAuuAGdTsdT-3' (sense)
5'-CuAAuAcAGGCcAAuAcAUdTsdT-3'(antisense)

EG5-siRNA: 5'-ucGAGAAucuAAAcuAAcudTsdT-3' (sense)
5'-AGUuAGUUuAGAUUCUCGAdTsdT-3' (antisense)

Cy3-AHA1-siRNA: (Cy3)-(NHC6)-5'-GGAuGAAGuGGAGAuuAGudTsdT-3' (sense)
5`-ACuAAUCUCcACUUcAUCCdTsdT-3' (antisense)

Dharmacon:

Ran-siRNA: 5´-ACCCGCTCGTCTTCCATAC-3' (sense)
5´-ATAATGGCACACTGGGCTTG-3' (antisense)

HBG was used as buffer and solvent.

1.2.3 Histopathology

Tissue – Tek Cryomold	Sakura Finetek (Heppenheim, Germany)
Tissue – Tek O.C.T. Compound	Sakura Finetek (Heppenheim, Germany)
Tissue – Tek Mega-Casette	Sakura Finetek (Heppenheim, Germany)

Bovine Serum Albumin	Sigma Aldrich (Hamburg, Germany)
Dako Pen	Dako (Glostrup, Denmark)
Super Frost Plus slides	Menzel (Braunschweig, Germany)
FluorSave™ Reagent	Merck (Darmstadt, Germany)
VECTASHIELD® Mounting	Biozol (Eching, Germany)
Texas Red Dextran 70 000 MW	Invitrogen (Karlsruhe, Germany)
FITC Dextran 2 000 000 MW	Invitrogen (Karlsruhe, Germany)
CD45 rat anti-mouse	BD Pharmingen (Heidelberg, Germany)
Alexa 647 goat anti-rat	Invitrogen (Karlsruhe, Germany)
Goat serum	Sigma Aldrich (Hamburg, Germany)
TUNEL ApopTag® Fluorescein kit	Qbiogene (Heidelberg, Germany)
4',6-Diamidino-2-phenylindol (DAPI)	
Hoechst 33342 dye	

1.2.4 Laboratory Animals

A/JOlaHsd	Harlan-Winkelmann (Borchen, Germany)
NMRI-*Foxn1*^{nude} (nu/nu)	Janvier (Le Genest-St-Isle, France)

1.3 Instruments

Luminometer Centro LB 960	Berchtold (Tuttlingen, Germany)
Tecan SpectraFluor Plus	Tecan (Crailsheim, Germany)
IVIS Lumina	Caliper Life Science (Rüsselsheim, Germany)
B. Braun Aesculap cordless animal clipper Isis GT420	(Melsungen, Germany)
Caliper Digi-Met	Peisser (Gammertingen, Germany)
PX2 Thermal Cycler	Thermo electron corporation (Karlsruhe, Germany)
Light Cycler 480	Roche Diagnostics (Mannheim, Germany)
Zeiss Axiovert 200 Fluorescence Microscope	Carl Zeiss AG (Göttingen, Germany)
Zeiss Laser Scanning Microscope LSM510 Meta	Carl Zeiss AG (Göttingen, Germany)
AxioCam	Carl Zeiss AG (Göttingen, Germany)
Thermo Scientific Excelsior™ Tissue Processor	Thermo Fisher Scientific (Massachusetts, USA)
Fully Automated Rotary Microtome Leica RM2265	Leica Microsystems GmbH (Wetzlar, Germany)
Leica EG1150 Modular Tissue Embedding Center	Leica Microsystems GmbH (Wetzlar, Germany)

Research Cryostat Leica CM3050 S	Leica Microsystems GmbH (Wetzlar, Germany)
Paraffin Tissue Floating Bath	MEDAX GmbH & Co.KG (Neumünster, Germany)
FastPrep®-24 Instrument	MP Biomedicals (Solon, USA)

1.4 Software

Graph Pad Prism 5 software	Graph Pad Software (San Diego, U.S.A.)
Living Image 3.2	Caliper Life Science (Rüsselsheim, Germany)
AxioVision LE^{TM} software	Carl Zeiss Microscopy GmbH (Jena, Germany)

2 Methods

2.1 Cell Culture

2.1.1 Maintenance of Cultured Cells

Mouse neuroblastoma Neuro2A cells (wildtype) and Neuro2A-eGFPLuc (stably transfected with the eGFPLuc gene), were grown in Dulbecco's modified Eagle's medium (DMEM). Medium was supplemented with 10% FCS, 4 mM stable glutamine, 100 U/mL penicillin and 100 µg/mL streptomycin. All cultured cells were grown at 37 °C in 5% CO_2 humidified atmosphere.

2.1.2. Luciferase Gene Silencing

Gene silencing experiments were performed using 0.5 µg/well (unless otherwise mentioned) of Luc-siRNA for silencing of the eGFPLuc protein, or control-siRNA as control. siRNA delivery was performed in 96-well plates with 5×10^3 cells per well in

triplicates. Cells were seeded into wells 24 hours prior to transfection and then growth medium was replaced with 80 µL fresh medium containing 10% FCS. Transfection complexes for siRNA delivery (20 µL formed in HBG) were added to each well and incubated at 37 °C for 48 hours in 5% CO_2 humidified atmosphere (unless otherwise mentioned). After transfection, cells were treated with 100 µL cell lysis reagent and luciferase activity in the cell lysate was measured from a 35 µl aliquot of the lysate using a luciferase assay kit and a plate reader luminometer. The relative light units (RLU) are presented as percentage of the luciferase gene expression obtained from with buffer treated control cells.

2.2 Animal Experiments

Animal experiments were performed according to the guideline of the German law of protection of animal life and were approved by the local animal experiments ethical committee. Mice were housed in individually vented cages (TECNIPLAST, Hohenpeißenberg) with up to 5 animals per cage under specific pathogen free conditions. Cages were equipped with wood shaving litter, a mouse house (TECNIPLAST, Hohenpeißenberg), a wooden rodent tunnel and cellulose bedding. Cages were changed once a week. Autoclaved water and standard breeding chow were provided *ad libitum.* A day and night cycle, 21 °C room temperature and 60% humidity were kept. Mice were allowed to adapt to the housing condition at least for one week before experiments started.

2.2.1 Subcutaneous Tumor Models for Histological Analysis of Systemic siRNA Delivery

For transfection studies female A/JOlaHsd mice, 6-8 week old mice were used.
Neuro2A cells were grown in cell culture as described above, despite being kept in antibiotic free DMEM medium supplemented with 10% FCS for at least one week prior to injection. For harvesting, cells were detached using trypsin/EDTA. Trypsin was inactivated with medium and cells were centrifuged (1000 rpm; 5 min). The cell pellet was washed three times with PBS and diluted in ice cooled PBS at a

concentration of 10^6 cells per 100 µl. The injection site of the mice was clipped one day prior to tumor cell injection, using an Aesculap cordless animal clipper, a 1 ml syringe and a 25 gauge needle was used to inoculate subcutaneously 1 × 10^6 Neuro2A cells in 150 µL of PBS into the left flank. After 10 days incubation 5 mice per group were injected intravenously via tail vein with conjugates containing 50 µg of siRNA (N/P 12) in 250 µL of HBG solution per 20 g of body weight.

2.2.2 Fluorescence Microscopy of Cy3 Labeled siRNA Distribution *in Vivo*

To detect siRNA distribution polyplexes containing Cy3 labeled siRNA were injected intravenously *via* tail vein. Mice were sacrificed 1 h after polyplex injection and organs (tumor, lung, liver, kidneys) were harvested. Organs were immobilized in TissueTek™ and immediately stored at -20° Celsius. 5 µm fine sections were cut using a cryotom. Slices were stained with Hoechst 33342 dye and results were documented using a Zeiss Axiovert 200 Fluorescence Microscope, a Zeiss Laser Scanning Microscope LSM510 and a MetaAxioCam.

2.2.3 Fluorescence Microscopy of Aster Formation *in Vivo*

24 h after EG5-siRNA containing polyplexes were injected intravenously via tail vein mice were sacrificed, tumors and organs (lung, liver, kidneys) were harvested. Organs were immobilized in TissueTek™ and immediately stored at -20° Celsius. 5 µm fine sections were cut using a cryotom. Slices were fixed with paraformaldehyde (4%), stained with DAPI and results were documented using a Zeiss Axiovert 200 Fluorescence Microscope, a Zeiss Laser Scanning Microscope LSM510 and a Meta Axio Cam.

2.2.4 TUNEL Stain and Fluorescence Microscopy of anti Ran Induced Apoptosis *in Vivo*

24 h after Ran-siRNA containing polyplexes were injected intravenously via tail vein mice were sacrificed and tumors were harvested. For determination of apoptosis the ApopTag® Fluorescein kit from Qbiogene (Heidelberg, Germany) was used according to the manufacturers' protocol. Briefly, organs were embedded in paraformaldehyde (4%), thereafter in paraffin and 5 µm fine sections were cut using a rotary microtome. Afterwards sections were deparaffinized and treated with 5 mg/mL proteinase K for 15 min at room temperature and inactivated endogenous peroxidase with 3 % H_2O_2. Sections were then incubated with TdT enzyme and biotin-labeled and –unlabeled deoxynucleotides at room temperature for 30 min in the dark. Nuclei were counterstained with 4', 6-Diamidino-2-phenylindol (DAPI). Results were documented using a Zeiss Axiovert 200 Fluorescence Microscope, a Zeiss Laser Scanning Microscope LSM510 Meta and a Carl Zeiss AxioCam.

2.2.5 Syngeneic Intrasplenic Tumor Model for Systemic siRNA Delivery

36 A/JOlaHsd mice, 6-8 week old mice were used.

A/JOlaHsd mice were clipped on the left lateral side of the abdomen behind the costal arch one day prior to tumor cell injection. Animals were anaesthetized by inhalation of isoflurane in oxygen (2.5% (v/v)) at a flow of 1 L/min and eye lube (Bepanthene® Augen- und Nasensalbe, Bayer, Leverkusen) was applied to prevent excessive eye drying. Rimadyl® (5 mg/kg) was injected subcutaneously prior to surgery. Mice were positioned on the right lateral side. The operating area was disinfected with ethanol 70% and Braunol® and thereafter the skin was carefully raised using a curved forceps and a vertical dermal incision of 5 mm caudal to the costal arche was set. The muscle-layer and the peritoneum were raised and another vertical incision was set to open the abdominal cavity. The lower part of the spleen was partially displaced out of the abdomen and 1 x 10^6 Neuro2A-eGFPLuc cells in 50 µl PBS were slowly injected into the spleen, using a 1 ml syringe with a 27G needle. A cotton swab was gently pressed on the injection site to prevent cell reflux and bleeding and the spleen was placed back into the abdomen. The peritoneum, muscle

layer and skin were sutured using Monosyn® 5/0. Mice were separately housed in heated cages until they fully recovered from anesthesia. Up to three days after surgery mice received 5 mg/kg Rimadyl® every 24 hours. Bodyweight was also determined every day up to three days after surgery for monitoring the general condition. Body condition of the mice was scored every second day and mice were sacrificed at a score of five.

Score System for survival experiment (N2A)

Parameter	Score 0	Score 1	Score 2	Score 3	day 0	day 1	day 2	day 3	day 4	day 5	day 6	day 7	day 8	day 9	day 10	day 11
Appearance	normal: bright eyes, well groomed hair coat	abnormal unkempt hair coat, dull fur	abnormal hunching, piloerection													
Natural behavior	normal: active, interactive in environment	slight decrease in activity, less interactive	abnormal pronounced decrease in activity, less interactive	abnormal possible selfmutilation, hyperactive or immobile												
Provoked behavior	normal: quickly moves away	slow to move away or exaggerated response	abnormal moves away after short period of time	abnormal does not move or react with excessively exaggerated response												
body condition score	normal		thin	emaciated												
body weight																
Total score																

Figure 6: Body condition scoring system.

For bioluminescence imaging mice were anaesthetized by inhalation of isoflurane in oxygen (2.5% (v/v)) at a flow of 1 L/min. Bepanthene® eye lube was applied to prevent excessive eye drying. Thereafter 100 µL luciferin solution (c = 60 mg/mL) was injected intraperitoneally and allowed to distribute 15 minutes prior to bioluminescent measurement. Bioluminescent signal was measured every second day by a cooled-charge-coupled device (CCD) camera (Ivis 100, Caliper Life Sciences, Hopkinton, MA, USA) from day 4. Animals were separated into three groups (n = 6) and injected intravenously *via* tail vein with conjugates containing 50 µg of EG5 siRNA, control-siRNA (N/P 16) in 250 µL of HBG solution per 20 g of body weight or 250 µL of HBG every second day. Results were analyzed using Living Image 3.0 software and statistical analysis was performed with Graph Pad Prism™ to compare siEG5, control-siRNA and HBG treated animals.

Figure 7: Intrasplenic injection of A/JOlaHsd mouse with 1 x 10^6 Neuro2A-eGFPLuc cells in 50 µl PBS.

2.2.6 Syngeneic Subcutaneous Tumor Model for Systemic and Intratumoral siRNA Delivery

36 A/JOlaHsd mice, female, 6-8 weeks old were used.

Neuro2A-eGFPLuc cells were grown in cell culture as described above, despite being diluted in 150 µl PBS. The injection site of the mice was clipped one day prior to tumor cell injection, using an Aesculap cordless animal clipper, a 1 ml syringe and a 25G needle was used to inoculate subcutaneously 1 × 10^6 Neuro2A-eGFPLuc cells in 150 µL of PBS into the left flank. Bioluminescent imaging was performed as described above on day 3, 6, 9 and 12. Animals were separated into 6 groups (n = 3) on day 3. Three groups were injected intravenously *via* tail vein with conjugates containing 50 µg of EG5 siRNA, control-siRNA (N/P 12) in 250 µL of HBG solution per 20 g of body weight or 250 µL of HBG on day 3, 6, 9 and 12. The other three groups were injected intratumorally with conjugates containing 50 µg of EG5 siRNA,

control-siRNA (N/P 12) in 50 µL of HBG solution per 20 g of body weight or 50 µL of HBG on day 3, 6, 9 and 12. For the intratumoral injection, mice were anaesthetized by inhalation of isoflurane in oxygen (2.5% (v/v)) at a flow of 1 L/min in a humidified chamber and eye lube (Bepanthene® Augen- und Nasensalbe, Bayer, Leverkusen) was applied to prevent excessive eye drying. Thereafter, the skin of the left flank was gently lifted using a sterile curved forceps and treatment was applied with a 1 ml syringe and a 27G needle. Tumor size was measured by a digital caliper every second day and determined as $a*(b^2)/2$ (a = length, b = width) until tumors reached a critical size. Afterwards size was determined every day. Mice were euthanized when first tumors reached a size of 1500 mm^3 at day 14. Tumor weight was determined after tumors were explanted.

Results were analyzed using Living Image 3.0 software and statistical analysis was performed with Graph Pad Prism™ to compare siEG5, control-siRNA and HBG treated animals as well as intravenous and intratumoral treatment.

2.2.7 Detection of CD45 Positive Cells in Neuro2A Murine Neuroblastoma Cell Tumors by Immunohistochemical Staining

To detect siRNA CD45 positive cells in Neuro2A tumors, they were explanted, immobilized in TissueTek™ and immediately stored at -20° Celsius. 5 µm fine sections were cut using a Leica cryotom. Tumor sections were marked with a CD45 purified rat anti-mouse antibody and stained with a donkey anti-rat Alexa Flour 594 antibody, nuclei were counterstained with DAPI. Results were documented using a Zeiss Axiovert 200 Fluorescence Microscope, a Zeiss Laser Scanning Microscope LSM510 Meta and a Carl Zeiss AxioCam.

2.2.8 Subcutaneous Xenograft Tumor Model for Intratumoral siRNA Delivery

21 NMRI-*Foxn1*^{nude} mice, female, 6-8 weeks old were used.

Neuro2A-eGFPLuc cells were grown in cell culture as described above, despite being diluted in 100 µl PBS. A 1 ml syringe and a 25G needle was used to inoculate subcutaneously 5×10^6 Neuro2A-eGFPLuc cells in 100 µL of PBS into the left flank.

Bioluminescent imaging was performed as described above on day 2, 4, 7, 9 and 11. Animals were separated into 7 groups (n = 3). Mice were injected intratumorally with conjugates containing 12,5 µg, 25 µg and 50 µg of EG5 siRNA or control-siRNA complexed with oligomer **49** (N/P 12) in 50 µL of HBG solution per 20 g of body weight or 50 µL of HBG on day 2, 4, 7, 9 and 11. Body weight was also determined on every treatment day for monitoring the general condition. Tumor size was measured by a caliper every second day and determined as $a*(b^2)/2$ (a = length, b = width) until tumors reached a critical size. Afterwards, size was determined every day. Mice were sacrificed when first tumors of control groups reached a size of 1500 mm^3.

Results were analyzed using Living Image 3.0 software and statistical analysis was performed with Graph Pad Prism™ to compare siEG5, control-siRNA and HBG treated animals.

2.2.9 Subcutaneus Xenograft Tumor Model for Intratumoral siRNA Delivery to Compare anti EG5 siRNA and anti RAN siRNA

40 NMRI-*Foxn1*^{nude} mice, female, 6-8 weeks old were used.

Neuro2A-eGFPLuc cells were grown in cell culture as described above, despite being diluted in 100 µl PBS. A 1 ml syringe and a 25 G needle were used to inoculate subcutaneously 5×10^6 Neuro2A-eGFPLuc cells in 100 µL of PBS into the left flank. Bioluminescent imaging was performed as described above on day 2, 4, 7, 9, 11 and 14. Animals were separated into 4 groups (n = 10) on day 2 and mice were injected intratumorally with conjugates containing 50 µg of EG5 siRNA, Ran siRNA or control-siRNA complexed with Oligomer **49** (N/P 12) in 50 µL of HBG solution per 20 g of body weight or 50 µL of HBG on day 2, 4, 7, 9, 11 and 14. Bodyweight was also determined on every treatment day for monitoring the general condition. Tumor size was measured by a caliper every second day and determined as $a*(b^2)/2$ (a = length, b = width) until tumors reached a critical size. Afterwards size was determined every day. Mice were sacrificed when the first tumor reached a size of 1500 mm^3.

Results were analyzed using Living Image 3.0 software and statistical analysis was performed with Graph Pad Prism™ to compare siEG5, siRan, control-siRNA and HBG treated animals.

2.2.10 Subcutaneous Xenograft Tumor Model for Intratumoral siRNA Delivery to Compare Oligomer 49, 229 and 386

30 NMRI-*Foxn1*^{nude} mice, female, 6-8 weeks old were used.
Neuro2A-eGFPLuc cells were grown in cell culture as described above, despite being diluted in 100 µl PBS. A 1 ml syringe and a 25G needle was used to inoculate subcutaneously 5 × 10^6 Neuro2A-eGFPLuc cells in 100 µL of PBS into the left flank. Bioluminescent imaging was performed as described above on day 2, 4, 8, 11 and 15. Animals were separated into 6 groups (n = 5). Mice were injected intratumorally with conjugates containing 50 µg of Ran siRNA or control-siRNA complexed with oligomer **49**, **229** and **386** (N/P 12) in 50 µL of HBG solution per 20 g of body weight on day 2, 4, 8, 11 and 15. Bodyweight was also determined on every treatment day for monitoring the general condition. Tumor size was measured by a caliper every second day and determined as a*(b^2)/2 (a = length, b = width) until tumors reached a critical size. Afterwards, size was determined every day. Mice were sacrificed 24h after the last treatment.
Results were analyzed using Living Image 3.0 software and statistical analysis was performed with Graph Pad Prism™ to compare siEG5, siRan, control-siRNA and HBG treated animals.

2.2.11 Subcutaneous Xenograft Tumor Model for Intratumoral siRNA Delivery to Compare Oligomer 49, 386, 332 and 454

34 NMRI-*Foxn1*^{nude} mice, female, 6-8 weeks old were used.
Neuro2A-eGFPLuc cells were grown in cell culture as described above and were diluted in 100 µl PBS. A 1 ml syringe and a 25G needle was used to inoculate subcutaneously 5 × 10^6 Neuro2A-eGFPLuc cells in 100 µL of PBS into the left flank. Bioluminescent imaging was performed as described above on day 2, 4, 8, 11, 14 and 16. Animals were separated into 8 groups (n = 3-5). Mice were injected intratumorally with conjugates containing 50 µg of Ran siRNA or control-siRNA complexed with oligomer **49**, **386**, **332** and **454** (N/P 12) in 50 µL of HBG solution per

20 g of body weight on day 2, 4, 8, 11 and 15. Bodyweight was also determined on every treatment day for monitoring the general condition. Tumor size was measured by a caliper every second day and determined as $a*(b^2)/2$ (a = length, b = width) until tumors reached a critical size. Afterwards size was determined every day. Mice were sacrificed when one tumor of a group reached a size of 1500 mm^3.

Results were analyzed using Living Image 3.0 software and statistical analysis was performed with Graph Pad Prism™ to compare siEG5, siRan, control-siRNA and HBG treated animals.

III Results

1 Transfection Efficacy of Oligomers 49, 229, 386 and 278

All synthesized oligomers were screened on the murine neuroblastoma cellline Neuro2A, stably transfected with the eGFPLuc reporter gene, for their gene silencing efficiency. In Figure 8, the efficiency of best performing oligomers of each topology classis is shown in Neuro2A-eGFPLuc murine neuroblastoma cells.

Especially the T-shape **49**, i-shape **229** and the three-armed **386** showed high transfection efficiency and were therefore chosen for further *in vivo* screening.

All of them displayed good siRNA binding capacity, T-shape **49** and i-shape **229** revealed pH-specific lytic potential and three-armed **386** high endosomal buffering capacity (data not shown). Unfortunately, the U-shape **278** showed severe toxicity in A/JOlaHsd mice when applied systemically.

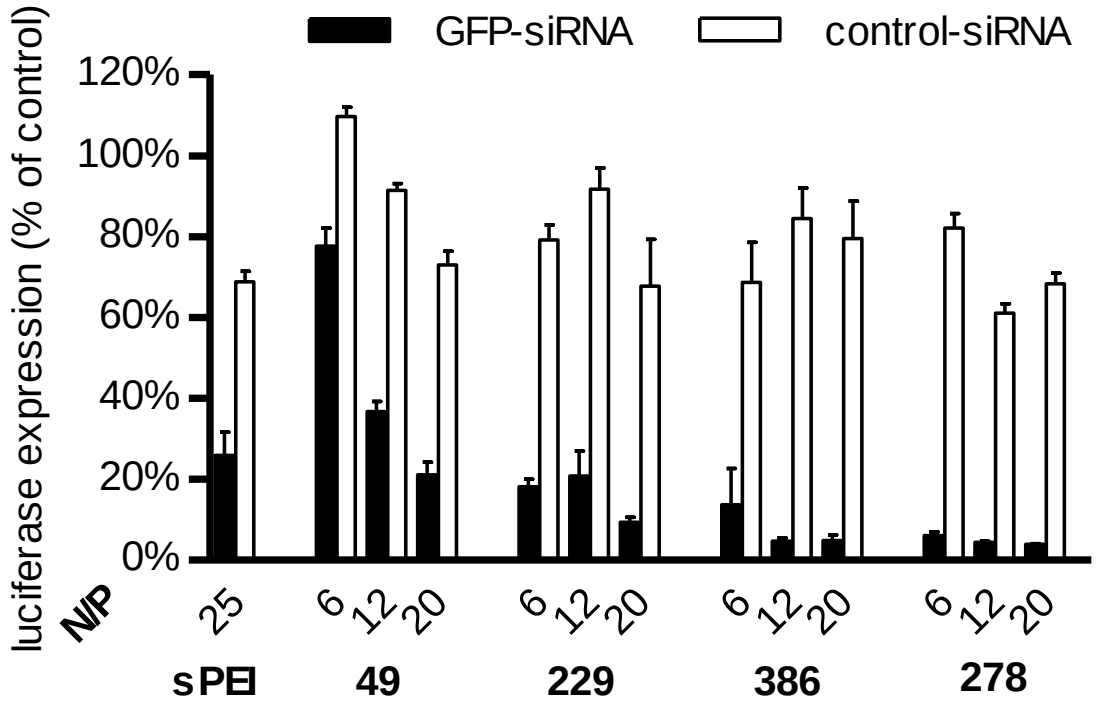

Figure 8: Gene silencing ability of selected oligomers of the four major molecular shapes in Neuro2A-eGFPLuc murine neuroblastoma cells, stably transfected with the eGFPLuc fusion protein. Positive control: succinylated PEI (sPEI).Black: GFP-siRNA, white: control-siRNA. Oligomer sequences: **49** C-Stp-Stp-K(K-OleA2)Stp-Stp-C, **229** (LinA)2K-C-Stp-Stp-Stp-C, **386** (C-Stp-Stp-Stp)2]K-Stp-Stp-Stp-C, **278** C-(LinA)2K]K-Stp-Stp-Stp-(LinA)2K]K-C. Data generated by Thomas Fröhlich, PhD thesis [LMU 2012].

2 Utilization of Mouse Models for Effective siRNA Delivery

2.1 Characterization of a Syngeneic Tumor Mouse Model for siRNA Delivery

2.1.1 Histopathological Evaluation of Cy3 labeled siRNA and anti EG5 siRNA in Subcutaneous Neuro2A Murine Neuroblastoma Cells

For the detection of successful siRNA delivery *in vivo* 1 x 10^6 Neuro2A cells were injected subcutaneously into the flank of A/JOlaHsd mice (n = 5). On day 10 after tumor cell implantation 50 µg of Cy3 fluorescently labeled siRNA was integrated into polyplexes with polymer **49**, **229** (N/P 12) and injected intravenously into the tail vein of tumor bearing mice. One hour after administration mice were sacrificed and several organs as well as the tumor were harvested, immobilized in TissueTek™, immediately stored at -20° Celsius and 5 µm fine sections were cut using a cryotom. Cell nuclei were stained with Hoechst 33342 dye. The tissue images confirmed polymer **229**, as well as polymer **49** are able to compact siRNA, protect it from degradation in the blood stream and deliver siRNA into murine tissue. The distribution of Cy3-siRNA in the kidney, lung, tumor, and liver is shown in Figure 9.

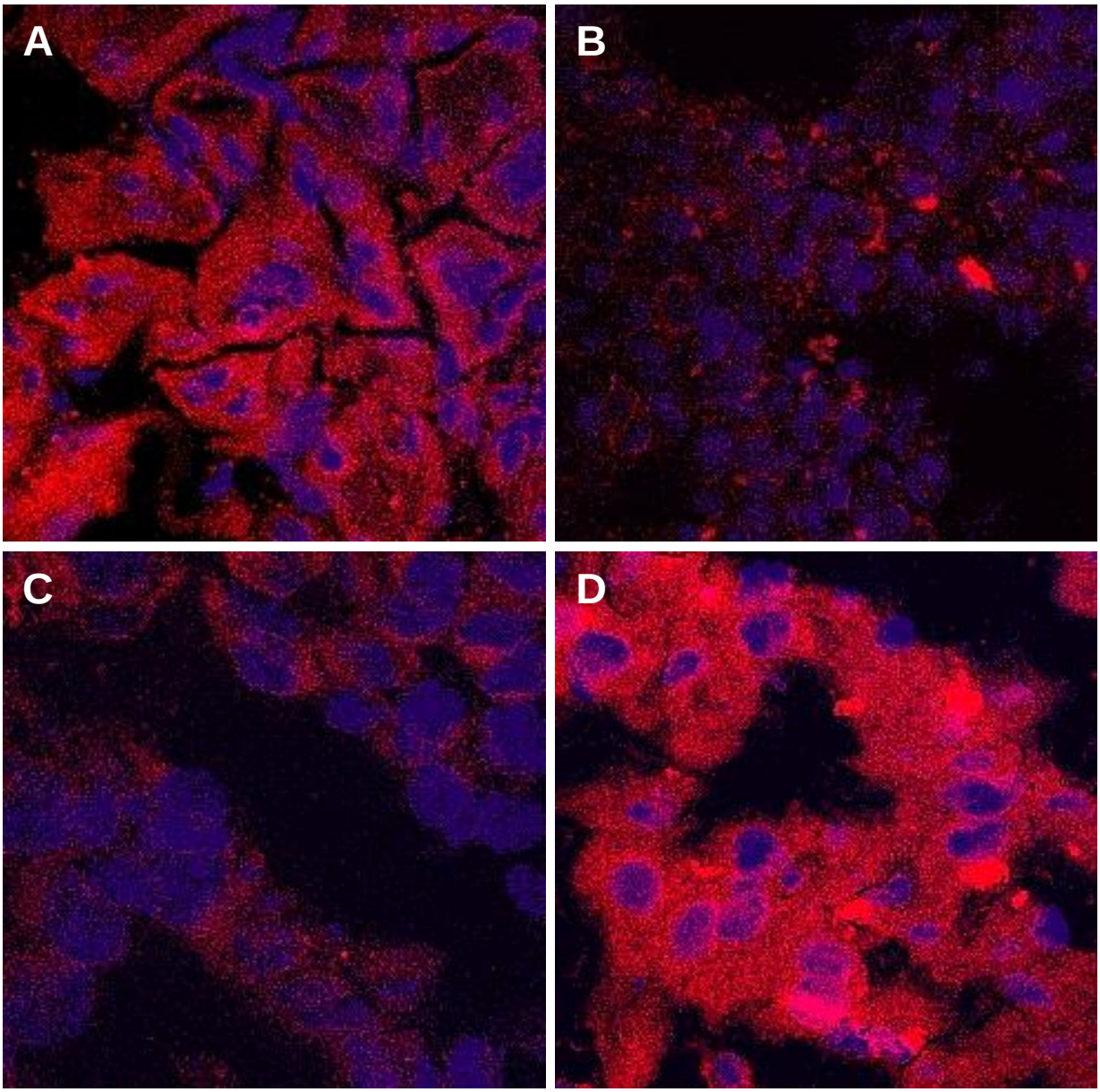

Figure 9: Representative tissue sections, illustrating siRNA distribution *in vivo* after systemic administration of polymer 49/Cy3-siRNA polyplexes (N/P 12; 50 µg siRNA per mouse) in tumor-bearing mice (5 mice per group). Blue color: Hoechst 33342 stained cell nuclei. Red color: Cy3-labeled siRNA. A) kidney, B) lung, C) tumor and D) liver**.**

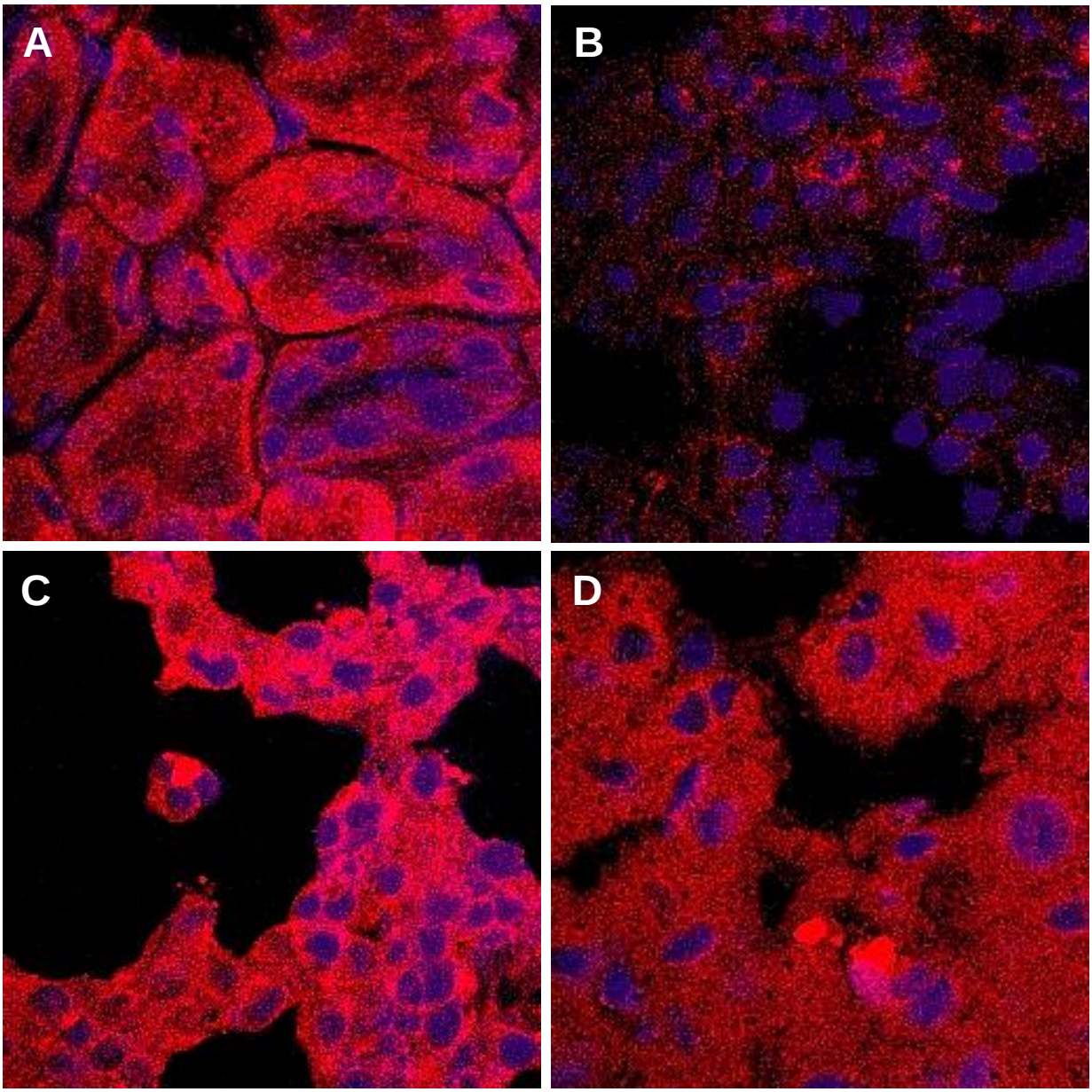

Figure 10: Representative tissue sections, illustrating siRNA distribution *in vivo* after systemic administration of polymer 229 / Cy3-siRNA polyplexes (N/P 12; 50 µg siRNA per mouse) in tumor-bearing mice (5 mice per group). Blue color: Hoechst 33342 stained cell nuclei. Red color: Cy3-labeled siRNA. A) kidney, B) lung, C) tumor and D) liver.

Polyplexes containing i-shape polymer **229** showed superior accumulation of Cy3-siRNA in tumors (Figure 9, Figure 10) over polyplexes with the t-shape polymer **49**.

To confirm that the tested polymers also mediate endosomal escape and to show target mRNA knockdown *in vivo*, the same polymers were formulated with therapeutic EG5 siRNA and administered intravenously into subcutaneous tumor bearing mice. 24 hours after polyplex injection the tumors were harvested,

immobilized in TissueTek™, immediately stored at -20° Celsius and 5 µm fine sections were cut using a cryotom. Cell nuclei were stained with DAPI and sections were examined for aster formation (Figure 11). Both polymer **49** and **229** were able to effectively knock down EG5 mRNA in Neuro2A tumors, which resulted in cell cycle arrest and in consequence in the typical aster formation. EG5 is a validated cancer target with well-characterized mechanisms mainly active in rapidly dividing cells [21]. The detection of aster formation in tumor sections is much harder than in cell culture because of the heterogeneity of tumor sections. However aster formation is a positive readout system and control-siRNA treated cells did not show any aster formation. The small amount of cells showing mitotic figures are a proof for target mRNA knockdown in tumors.

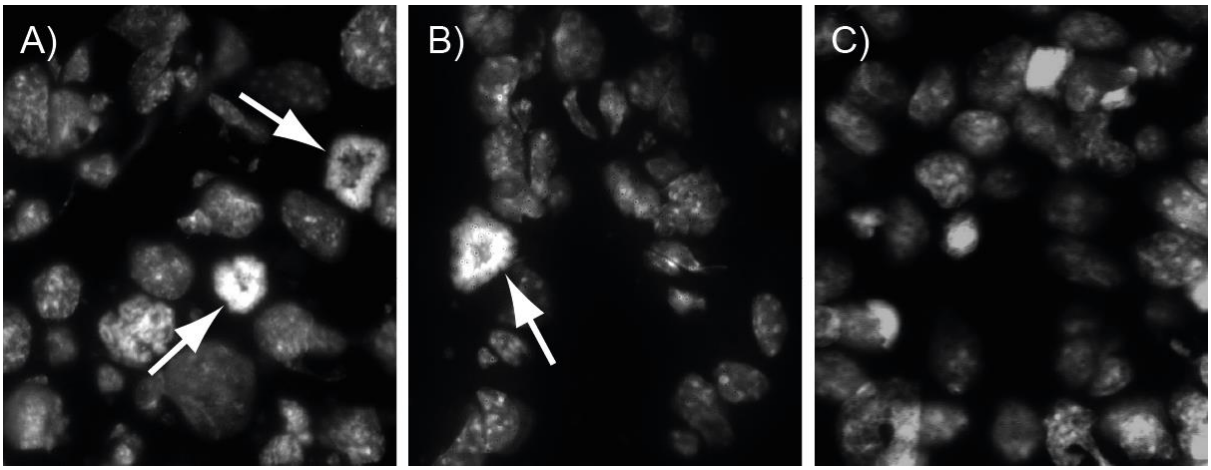

Figure 11: Representative images of *in vivo* aster formation in tumor sections of Neuro2A tumor-bearing A/JOlaHsd mice (5 mice per group), 24 hours after treatment with A) polymer **49** / EG5-siRNA polyplexes, B) polymer **229** / EG5-siRNA polyplexes (N/P 12; 50 µg siRNA per mouse), C) plain siRNA. Cell nuclei were stained with DAPI.

2.1.2 Histopathological Evaluation anti Ran siRNA *via* TUNEL Stain in Subcutaneous Neuro2A Murine Neuroblastoma Cells

For the detection of successful siRNA delivery the Ran protein was used as a second target. Hence 1 x 10^6 Neuro2A cells were injected subcutaneously into the flank of A/JOlaHsd mice (n = 3). On day 10 after tumor cell implantation 50 µg of Ran-siRNA or control-siRNA complexed with polymer **49** (N/P 12) were intratumorally injected. 24 hours after administration mice were sacrificed and livers as well as the tumor

were harvested, embedded in paraformaldehyde (4%), thereafter in paraffin and 5 µm fine sections were cut using a rotary microtome. Afterwards sections were TUNEL stained for apoptosis, cell nuclei were counterstained with DAPI. The tissue images confirmed again, that polymer **49** is able to compact siRNA, protect it from degradation and deliver siRNA into murine tumors resulting in apoptosis of tumor cells whereas liver tissue remained untreated (Figure 12).

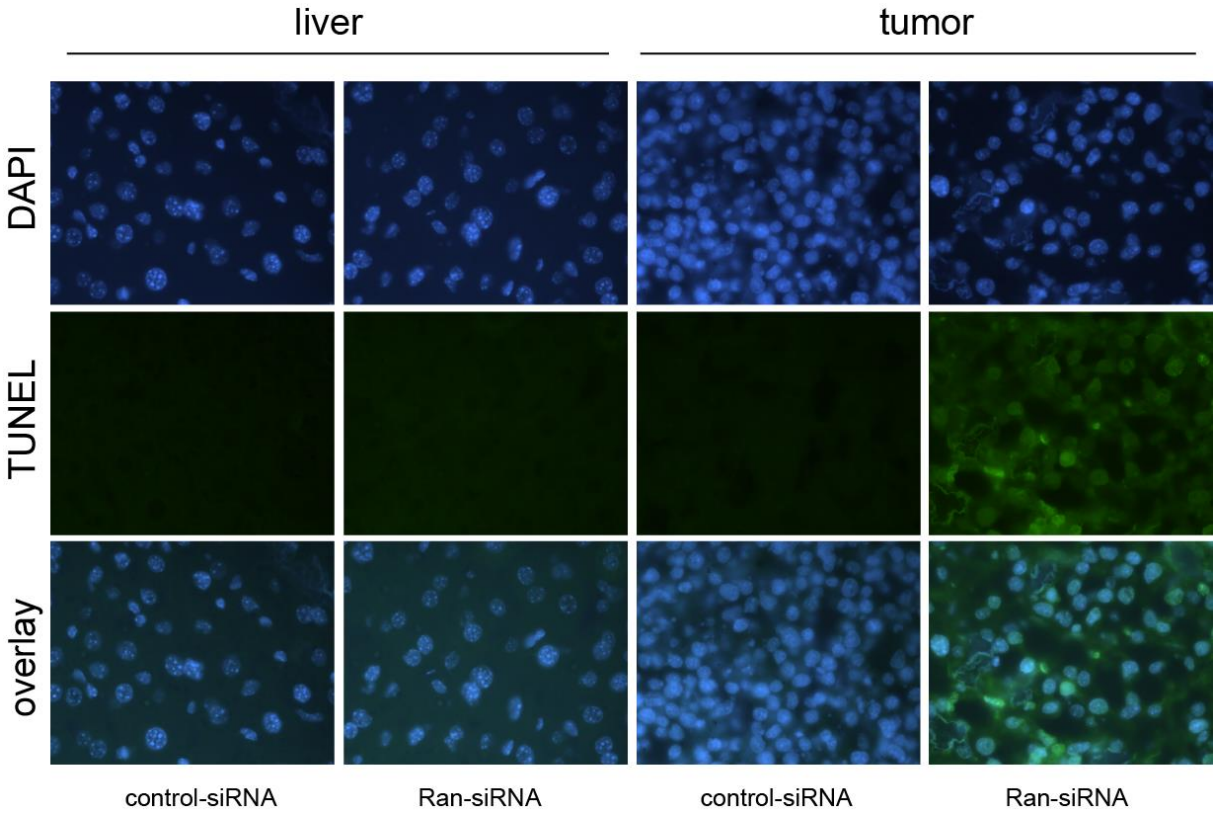

Figure 12: Representative images of *in vivo* siRNA mediated apoptosis in tumor and liver sections of Neuro2A tumor-bearing A/JOlaHsd mice (3 mice per group), 24 hours after treatment with polymer **49** / Ran-siRNA polyplexes (N/P 12; 50 µg siRNA per mouse) and polymer **49** / control-siRNA (N/P 12; 50 µg siRNA per mouse). Green color: TUNEL-positive fractions, cell nuclei were counterstained with DAPI**.**

2.1.3 Tumor Growth Inhibition of Intrasplenically Injected Neura2A-eGFPLuc Cells with anti EG5 siRNA

Efficacy of polymer **49** was further determined in a treatment experiment with EG5 siRNA. An intrasplenic injection of $1x10^6$ Neuro2A-eGFPLuc cells was performed and mice were treated by repeated intravenous application of polyplexes containing 50 µg EG5 siRNA, control-siRNA and polymer **49** (N/P 16) in 250 µl of HBG or HBG only. Successful delivery of EG5 siRNA into tumor cells results in cell cycle arrest and apoptosis of cells and should therefore slow down primary tumor progression in the spleen and metastatic spread of tumor cells with the blood circulation. As the tumor cells stably express the luciferase protein and can therefore be visualized using a bioimager, a higher bioluminescent signal indicates a larger number of tumor cells and hence a higher tumor burden. The intrasplenic tumors were treated from day 4 on after inoculation and the bioluminescent signal from the stably eGFPLuc gene expressing tumor cells was collected every second day until euthanasia. As it is not possible to measure the exact size of a non-subcutaneous tumor, a body condition scoring system was created to determine a human endpoint for the experiment. Body condition scores and body weight were determined every second day until mice reached a critical amount of scoring points, thereafter scores were determined every day and mice were sacrificed when they reached a total of 5 points. The average bioluminescent signal of each group was compared until the first mouse of the group had to be sacrificed and a slight positive effect of the polymer/siRNA formulation on tumor growth compared to the HBG group could be observed but was not significant on any time point (Figure 13). Likewise the bioluminescent signal of the EG5 siRNA treated group did not differ from the signal of the control-siRNA treated group (Figure 13).

Based on the body condition scoring system, a Kaplan-Meier survival analysis was performed. HBG treated mice lived significantly shorter than siRNA/polyplex treated animals but no significant prolonged survival could be detected within the siRNA/polyplex treated groups (Figure 14).

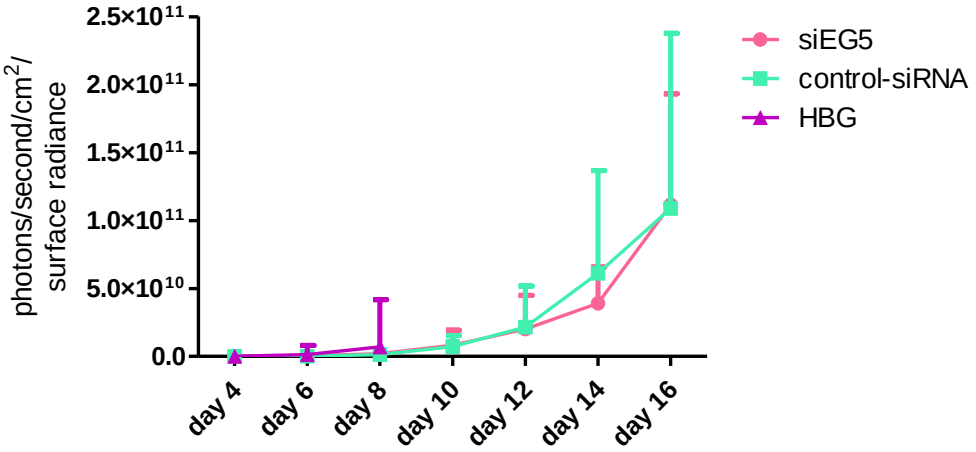

Figure 13: Tumor growth of intrasplenic Neuro2A-eGFPLuc tumors in A/JOlaHsd mice after repeated systemical treatment (6 mice per group) with polymer 49 and EG5 siRNA, control-siRNA (N/P 16) polyplexes or HBG. Tumor size was determined by imaging the bioluminescent signal of the Neuro2A-eGFPLuc cells after peritoneal injection of luciferin. Significance of the results was evaluated by t-test.

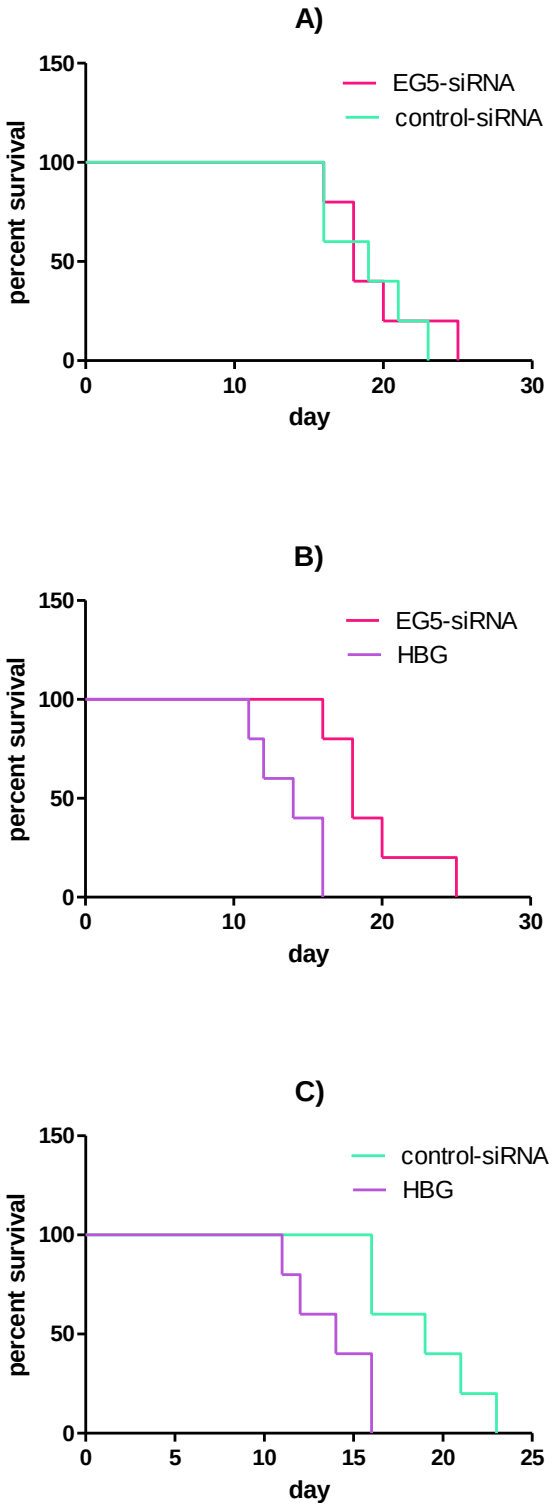

Figure 14: A – D) Kaplan Maier survival analysis of intrasplenic Neuro2A-eGFPLuc tumors in A/JOlaHsd mice after repeated systemical treatment (5 mice per group) with polymer 49 and EG5 siRNA, control-siRNA (N/P 16) polyplexes and HBG. Animals were treated with A) 50 µg EG5 or control-siRNA per mouse, B) 50 µg EG5-siRNA or 250 µl HBG per mouse or C) 50 µg control-siRNA or HBG per mouse at every second day from day 4 on. Significance of the results was evaluated by t-test.

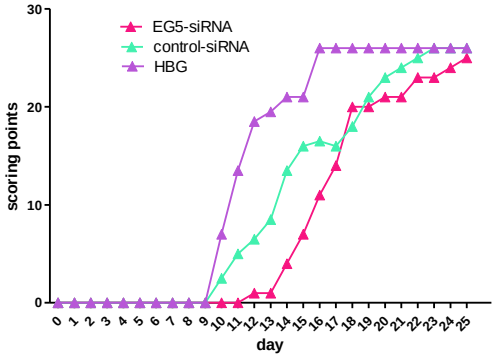

Figure 15: Body Condition Scoring of A/JOlaHsd mice bearing subcutaneous Neuro2A-eGFPLuc tumors in A/JOlaHsd mice after repeated systemical treatment (5 mice per group) with polymer 49 and EG5 siRNA, control-siRNA (N/P 16) polyplexes and HBG. Mice were euthanized when scored a five. Total scoring points per group.

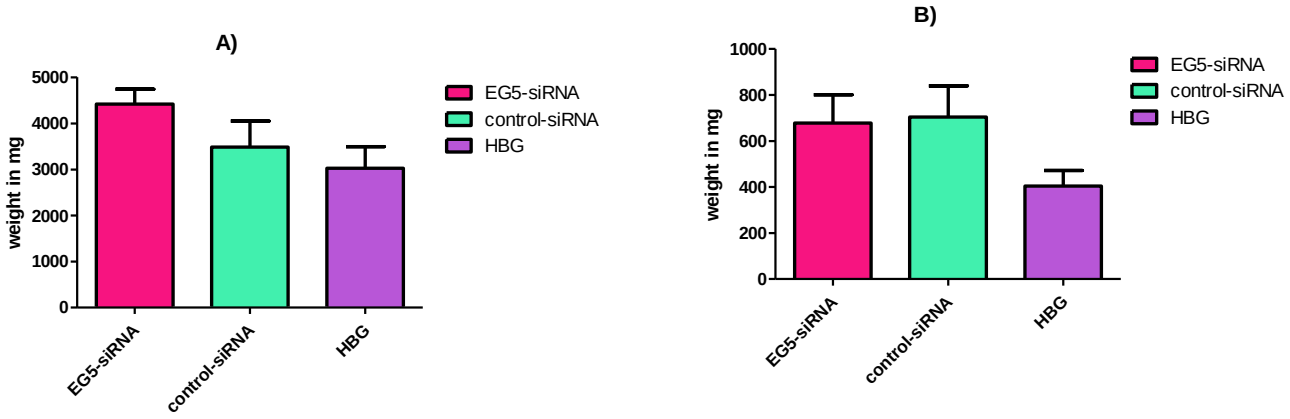

Figure 16: A) & B) Tissue weight of A/JOlaHsd mice inoculated with Neuro2A-eGFPLuc cells into the spleen and therefore metastases in the liver after repeated systemic treatment (5 mice per group) with polymer 49 and EG5 siRNA, control-siRNA (N/P 16) polyplexes or HBG. A) liver and B) spleen. Significance of the results was evaluated by t-test.

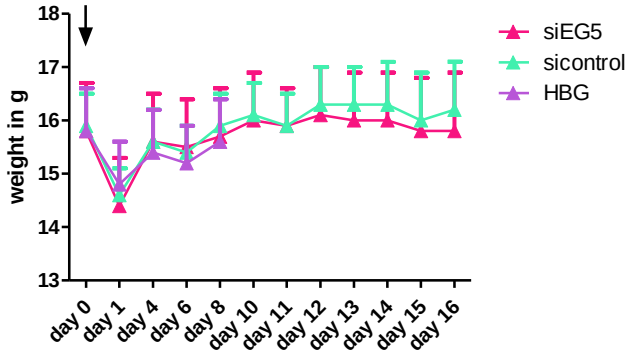

Figure 17: Body weight of A/JOlaHsd mice inoculated with subcutaneous Neuro2A-eGFPLuc tumors during repeated systemic treatment (5 mice per group) with polymer 49 and EG5 siRNA, control-siRNA (N/P 16) polyplexes or HBG. Black arrow: time point of intrasplenic tumor cell injection.

2.1.4 Tumor Growth Inhibition of Subcutaneous Neura2A-eGFPLuc Tumors with anti EG5 siRNA/Polymer 49 Formulation

In order to compare the intravenous to the intratumoral treatment with EG5 siRNA/polymer **49** formulations, an experiment with syngeneic subcutaneous tumors was set up. 36 A/JOlaHsd mice were inoculated with $1x10^6$ Neuro2A-eGFPLuc cells and divided into 6 groups on day three. The subcutaneous tumors were treated from day three on after inoculation either intravenously or intratumorally with polyplexes comprising 50 µg EG5 siRNA, control-siRNA and polymer 49 (N/P 12) in HBG or HBG two times a week. As explained in chapter 2.2.2 bioluminescent signal and digital caliper measurement was used to determine tumor burden and performed at indicated time points. Experiments were terminated when first tumors reached a size of 1500 mm^3. After euthanasia tumors were explanted and weight was determined. In the intravenously treated groups no significant difference, neither with caliper measurement, nor with bioluminescent imaging was detectable (Figure 18). Tumor weight shows a similar result (Figure 19). Body weight and behavior of mice stayed relatively constant over time indicating no excessive systemic toxicity of polymer **49** at an N/P ratio of 12 with 50 µg siRNA. Within the intratumoral experiment the siRNA formulations hampered tumor growth significantly compared to HBG treated animals that served as control, confirmed by statistical analysis of the results. Unfortunately,

no difference in tumor growth between control and EG5 siRNA treated groups could be observed (Figure 18, Figure 19).

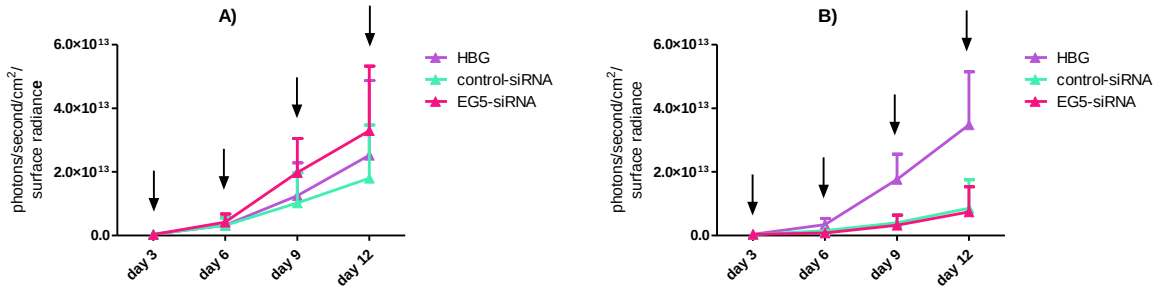

Figure 18: A) & B) Tumor growth of subcutaneous Neuro2A-eGFPLuc tumors in A/JOlaHsd mice after repeated intratumoral or intravenous treatment (6 mice per group) with polymer 49 and EG5 siRNA or control-siRNA (N/P 12) polyplexes. Animals were treated with A) 50 µg siRNA per mouse intravenously, B) 50 µg siRNA per mouse intratumorally at day 3, 6, 9 and 12 after inoculation of the tumor cells. Tumor size was determined by imaging the bioluminescent signal of the Neuro2A-eGFPLuc cells after peritoneal injection of luciferin. Significance of the results was evaluated by t-test.

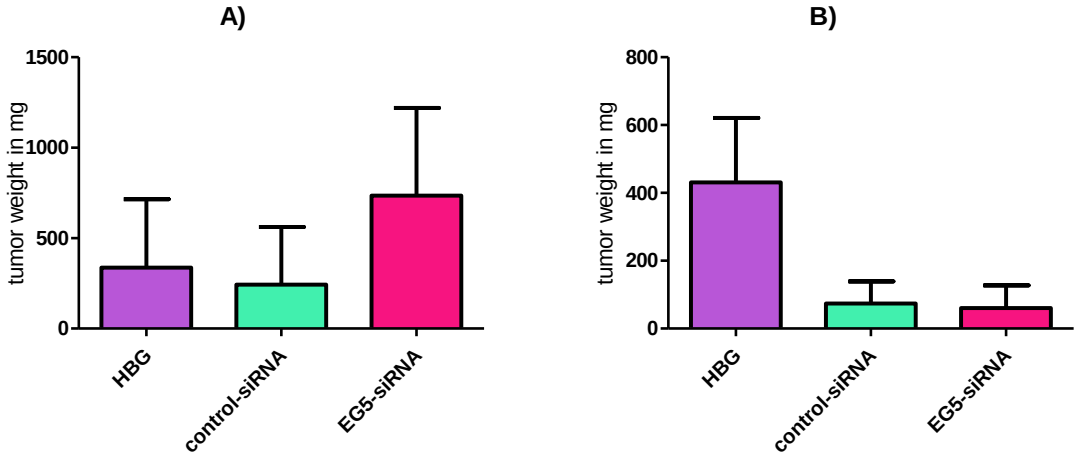

Figure 19: A) & B) Tumor weight of subcutaneous Neuro2A-eGFPLuc tumors in A/JOlaHsd mice after repeated intratumoral or intravenous treatment (6 mice per group) with polymer 49 and EG5 siRNA or control-siRNA (N/P 12) polyplexes. Animals were treated with A) 50 µg siRNA per mouse intravenously, B) 50 µg siRNA per mouse intratumorally at day 3, 6, 9 and 12 after inoculation of the tumor cells. Tumor size was determined after explantation. Significance of the results was evaluated by t-test.

2.1.4.1 Induction of Immune Response in Syngeneic Tumor Bearing Mice

As explained in chapter 2.2.3 in the intratumorally treated group a huge difference between the HBG and the siRNA/polymer treated group occurred concerning bioluminescent imaging as well as tumor weight. At the same time mice showed typical signs of inflammation as *calor*, *rubor*, *dolor* and *tumor*. Therefore, the question came up whether an activation of the mice immune system could be involved. As the experiments were performed under sterile conditions, a sterile inflammation was presumably present as there are many ways of induction [158]. Possible causing agents could be bacterial DNA that is incorporated in the Neuro2A-eGFPLuc cells and in addition expressing firefly luciferase, a foreign protein in the immunocompetent organism of a A/JOlaHsd mouse [159]. Likewise, synthetic siRNAs can sequence-dependently stimulate the immune response [160]. After explantation tumors were stained for CD45 targeting monocytes, B & T lymphocytes, granulocytes and thrombocytes. siRNA/polymer treated groups showed higher accumulation of CD45 positive cells than HBG treated ones (Figure 20).

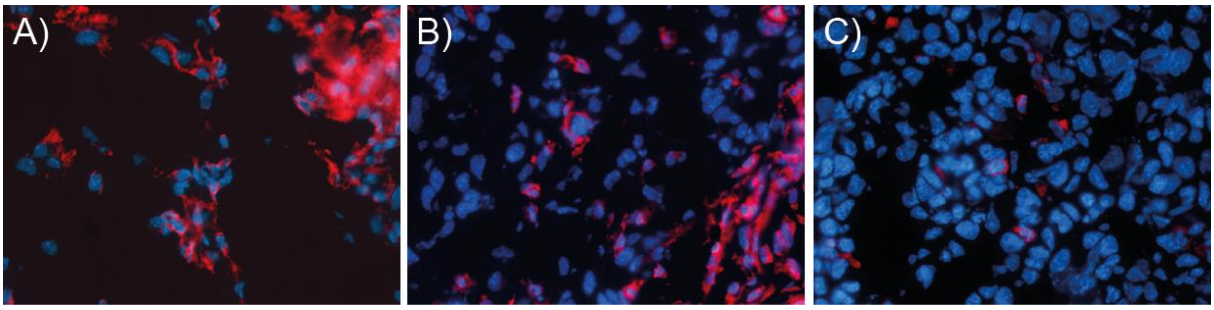

Figure 20: A-C) Representative tumor sections of subcutaneous Neuro2A-eGFPLuc tumors in A/JOlaHsd mice after repeated intratumoral treatment (6 mice per group) with polymer 49 and EG5 siRNA, control-siRNA (N/P 12) polyplexes or HBG. Animals were treated intratumorally with A) 50 µg EG5 siRNA formulated with polymer **49** per mouse, B) 50 µg control-siRNA formulated with polymer **49** per mouse at day 3, 6, 9 and 12 after inoculation of the tumor cells. Tumor sections were marked with a CD45 purified rat anti-mouse antibody and stained with a donkey anti-rat Alexa Flour 594 antibody, nuclei were counterstained with DAPI.

2.2 Characterization of a Xenograft Tumor Mouse Model for siRNA Delivery

2.2.1 Tumor Growth Inhibition of Subcutaneous Neura2A-eGFPLuc Tumors with Various Concentrations of anti EG5 siRNA

According to the findings that our treatment, in combination with luciferase expression of the Neuro2A cells, caused immune system activation in immunocompetent mice, a new mouse strain was chosen for the following experiments. The NMRI-Foxn1^{nude} mouse strain has a thymic dysgenesis and is T-cell deficient. Therefore no specific immune reaction is possible. A dose response experiment was performed by repeated intratumoral application of 12.5 µg, 25 µg or 50 µg EG5 siRNA or control-siRNA containing polyplexes in subcutaneous Neuro2A-eGFPLuc tumors. Successful delivery of EG5 siRNA results in cell cycle arrest and apoptosis of tumor cells and should therefore slow down tumor progression. The subcutaneous tumors were treated from day two on after inoculation and the bioluminescent signal from the stably eGFPLuc gene expressing tumor cells was collected at indicated time points (Figure 21). Experiments had to be terminated on day 14 and 11, respectively, because of excessive tumor growth in the control groups. With a concentration of 12.5 µg siRNA, no positive effect of the polymer/EG5 siRNA formulation on tumor growth could be observed after eleven days, whereas at 25 µg EG5 siRNA per treatment a slight regression of growth was detected over time, although with a relatively large variation within the treatment group. For 50 µg EG5 siRNA a significant decrease was measurable compared to control-siRNA treated animals, confirmed by statistical analysis of the results. Body weight stayed constant over time indicating that polymer **49** is not a high burden for the mouse organism when applied locally in utilized concentrations (Figure 22). The experiment demonstrates the ability of this new class of polymers to deliver siRNA *in vivo* and enable the siRNA to unfold its therapeutic potential.

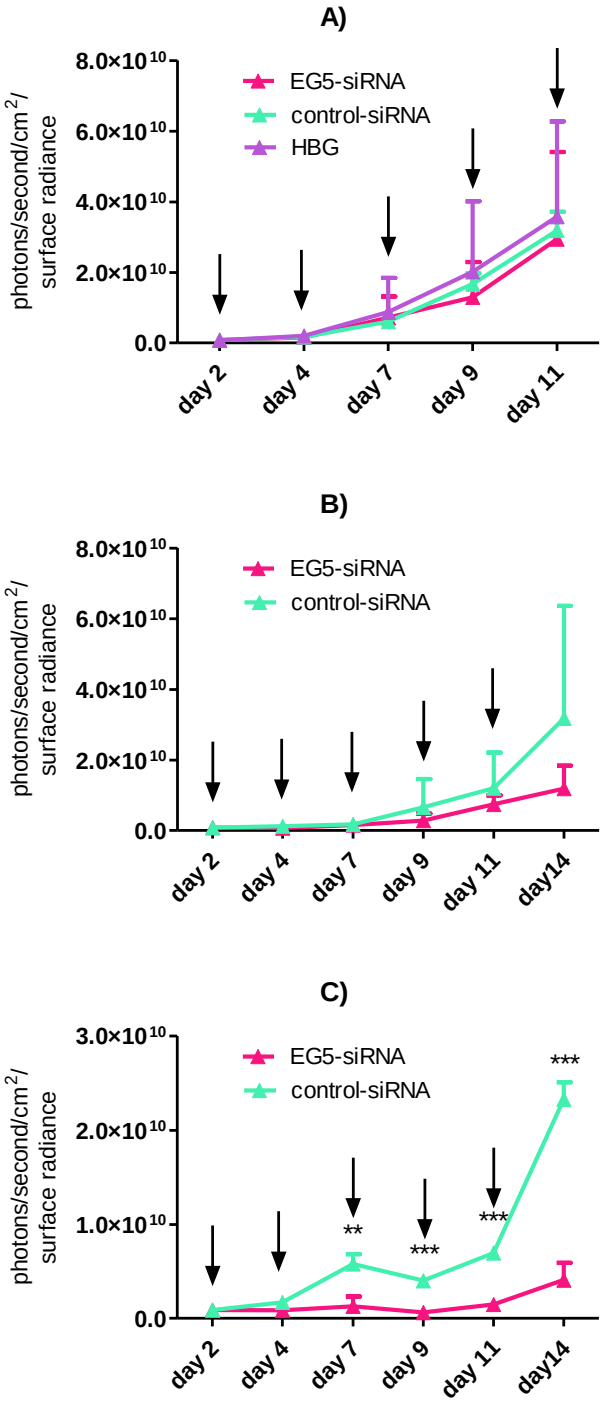

Figure 21: A – C) Tumor growth of subcutaneous Neuro2A-eGFPLuc tumors in mice after repeated intratumoral treatment (3 mice per group) with polymer 49 and EG5 siRNA or control-siRNA (N/P 12) polyplexes. Animals were treated with A) 12,5 µg siRNA per mouse, B) 25 µg siRNA per mouse, C) 50 µg siRNA per mouse at day 2, 4, 7, 9 and 11 after inoculation of the tumor cells. Tumor size was determined by imaging the bioluminescent signal of the Neuro2A-eGFPLuc cells after peritoneal injection of luciferin. The treatment group with 12.5 µg siRNA was terminated on day 11 due to excessive tumor size. Significance of the results was evaluated by t-test.

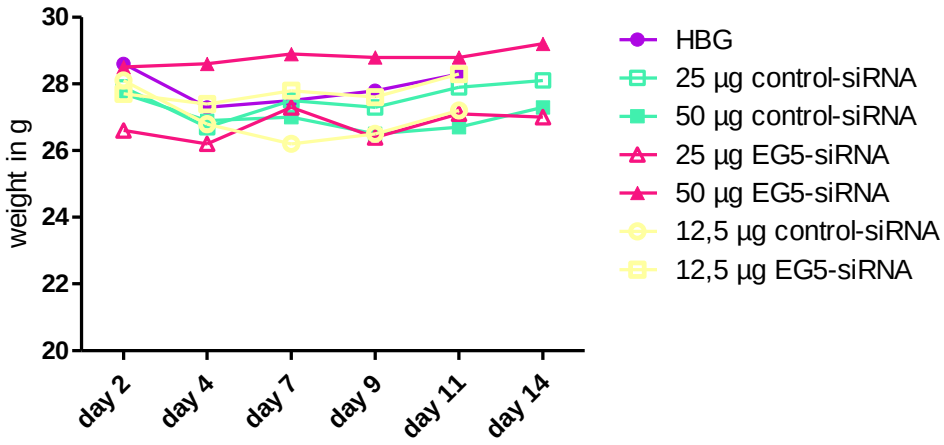

Figure 22: Body weight of NMRI-*Foxn1*^{nude} mice inoculated with subcutaneous Neuro2A-eGFPLuc tumors during repeated intratumoral treatment (3 mice per group) with polymer 49 and EG5 siRNA, control-siRNA (N/P 12) polyplexes or HBG.

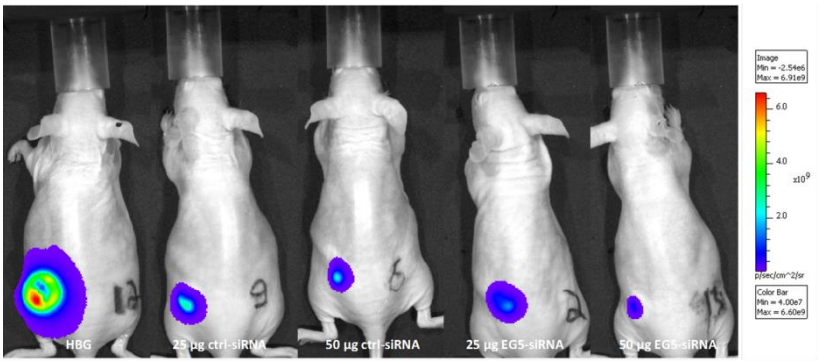

Figure 23: Representative pictures as seen by the CCD camera on day 11 after tumor cell inoculation.

2.2.2 Comparison of Tumor Growth Inhibition Efficacy of anti EG5 siRNA and anti Ran siRNA

Due to promising cell culture data (performed by Daniel Edinger; PhD Thesis LMU, in progress), Ran siRNA was chosen for an *in vivo* experiment to slow down tumor progression. As described above the Ran protein is a nuclear import protein and its downregulation leads to apoptotic cell death. Therefore we hypothesized Ran siRNA to be even more effective in hampering tumor growth than anti EG5, because no cell division is needed to kill cells. A survival experiment was performed by repeated intratumoral application of 50 µg EG5 siRNA, Ran siRNA or control-siRNA containing polyplexes formulated in HBG or only HBG in subcutaneous Neuro2A-eGFPLuc tumors. Animals were inoculated with $5x10^6$ Neuro2A-eGFPLuc cells and divided into 4 (n = 9) groups on day two.

The subcutaneous tumors were treated intratumorally from day two on after inoculation, the bioluminescent signal from the stably eGFPLuc gene expressing tumor cells and tumor size were collected as described above at indicated time points (Figure). siRNA formulation and HBG were applied 6 times. Mice were sacrificed when tumors reached a size of 1500 mm^3 and bioluminescent signal was compared until the first mouse of a group had to be euthanized. After euthanasia tumors were explanted, and weight was determined to prove that mice were sacrificed at equal time points. With a concentration of 50 µg siRNA, both in the siEG5 and in the siRan treated group a significant regression of tumor growth was detectable from day 9 on. siRan did not lead to a significant, but clearly visible tumor growth reduction compared to siEG5, therefore siRan was chosen for further *in vivo* experiments. Unfortunately control-siRNA treatment led to smaller tumors than HBG treatment, revealing a slight local unspecific toxicity of polymer **49**. The Kaplan Maier analysis, confirming the result of the bioluminescence imaging, showed that again, both siEG5 (median survival = 25d) and siRan (median survival = 28d) treated mice, lived significantly longer than control-siRNA treated ones (median survival = 20,5d). Control-siRNA treated animals did not survive significantly longer than HBG treated ones (median survival = 18d) (Figure).

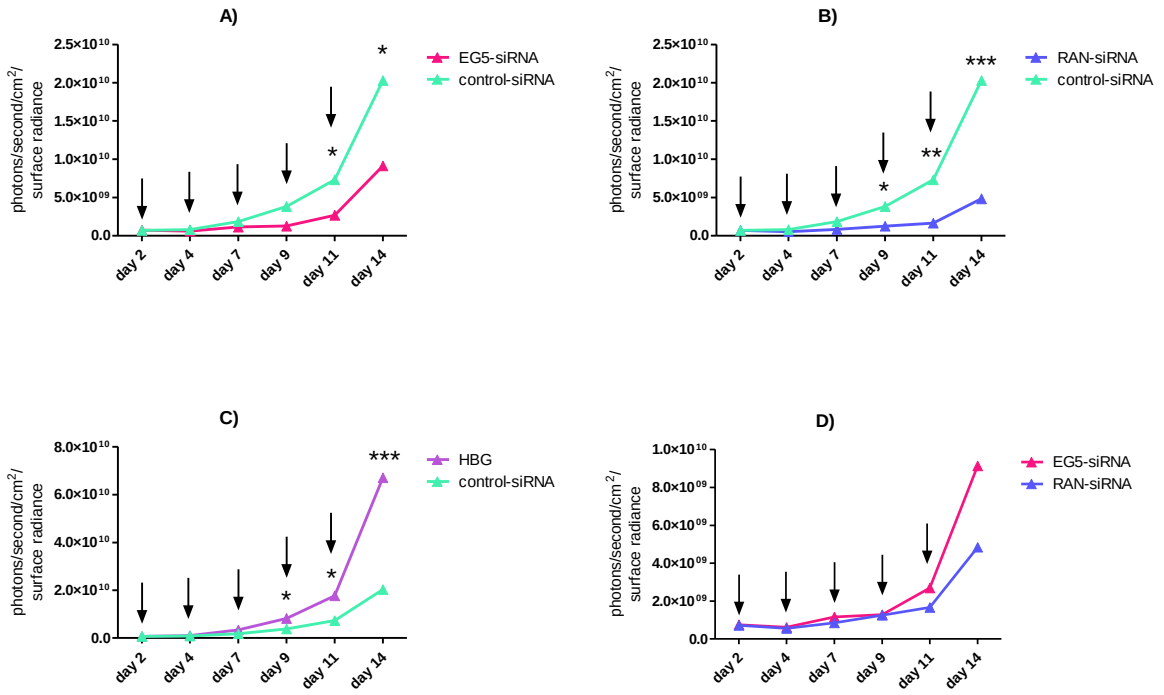

Figure 24: A – D) Tumor growth of subcutaneous Neuro2A-eGFPLuc tumors inNMRI-Foxn1nu mice after repeated intratumoral treatment (9 mice per group) with polymer 49 and EG5 siRNA, Ran siRNA, control-siRNA (N/P 12) polyplexes and HBG. Animals were treated with A) 50 µg EG5 or control-siRNA per mouse, B) 50 µg Ran or control-siRNA per mouse, C) 50 µg control-siRNA or 50µl HBG per mouse or D) 50 µg EG5 or Ran siRNA per mouse at day 2, 4, 7, 9, 11 and 14 after inoculation of the tumor cells. Tumor size was determined by imaging the bioluminescent signal of the Neuro2A-eGFPLuc cells after peritoneal injection of luciferin. Significance of the results was evaluated by t-test.

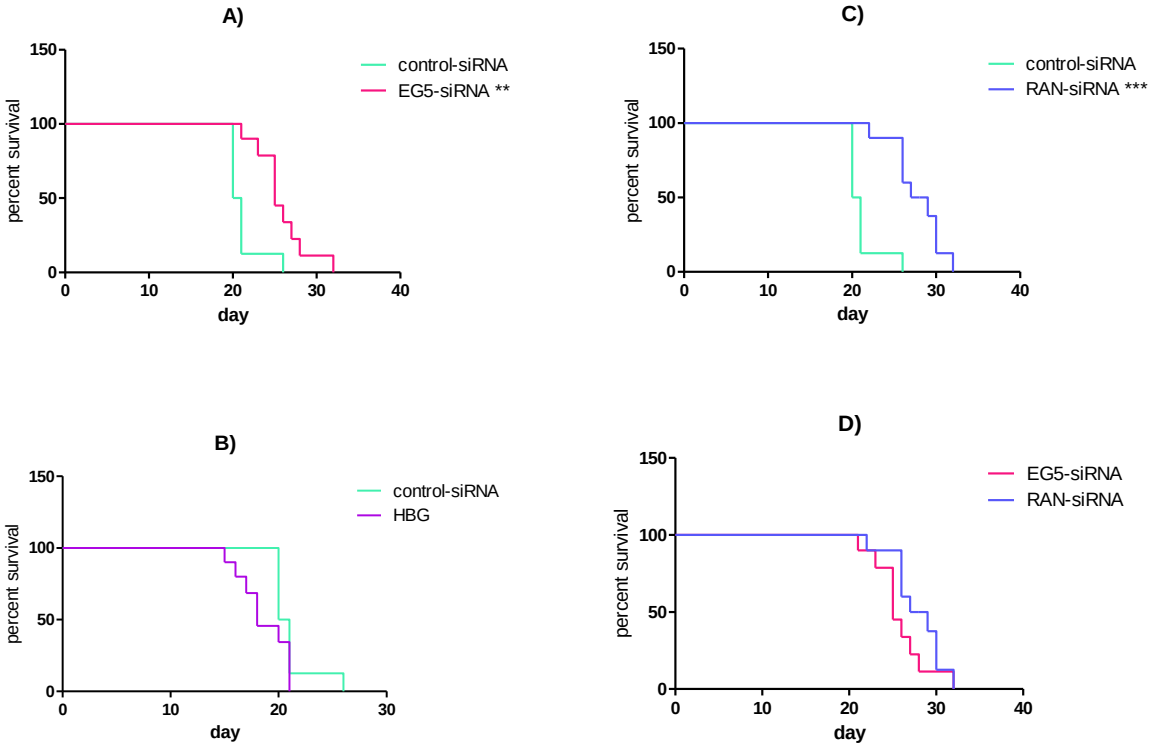

Figure 25: A – D) Kaplan Maier survival analysis of subcutaneous Neuro2A-eGFPLuc tumors inNMRI-Foxn1nu mice after repeated intratumoral treatment (9 mice per group) with polymer 49 and EG5 siRNA, Ran siRNA, control-siRNA (N/P 12) polyplexes and HBG. Animals were treated with A) 50 µg EG5 or control-siRNA per mouse, B) 50 µg Ran or control-siRNA per mouse, C) 50 µg control-siRNA or 50µl HBG per mouse or D) 50 µg EG5 or Ran siRNA per mouse at day 2, 4, 7, 9, 11 and 14 after inoculation of the tumor cells. Tumor size was determined by caliper measurement. Significance of the results was evaluated by t-test.

2.2.3 Comparison of Tumor Growth Inhibition Efficacy of anti Ran siRNA with Oligomer 49, Oligomer 229 and Oligomer 386

In the last experiment siRan was shown to be more effective in hampering tumor growth. As the aim of this thesis was to compare the *in vivo* transfection efficacy of polymers, the first *in vivo* comparison experiment was set up. Animals were subcutaneously inoculated with $5x10^6$ Neuro2A-eGFPLuc cells as described above and divided into 6 (n = 5) groups on day two.

The subcutaneous tumors were treated intratumorally from day two on after inoculation with 50 µg siRan or control-siRNA, respectively, formulated with oligomer **49**, that had been used in the prior experiments, oligomer **229**, that had been used in the siGlo trial, and oligomer **386** which had shown excellent *in vitro* knockdown efficacy. The bioluminescent signal from the stably eGFPLuc gene expressing tumor cells and tumor sizes were collected as described above at indicated time points (Figure). siRNA formulations were applied twice a week and 5 times in total. Mice were sacrificed on day 17, two days after the last treatment and bioluminescent signal was compared till day 15. After euthanasia tumors were explanted to compare their weight (Figure). With a concentration of 50 µg siRNA both, treatment twice a week and 5 applications in total no significant regression of tumor growth could be detected within a timeframe of 15 days neither in the bioluminescence imaging nor in tumor weight. Within the oligomer **49** and **386** treated groups a clearly visible tumor growth reduction could be detected, regarding siRan treated animals in contrast to control-siRNA treated ones. But in both cases a relatively high variation within the treatment group hindered a significant difference.

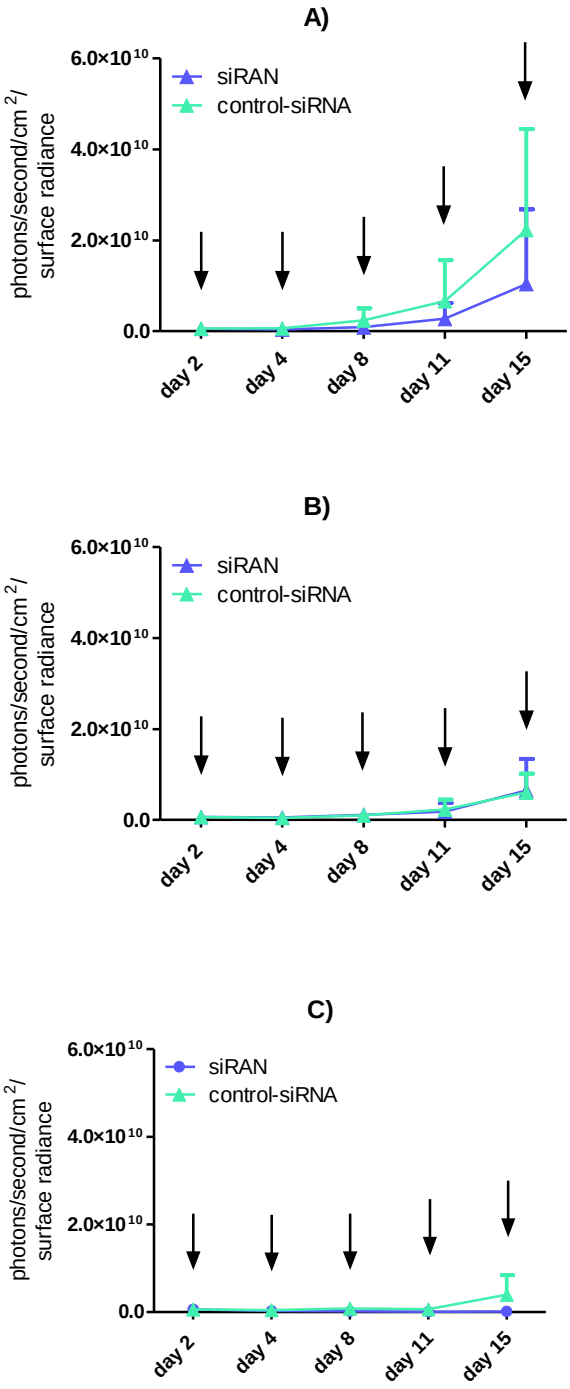

Figure 26: A – C) Tumor growth of subcutaneous Neuro2A-eGFPLuc tumors in NMRI-Foxn1nu mice after repeated intratumoral treatment (5 mice per group) with polymer 49, 229, 386 and EG5 siRNA, Ran siRNA, control-siRNA (N/P 12) polyplexes and HBG. Animals were treated with A) 50 µg Ran or control-siRNA complexed with polymer **49** per mouse, B) 50 µg Ran or control-siRNA complexed with polymer **229** per mouse, C) 50 µg Ran or control-siRNA complexed with polymer **386** per mouse at day 2, 4, 8, 11 and 15 after inoculation of the tumor cells. Tumor size was determined by imaging the bioluminescent signal of the Neuro2A-eGFPLuc cells after peritoneal injection of luciferin. Significance of the results was evaluated by t-test.

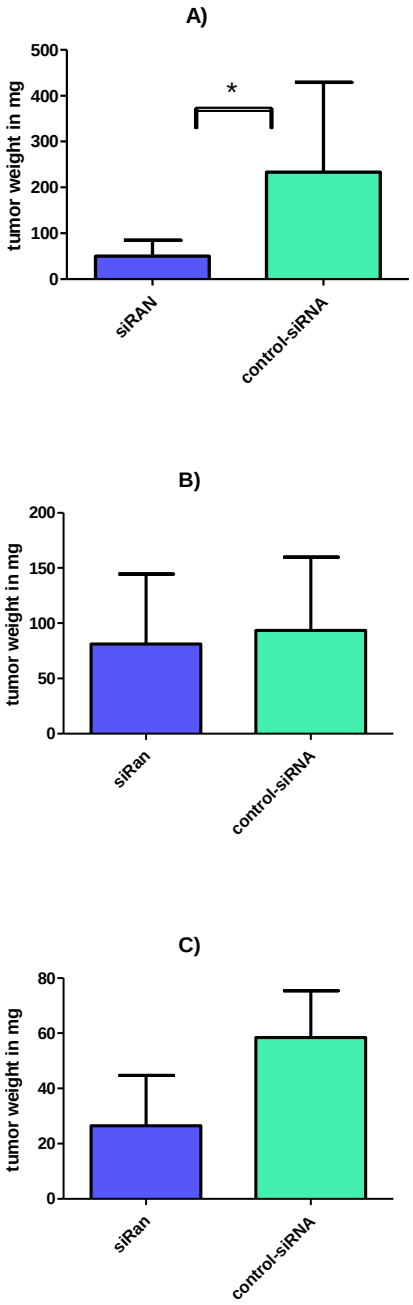

Figure 27: A – C) Tumor weight of subcutaneous Neuro2A-eGFPLuc tumors inNMRI-Foxn1nu mice after repeated intratumoral treatment (5 mice per group) with polymer 49, 229, 386 and EG5 siRNA, Ran siRNA, control-siRNA (N/P 12) polyplexes and HBG. Animals were treated with A) 50 µg Ran or control-siRNA complexed with polymer **49** per mouse, B) 50 µg Ran or control-siRNA complexed with polymer **229** per mouse, C) 50 µg Ran or control-siRNA complexed with polymer **386** per mouse at day 2, 4, 8, 11 and 15 after inoculation of the tumor cells. Tumor size was determined after explantation. Significance of the results was evaluated by t-test.

2.2.3 Comparison of Tumor Growth Inhibition Efficacy of anti Ran siRNA with Oligomer **49**, **386**, **332** and **454**

In the following experiment polymer **49** to **386**, **332** and 454 were compared. Especially the last two structures showed excellent transfection efficacy and in addition prolonged serum stability. Therefore, animals were subcutaneously inoculated with $5x10^6$ Neuro2A-eGFPLuc cells as described above and divided into 8 (n = 3-5) groups on day two.

The subcutaneous tumors were treated intratumorally from day two on after inoculation with 50 µg siRan or control-siRNA, respectively, formulated with oligomer **49**, oligomer **332**, oligomer **454** and oligomer **386** which showed its therapeutic potential in the last *in vivo* experiment. Oligomer **332** and oligomer **454** had shown excellent *in vitro* knockdown efficacy as well as prolonged serum stability. The bioluminescent signal from the stably eGFPLuc gene expressing tumor cells and tumor sizes were collected as described above at indicated time points (Figure). siRNA formulations were applied twice a week and 5 times in total. Mice were sacrificed on day 16 and 18, respectively and bioluminescent signal was compared till euthanasia day. After euthanasia tumors were explanted to compare their weight (Figure). With a concentration of 50 µg siRNA both, treatment twice a week and 5 applications in total a significant regression of tumor growth could be detected in the polymer **386**/Ran siRNA treated group. The bioluminescence signal in this group was significantly lower than the control-siRNA treated groups from day 14. No significant difference was measurable within the other groups. Nevertheless, distinct but not significant hampering of tumor progression was visible in the polymer **49** and **332** treatment groups.

But in both cases a relatively high variation within the treatment group hindered a significant difference. No local or systemic toxicity was observed.

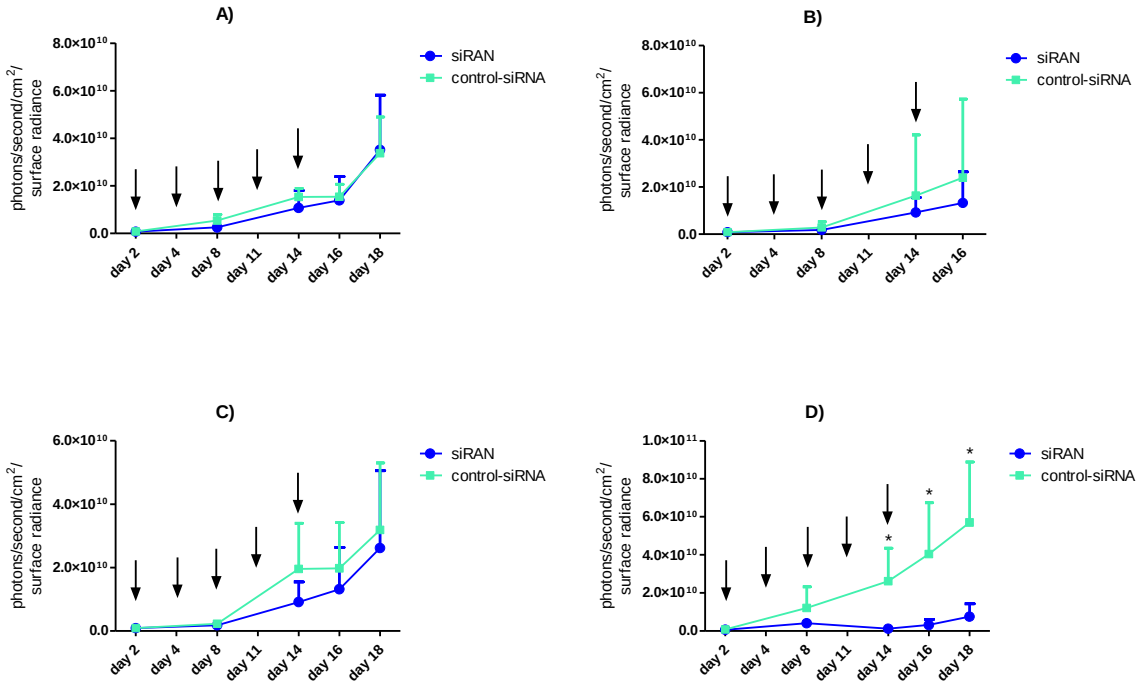

Figure 28: A – D) Tumor growth of subcutaneous Neuro2A-eGFPLuc tumors in NMRI-*Foxn1*^{nude} mice after repeated intratumoral treatment (3-5mice per group) with polymer 49, 332, 454, 386 and Ran siRNA, control-siRNA (N/P 12) polyplexes or HBG. Animals were treated with A) 50 µg Ran or control-siRNA complexed with polymer **49** per mouse, B) 50 µg Ran or control-siRNA complexed with polymer **332** per mouse, C) 50 µg Ran or control-siRNA complexed with polymer **454** per mouse D) 50 µg Ran or control-siRNA complexed with polymer **386** per mouse at day 2, 4, 8, 11 and 14 after inoculation of the tumor cells. Tumor size was determined by imaging the bioluminescent signal of the Neuro2A-eGFPLuc cells after peritoneal injection of luciferin. Significance of the results was evaluated by t-test.

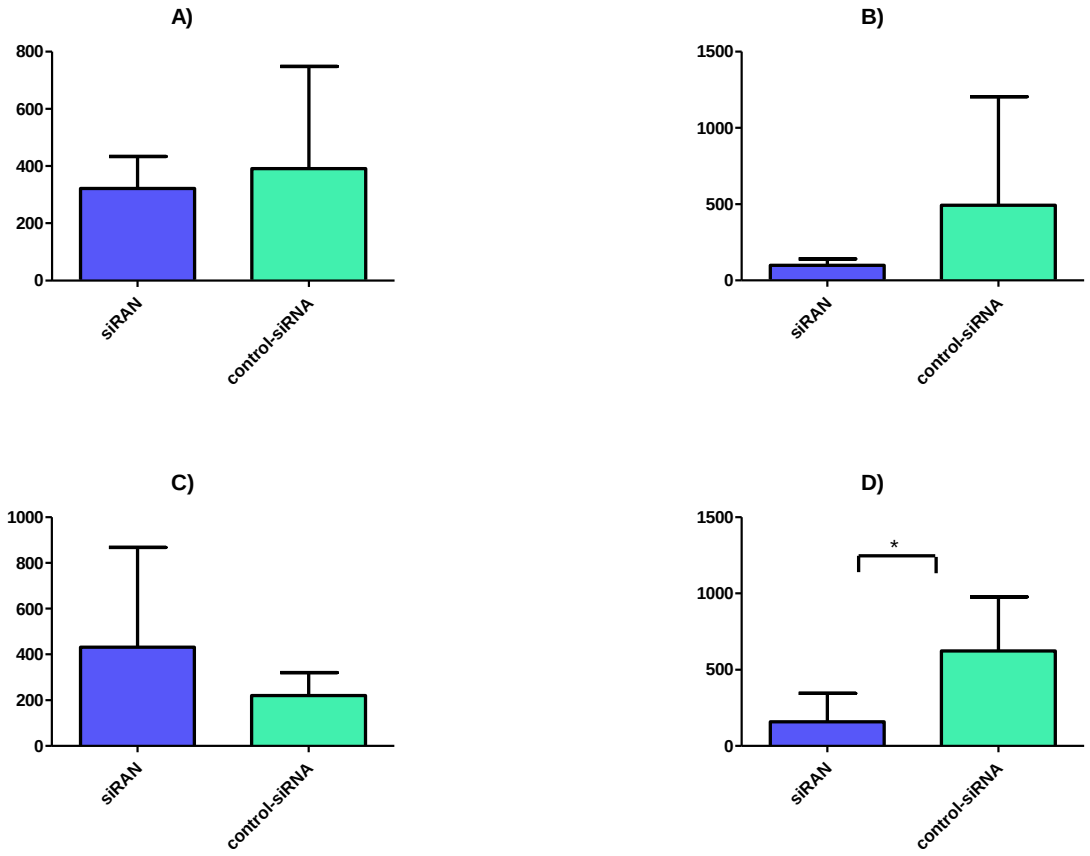

Figure 29: **A – D) Tumor weight of subcutaneous Neuro2A-eGFPLuc tumors in NMRI-*Foxn1*^{nude} mice after repeated intratumoral treatment (3-5mice per group) with polymer 49, 332, 454, 386 and Ran siRNA, control-siRNA (N/P 12) polyplexes or HBG.** Animals were treated with A) 50 µg Ran or control-siRNA complexed with polymer **49** per mouse, B) 50 µg Ran or control-siRNA complexed with polymer **332** per mouse,C) 50 µg Ran or control-siRNA complexed with polymer **454** per mouse D) 50 µg Ran or control-siRNA complexed with polymer **386** per mouse at day 2, 4, 8, 11 and 14 after inoculation of the tumor cells. Tumor size was determined after explantation. Significance of the results was evaluated by t-test.

VI Discussion

1. Choice of Mouse Strains

The most prominent advantage of using mice in the field of research is the simple and relatively cost-effectively animal husbandry, even in greater quantities and the short reproduction time. With regard to bioluminescence imaging another advantage is the relatively small body size. Moreover were Neuro2A wild type are used in our laboratory for transfection experiments and a subcutaneous tumor model in A/JOlaHsd mice had already been established as well as *in vivo* bioluminescence imaging of various cell types.

1.1 A/JOlaHsd

The A/OlaHsd mouse strain is an albino inbred strain that was generated by Dr. LC Strong in 1921, by crossing the Cold Spring Harbor and Bagg albino random bred [161]. They are therefore related to Balb/C mice. Strain A was the third most widely used strain in cancer and immunology research [162]. Their breeding performance is intermediate, whereas the litter size is about 4.9, the sterility rate around 11.5%. A/JOlaHsd mice have a low intra-strain aggression and which is beneficial when housing them in groups and later on mixing the groups because of division into treatment and control groups [161]. Iwakawa et *al* generated already in 1994 a reproducible tumor model by injection of murine neuroblastoma cells. Animals were used in treatment groups as well as in control groups.

1.2 NMRI-*Foxn1*^{nude}

Flanagan described in 1966 a spontaneous mutation resulting in nude mice which was found in the animal colony of the Virus Laboratory in the Ruchill Hospital, UK [161]. Pantelouris observed in 1968 that these mice lacked a thymus. In 1972 the institute of Animal Genetics (now Harlan Laboratories) crossed the nude gene into

the Swiss mouse NMRI, resulting in an outbred NMRI-*nude* stock [161]. NMRI-*Foxn1*^{nude} suffer, as described above, from a *Foxn1* gene mutation leading to a thymic dysgenesis and a T-cell deficiency [163], this is especially advantageous for the Neuro2A-eGFPLuc cell model that stably expresses luciferase that is measured in this work because no severe interaction with the immune system was expected. Animals were used in treatment groups as well as in control groups.

2 Utilization of Mouse Models for Detection of Effective siRNA Delivery

As in our lab a new library of biodegradable polymers for siRNA delivery was synthesized, a screening system for *in vivo* efficacy had to be developed. For this intend fluorescence labeled siRNA and bioluminescent imaging of firefly luciferase expressing tumor cells appeared to be most advantageous [128, 157, 164, 165].
In addition to the traditional negative readout system of bioluminescent imaging, a positive readout system with Cy3 labeled siRNA was evaluated. Neuro2A-eGFPLuc cells were chosen for *in vivo* studies because polymers used in this work had successfully proven their transfection capacity *in vitro* in this particular cell line [104]. Polymers were first screened for their systemic delivery efficacy *via* Cy3 labeled siRNA and analyzed histopathologically. Thereafter, therapeutic siRNA was introduced in systemic as well as local applications of polyplexes in various tumor and mouse models.

2.1 Utilization of Cy3 Labeled siRNA for Detection of Effective siRNA Delivery

The selected Neuro2A-eGFPLuc murine neuroblastoma tumor mouse model had to be specifically adapted according to the demands of siRNA delivery studies. Hence it's a positive readout system, fluorescence labeled siRNA is especially beneficial for efficacy testing. Immunocompetent AJ mice were used for all histopathologic evaluation because the siRNA/polymer formulation was only injected once and experiments were terminated 1 hour after application and therefore an activation of the immune system should not interfere with the experiment. Tissue sections revealed that both, polymer **49** and **229** accumulate, as expected due to

their fatty acids, in liver and also kidneys where they are cleared. They serendipitously accumulate just marginally in the lung, regarding side effects such as lung embolism. Polymer **229** showed a higher accumulation of Cy3-labeled siRNA in the tumor, indicating a good Neuro2A-eGFPLuc transfection capacity.

2.2 Utilization of Functional siRNA for Detection of Effective siRNA Delivery

2.2.1 Utilization of anti EG5 siRNA for Detection of Effective siRNA Delivery

In one part of the thesis the potential therapeutic effect of anti-EG5 siRNA in Neuro2A-eGFPLuc cells was studied. EG5 is a member of the Bim-C class of kinesin related proteins and influences the assembly and organization of the mitotic spindle that orchestrates chromosome segregation in dividing cells [148]. The EG5 protein plays a pivotal role in cell division. If there is no EG5 in the cytoplasm, abnormal monopolar spindles occur, hampering successful cell division [149].
We utilized a siRNA directed against the EG5 mRNA to silence protein translation. Because of its pivotal role in cell division, our hypothesis was that downregulation of the EG5 protein results in apoptosis of our targeted cells.

2.2.1.1 Histological Evaluation of Effective anti EG5 siRNA Delivery

As the previous experiment with fluorescently labeled siRNA revealed a good accumulation of siRNA in the tumor, the next step was to incorporate functional siRNA into the polyplexes. The two lead candidates of the library were formulated with therapeutic anti-EG5 siRNA, which lead to cell cycle arrest in neuroblastoma cells *in vitro*. The aim was to determine if the polymers are not only capable to transfer siRNA into target cells *in vivo* but also mediate endosomal escape and thereafter allow the siRNA to be functional inside the cells. The experimental design was similar to the previous one, polyplexes were applied systemically and mice were sacrificed 24 hours after treatment. Functional EG5 siRNA leads to mitotic figures that can be visualized by DNA staining. In this case DAPI was the stain of choice.

Luckily mitotic figures could only be detected in tumor sections of mice treated with polymer **49** and **229** and neither in control-siRNA treated tumors nor in other tissues such as liver, kidney, lung or muscle. But mitotic figures in general are far less frequently found in tumor tissue than in similarly treated cells *in vitro*. All in all histological evaluation of siRNA transfection *in vivo* is a good method to prove qualitative delivery capacity of polymers but a meaningful quantitative statement still remains difficult.

2.2.1.2 Hampering of Tumor Growth with Therapeutical anti EG5 siRNA

As systemic delivery of polyplexes with EG5 siRNA could be proven in tumor sections, the therapeutic scale was investigated in various tumor models and application methods.

First, an intrasplenic injection of $1x10^6$ Neuro2A-eGFPLuc cells was performed resulting in a solid tumor in the spleen and metastases in the liver. Tumor size was determined by bioluminescent imaging. A critical point in bioluminescent imaging is the application method of the luciferin substrate, including time point, amount and application site [166]. In the past 150 mg/kg body weight luciferin was injected, but it was also demonstrated that with this concentration it was not possible to evoke maximized bioluminescent signals [143]. Therefore 300 mg/kg body weight luciferin was used in the present studies as reported by Hildebrandt et al. [167].

According to the findings of Dr. Gelja Maiwald (vet MD thesis [LMU 2010]), luciferin was injected intraperitoneally and bioluminescence imaging was performed 15 minutes after application of the luciferin substrate. A further parameter that has an impact on the outcome of bioluminescent measurements is the position of the tissue to be evaluated and CCD camera to each other. Dr. Gelja Maiwald demonstrated in her work [LMU 2010] that slight changes in the position can alter the outcome of the measurement. Therefore tumor tissue was directly placed under the CCD-camera. A pivotal role in evaluation of tumor size by bioluminescent imaging of plays the fact that tumor progression develops differently in each individual, which over time causes increasing interindividual variances in treatment groups. Consequently, it is generally recommended to start tumor treatment as soon as possible. On the other hand successful systemic siRNA/polymer treatment relies on accessibility of tumors

via the tumor vascularization, depending on the tumor size. This hurdle is overcome by some working groups via utilization of a correction factor [168] or more simply by intratumoral injections. Another strategy of liver metastases that should be well supplied by the liver vascularization and therefore be accessible to systemic treatment, was investigated. A further point that has to be taken into account is anesthesia depth while bioluminescent measurement. During isoflurane inhalation, which is the method of choice when performing bioluminescence imaging, oxygen level in the mouse body decreases as well as the body temperature. These factors can have an influence on the distribution of reporter molecules [169]. Hence a standardized way of animal preparation and bioluminescence imaging was utilized to limit the effects from these factors. As described above mice were anaesthetized by inhalation of isoflurane in oxygen (2.5% (v/v)) at a flow of 1 L/min, thenceforth 100 µL luciferin solution (c = 60 mg/mL PBS ≙ 300 mg/kg body weight luciferin) were injected intraperitoneally and allowed to distribute for 15 minutes prior to bioluminescence measurement. In the beginning of this thesis the *in vivo* efficacy of polymer **49**/EG5 siRNA (50 µg siRNA; N/P 16) complexes were evaluated in contrast to polymer **49**/control-siRNA polyplexes and HBG treated animals. Therefore, $1x10^6$ Neuro2A-eGFPLuc cells were injected into the spleen of immunocompetent A/JOlaHsd mice, resulting in a solid spleen tumor with metastases in the liver. Animals were treated every second day from day 4 on. Polyplex treated animals lived longer than HBG treated ones indicating an unspecific local toxic effect and also tumor and liver blood vessels might have been blocked leading to a depletion of blood supply and hence resulting in tissue necrosis. In the following experiment $1x10^6$ Neuro2A-eGFPLuc cells were injected *subcutaneously* into immunocompetent A/JOlaHsd mice. The subcutaneous tumors were treated from day three on after inoculation whether intravenously or intratumorally with polyplexes comprising 50 µg EG5 siRNA, control-siRNA and polymer **49** (N/P 12) in HBG or HBG two times a week. In the intravenously treated groups no significant difference, neither with caliper measurement nor with bioluminescent imaging was detectable. This could have been caused by the lower N/P ratio (N/P 12 instead of N/P 16) or by interactions of the positively charged polyplexes with blood compounds and rapid clearance from the blood system. Body weight and behavior of mice stayed relatively constant over time indicating no excessive systemic toxicity of polymer **49** at an N/P ratio of 12 with 50 µg siRNA.

Within the intratumoral experiment the siRNA formulations hampered tumor growth significantly compared to HBG treated animals that served as control, confirmed by statistical analysis of the results. Unfortunately, no difference in tumor growth between control and EG5 siRNA treated groups could be observed, this might be evoked by activation of the immune system confirmed by histopathological results.

Consequently in the next study NMRI-Foxn1^{nude} mice with a thymic dysgenesis and are T-cell deficiency were used. A dose response experiment was performed by repeated therapeutic intratumoral application of 12.5 µg, 25 µg or 50 µg EG5 siRNA or control-siRNA containing polyplexes in subcutaneous Neuro2A-eGFPLuc tumors. Successful delivery of EG5 siRNA results in cell cycle arrest and apoptosis of tumor cells and should therefore slow down tumor progression. The subcutaneous tumors were treated from day two on after inoculation 3 times a week, five times in total. Experiments had to be terminated on day 11 and 14, respectively, because of excessive tumor growth in the control groups. With a concentration of 12.5 µg siRNA, no positive effect of the polymer/EG5 siRNA formulation on tumor growth could be observed after eleven days, whereas at 25 µg EG5 siRNA per treatment a slight regression of growth was detected over time, although with a relatively large variation within the treatment group. For 50 µg EG5 siRNA a significant decrease was measurable compared to control-siRNA treated animals, confirmed by statistical analysis of the results. Body weight stayed constant over time indicating that polymer **49** is not a high burden for the mouse organism when applied locally in utilized concentrations. The experiment demonstrates that 50 µg siEG5 complexed with polymer **49** (N/P 12) is necessary for significant gene silencing *in vivo* when applied 3 times a week.

In the following experiment the therapeutic effect of anti EG5 siRNA and anti Ran siRNA was compared. As described above, the Ran protein is a nuclear import protein and its downregulation leads to apoptotic cell death. Therefore we hypothesized Ran siRNA to be even more effective in hampering tumor growth than anti EG5 because no cell division is needed to kill cells. A survival experiment was performed by repeated intratumoral application of 50 µg EG5 siRNA, Ran siRNA or control-siRNA containing polyplexes formulated with polymer **49** in HBG or only HBG in subcutaneous Neuro2A-eGFPLuc tumors. The subcutaneous tumors were treated

intratumorally three times a week from day two on after inoculation, 6 times in total. After euthanasia tumors were explanted and weight was determined to prove that mice were sacrificed at equal time points. With a concentration of 50 µg siRNA both, in the siEG5 treated group a significant regression of tumor growth was detectable from day 11 on whereas in the siRan treated group, a significant regression was detectable from day 9 on, indicating a higher efficacy in killing target cells. The difference was not clearly significant, but obviously visible. Therefore siRan was chosen for further *in vivo* experiments. Unfortunately control-siRNA treatment led to smaller tumors than HBG treatment revealing a slight local toxicity of polymer **49** which was also partly visible at the injection sites. The Kaplan Maier analysis, confirming the result of the bioluminescence imaging, showed again that both siEG5 (median survival = 25d) and siRan (median survival = 28d) treated mice, lived significantly longer than control-siRNA treated ones (median survival = 20,5d). Control-siRNA treated animals did not survive significantly longer than HBG treated ones (median survival = 18d).

2.2.2 Utilization of Ran siRNA for Detection of Effective siRNA Delivery

2.2.2.1 Histological Evaluation of Effective anti Ran siRNA Delivery

As another therapeutic siRNA should be screened as tool for tumor therapy with the newly synthesized oligomers, histopathological evaluation was the first step. Tietze et al. had already shown that apoptosis can be achieved by a downregulation of Ran [88]. In our case polymer **49** of the library was formulated with therapeutic anti Ran siRNA, which lead to apoptosis in neuroblastoma cells *in vitro* (performed by Daniel Edinger; PhD Thesis, LMU, in progress). The aim was to determine if the new polymer **49** was capable to transfer anti Ran siRNA into target cells *in vivo* and allow the siRNA to be functional inside the cells. The experimental design was similar to the anti EG5 siRNA one but polyplexes were applied intratumorally and A/JOlaHsd mice were sacrificed 48 hours after treatment. Functional Ran siRNA causes cell

apoptosis that can be visualized by TUNEL staining. In this case cell nuclei were counterstained with DAPI. Fortunately, apoptotic cell were only visible in tumor sections of mice treated with polymer **49**/siRNA and neither in control-siRNA treated tumors nor in liver tissue. All in all histological evaluation of anti Ran siRNA transfection *in vivo* is a beneficial qualitative method to prove delivery capacity of polymers but as the aim of the thesis was to create a method to compare polymer transfection efficacy *in vivo* a quantitative method is obligatory.

2.2.2.2 Hampering of Tumor Growth with Therapeutical anti Ran siRNA

In the last treatment experiment siRan was shown to be more effective in hampering tumor growth than siEG5 and as the aim of this thesis was to compare the *in vivo* transfection efficacy of polymers the best performing siRNA is needed to evaluate the transfection efficacy of diverse polymers of the library. Therefore, the first *in vivo* comparison experiment was set up. Animals were subcutaneously inoculated again with $5x10^6$ Neuro2A-eGFPLuc cells as described above and divided into 6 groups on day two. The subcutaneous tumors were treated intratumorally from day two on after inoculation with 50 µg siRan or control-siRNA, respectively, formulated with oligomer **49**, that had been used in the prior experiments, oligomer **229**, that had been used in the siGlo trial, and oligomer **386** which had shown excellent *in vitro* knockdown efficacy. siRNA formulations were applied twice a week and five times in total. Mice were sacrificed on day 17, two days after the last treatment. After euthanasia tumors were explanted to compare their weight. With a concentration of 50 µg siRNA both, treatment twice a week and 5 applications in total no significant regression of tumor growth could be detected within a timeframe of 15 days neither in the bioluminescence imaging nor in tumor weight. Within the oligomer **49** treated groups a clearly visible tumor growth reduction could be detected, regarding siRan treated animals in contrast to control-siRNA treated ones. But a relatively high variation within the treatment group hindered a significant difference. A significant difference could only be detected within tumor weight. Oligomer **386** seemed to show the most prominent tumor reduction in both groups, most likely because of incorporation of TFA salt. Nevertheless a distinct difference between the control-siRNA and the siRAN treated group could be observed, demanding a repetition of the experiment.

Consequently, the experiment was repeated to explore whether oligomer **49** is capable to hinder tumor growth with two applications a week and whether oligomer **386** can also prevent tumor growth progression without TFA salt. In the meantime new polymers were synthesized and showed, apart from excellent *in vitro* knockdown efficacy, prolonged serum stability which is beneficial for an enlarged application interval. This time, oligomer **49**, **386**, **332** and **454** were investigated. Therefore animals were subcutaneously inoculated with $5x10^6$ Neuro2A-eGFPLuc cells as described above and divided into 8 groups on day two. Animals were treated intratumorally from day two on after inoculation with 50 µg siRan or control-siRNA, respectively, formulated with oligomer **49**, oligomer **332**, oligomer **454** and oligomer **386**. Ran-siRNA formulations were applied twice a week and 5 times in total. Mice were sacrificed on day 16 and 18, respectively. With a concentration of 50 µg siRNA both, treatment twice a week and 5 applications in total, a significant regression of tumor growth could be detected in the polymer **386**/Ran siRNA treated group. The bioluminescence signal in this group was significantly lower than the control-siRNA treated groups from day 14, revealing an excellent *in vivo* knockdown efficacy without TFA salt. No significant difference was measurable within the other groups. Nevertheless, distinct but not significant hampering of tumor progression was visible in the polymer **332** treatment group. But in this case a relatively high variation within the treatment group hindered significance. No significant tumor progression hampering was detected within the other groups. During the whole experiment no local or systemic toxicity was observed which allows the conclusion to be drawn that the oligomers are biocompatible as desired. Assuming that polymer **49** has shown *in vivo* efficacy several times when applied 3 times and was not effective when applied twice, 3 treatments are obligatory or polymers with higher serum stability are needed. Polymer **332** already showed a promising tendency and should be analyzed in a higher ratio. With those stable polymers as well as polymer **386** an excellent step towards tumor cell killing with intratumoral applications is achieved. Nevertheless, systemic therapeutic effects still remain a challenge but even this hurdle can be overcome by stable particles with prolonged circulation half-life, shielding (e.g. with PEG) and the incorporation of targeting ligands to enhance directed cellular uptake.

V Summary

The field of nucleic acid-based therapy holds enormous promise in the treatment of a broad range of genetic and acquired diseases by targeting their cause, at gene level. Thereby, a genetic defect can be compensated or target genes, which are either pathogenic or indispensable for cell viability, can be silenced, resulting in an indirectly mediated therapeutic effect. For achieving this goal, appropriate delivery agents are necessary for accumulation of the cargo inside target cells and polymers represent an interesting class of carriers for this purpose.

For the development of potent siRNA delivery systems different factors have to be optimized. Ideal polycations protect the nucleic acids in blood flow and transport them securely and predominantly to the target cells. They should be biocompatible and not toxic, can be degraded by the organism to nontoxic metabolites and therefore be excreted from the body. This thesis describes *in vivo* studies to find and furthermore optimize *in vivo* models in which especially siRNA is delivered by new polymers created in our laboratory. A second aim was to investigate desired effects of therapeutic siRNA as well as potential toxic effects of delivery systems following systemic and intratumoral application.

The first part describes the histopathological analysis of effective *in vivo* delivery of one labeled siRNA and afterwards of two therapeutic siRNA in subcutaneous Neuro2A murine neuroblastoma cells in A/JOlaHsd mice.

Polymer **49**, a T-shape structure and polymer **229**, an i-shape structure, were evaluated for siRNA delivery in Neuro2A murine neuroblastoma cells *in vivo*, where polymer **229** showed a slightly higher accumulation.

The first therapeutic siRNA was against the kinesin EG5, which is a member of the Bim-C class of kinesin related proteins influencing the assembly and organization of the mitotic spindle. If there is no EG5 in the cytoplasm, abnormal monopolar spindles occur, which prevent successful cell division [148]. Effective transfection was detected in the tumor sections by mitotic figures when stained with DAPI. The second siRNA used was against the Ras-related nuclear protein Ran, because it was recently identified as possible target in cancer therapy [156]. We utilized a siRNA directed against the Ran mRNA to silence protein translation. Because of its pivotal role in nuclear transport, our hypothesis was that downregulation of the Ran protein results in apoptosis of our targeted cells. Effective transfection was in this case

observed by staining of apoptotic cells by TUNEL stain. Both experiments were performed with polymer **49** and in case of EG5 also in addition with polymer **229**.

In the second part retardation of tumor growth was investigated in several tumor models. At first with intrasplenically injected Neuro2A-eGFPLuc cells in A/JOlaHsd mice, several systemic anti-EG5 siRNA/polymer **49** polyplex treatments resulted in tumor growth reduction, but no siRNA specific tumor growth reduction was detectable. The systemic vs. intravenous anti-EG5 treatment was compared in subcutaneous Neuro2A-eGFPLuc cells in A/JOlaHsd mice, but again the tumor growth reduction was not siRNA-specific.

According to the findings that our treatment, in combination with the artificial luciferase expression of the Neuro2A cells, caused immune reactions in immunocompetent mice, NMRI-*Foxn1*^{nude} mouse strain was used.

A dose response experiment was performed by repeated intratumoral application of 12.5 µg, 25 µg or 50 µg EG5 siRNA or control-siRNA containing polyplexes in NMRI-*Foxn1*^{nude} mice bearing subcutaneous Neuro2A-eGFPLuc tumors. For 50 µg EG5 siRNA a significant decrease was measurable compared to control-siRNA treated animals. Body weight stayed constant over time indicating that polymer **49** is not a high burden for the mouse organism when applied locally in utilized concentrations.

In the next part a survival experiment was performed by repeated intratumoral application of 50 µg EG5 siRNA, Ran siRNA or control-siRNA containing polyplexes formulated in HBG or only HBG in subcutaneous Neuro2A-eGFPLuc tumors to compare the growth inhibition efficacy of siRNA and siEG5. With a concentration of 50 µg siRNA both, in the siEG5 and in the siRan treated group, a significant regression of tumor growth was detectable from day 9 on. siRan did not lead to a significant, but clearly visible tumor growth reduction compared to siEG5. Therefore siRan was chosen for further *in vivo* experiments. Unfortunately control-siRNA treatment led to smaller tumors than HBG treatment revealing a slight local toxicity of polymer **49**. The Kaplan Maier analysis, confirming the result of the bioluminescence imaging, showed again that both siEG5 (median survival = 25d) and siRan (median survival = 28d) treated mice, lived significantly longer than control-siRNA treated ones (median survival = 20,5d). Control-siRNA treated animals did not survive significantly longer than HBG treated ones (median survival = 18d).

Therefore, siRAN was used in the next experiment. As the aim of the thesis was to establish an *in vivo* model to compare various polymers in their transfection capacity

in vivo, we used polymer **49**, polymer **229** and polymer **386**. Animals were subcutaneously inoculated with $5x10^6$ Neuro2A-eGFPLuc and treated with a 50 µg siRNA. With a treatment twice a week and 5 applications in total no significant regression of tumor growth could be detected within a timeframe of 15 days. Within the oligomer **49** and **386** treated groups a clearly visible tumor growth reduction could be detected, regarding siRan treated animals in contrast to control-siRNA treated ones.

In the last experiment polymer **49**, **386**, **332** and **454** were compared within the established tumor model. Especially the last two structures showed excellent transfection efficacy and in addition prolonged murine serum stability *in vitro*. siRNA formulations were applied twice a week and 5 times in total. With a concentration of 50 µg siRNA, treatment twice a week and 5 applications in total, a significant regression of tumor growth could be detected in the polymer **386**/Ran siRNA treated group from day 14. No significant difference was measurable within the other groups. Nevertheless, distinct but not significant hampering of tumor progression was visible in the polymer **332** treated group, but a relatively high variation within the treatment group hindered a significant difference. No local or systemic toxicity was observed. This work demonstrates within the newly established *in vivo* model the ability of this new class of polymers to deliver siRNA *in vivo* and enable the siRNA to unfold its therapeutic potential.

VI Zusammenfassung

Die Anwendung von therapeutischen Nukleinsäuren verspricht enorme Fortschritte in der biomedizinischen Forschung zur Behandlung von angeborenen sowie erworbenen Krankheitsbildern, indem sie an deren Ursprung, den Genen, ansetzt. Dabei können genetische Defekte kompensiert werden oder die Expression von Genbereichen, die entweder pathogen, oder unabdingbar für das Überleben von Zellen sind, gezielt herunterreguliert werden. Es müssen geeignete Träger für den Transport von Nukleinsäuren in die Zielzellen gefunden werden. Die in unserem Labor entwickelten Polymere stellen einen interessanten Ansatz dar, um dieses Ziel zu erreichen.

Für die Entwicklung von potenten siRNA-Delivery-Systemen müssen unterschiedliche Komponenten optimiert werden. Ideale Polykationen schirmen siRNAs von Blutkomponenten ab und transportieren sie sicher zu den Ziel-Zellen. Sie sollten biokompatibel und nicht toxisch sein und durch den Organismus abgebaut, somit zu nicht toxischen Metaboliten umgewandelt und damit aus dem Körper ausgeschieden werden können.

Diese Arbeit beschreibt *in vivo* Studien, für die *in vivo* Modelle etabliert und optimiert wurden, mit dem Ziel, die von unserem Labor entwickelten Polymere auf ihre siRNA Transfer Kapazität zu testen und untereinander zu vergleichen.

Ein weiteres Ziel war es, die erwünschte therapeutische Wirkung von siRNAs, sowie mögliche toxische Wirkungen von Delivery-Systemen nach intratumoraler und systemischer Applikation zu untersuchen.

Der erste Teil beschreibt die histopathologische Analyse einer erfolgreichen *in vivo* Verabreichung von markierter siRNA und zwei therapeutischen siRNAs in subkutanen Tumoren aus murinen Wildtyp-Neuroblastomzellen Neuro2A in A/JOlaHsd-Mäusen. Polymer **49**, eine T-shape Struktur und Polymer **229** ein i-shape Struktur, wurden, komplexiert mit siRNA, systemisch verabreicht und anhand von Tumorschnitten beurteilt, wobei Polymer **229** eine leicht höhere Akkumulation zeigte.

Der erste therapeutische siRNA Versuch war gegen das Kinesin Spindle Protein EG5 gerichtet. EG5 gehört zur Bim-C-Klasse der Kinesine und ist essenziel für die eukaryotische bipolare Spindelformation während der Zellteilung. Wenn kein EG5 in der Zelle vorhanden ist, bilden sich abnorme monopolare Spindeln, die die

erfolgreiche Zellteilung verhindern. Effektiver siRNA-Transfer wurde durch DAPI angefärbte, abnorme mitotische Formationen in Tumorschnitten gezeigt.

Die zweite, in dieser Arbeit verwendete siRNA, ist gegen die mRNA des Ran-Proteins gerichtet. Da es vor kurzem als möglicher Ansatzpunkt in der Krebstherapie entdeckt wurde [156], nutzten wir die Ran-siRNA um die Proteintranslation von Ran vermindern. Da Ran eine pivotale Rolle im Zellkerntransport einnimmt, war unsere Hypothese, dass eine Herunterregulierung des Ran-Proteins in Apoptose der betreffenden Zelle resultiert. In diesem Fall wurde die erfolgreiche Transfektion der Zielzellen durch TUNEL-Färbung der apoptotischen Zellen demonstriert. Beide Experimente wurden mit Polymer **49** durchgeführt, der EG5-Versuch zusätzlich mit Polymer **229**.

In dem zweiten Abschnitt der Arbeit wurden die Auswirkungen der siRNAs, komplexiert mit diversen Polymeren, auf das Tumorwachstum in verschiedenen Tumormodellen untersucht. Zu Beginn wurden Neuro2A-eGFPLuc Zellen intrasplenisch in A/JOlaHsd-Mäuse injiziert und diese mehrmals mit anti-EG5 siRNA/ Polymer **49** Polyplexen behandelt, wobei keine siRNA spezifische Reduktion des Tumorwachstums nachweisbar war. Zudem wurde systemische und intratumorale Behandlung von subkutanen Neuro2A-eGFPLuc Tumoren in A/JOlaHsd Mäusen verglichen, doch wurde auch hier kein spezifischer Effekt nachgewiesen.

Nachdem wir in Zusammenhang mit der Behandlung und den Luciferase exprimierenden Neuro2A-eGFPLuc Tumoren entzündliche immunologische Reaktionen in den immunkompetenten A/JOlaHsd-Mäuse festgestellt hatten, wurde auf NMRI-*Foxn* ^{nude} Mäuse umgestellt. Eine Dosis-Wirkungs-Studie wurde mit 12.5 µg, 25 µg, 50 µg EG5 siRNA und der jeweiligen Menge Kontroll-siRNA in subkutanen Neuro2A-eGFPLuc-Tumoren in NMRI-*Foxn1*^{nude} Mäusen durchgeführt. Bei einer Menge von 50 µg EG5 siRNA konnte ein deutlich messbarer Rückgang des Tumorwachstums gegenüber den Kontrolltieren festgestellt werden, wobei das Körpergewicht aller Tiere über die Behandlungszeit konstant blieb. Dies bezeugt, dass Polymer **49** in den eingesetzten Konzentrationen keine höhere Belastung für den Organismus darstellt.

Im nächsten Teil wurden EG5-siRNA mit Ran-siRNA, Kontroll-siRNA und HBG in einem Überlebensexperiment miteinander verglichen. Komplexiert mit Polymer **49** wurden wiederholt intratumorale Applikationen durchgeführt.

Bei einer Konzentration von 50 µg zeigte sich bei siEG5 und siRan eine signifikante Regression des Tumorwachstums ab Tag 9. siRan zeigte eine zwar nicht signifikante aber doch deutlich stärkere Wirkung als siEG5 und wurde deshalb für weitere *in vivo* Experimente verwendet. Unglücklicherweise führte die Kontroll-siRNA Behandlung zu kleineren Tumoren als die Behandlung mit HBG, was auf eine leichte lokale Toxizität von Polymer **49** schließen lässt. Die Kaplan Maier Analyse bestätigte das Ergebnis der Biolumineszenz-Auswertung indem sie zeigte, dass die mit siEG5 (mediane Überlebenszeit = 25d) und siRan (mediane Überlebenszeit = 28d) behandelten Mäuse länger überlebten als kontrollbehandelte Tiere (mediane Überlebenszeit d = 20,5), wobei diese nicht signifikant länger lebten als die mit HBG behandelten Tiere (mediane Überlebenszeit = 18d).

Deshalb wurde im darauffolgenden Experiment anti-Ran siRNA verwendet. Da es Ziel dieser Arbeit war, ein *in vivo* System zu entwickeln, in dem verschiedene Polymere auf ihre Transfektionskapazität getestet werden können, wurden Polymer **49**, **229** und **386** zum ersten Mal *in vivo* parallel eingesetzt. $5x10^6$ Neuro2A-eGFPLuc Zellen wurden subkutan in die Flanken von NMRI- Mäusen injiziert und zweimal die Woche mit 50 µg Ran-siRNA behandelt, wobei innerhalb eines Zeitrahmens von 15 Tagen zwar keine signifikante Regression des Tumorwachstums in den Behandlungsgruppen nachgewiesen werden konnte. Dennoch war in der Oligomer **49** und **386** Gruppe eine deutlich sichtbare Reduktion des Tumorwachstums bei den mit Ran-siRNA behandelten Tieren zu erkennen.

Im letzten Experiment wurden die Polymere **49**, **386**, **332** und **454** innerhalb des etablierten Tumormodells verglichen. Besonders die letzten beiden Strukturen zeigten exzellente Transfektionseffizienz *in vitro* und hohe Stabilität in murinem Serum. Die siRNA-Formulierungen wurden zweimal pro Woche und fünfmal insgesamt appliziert. Bei einer Konzentration von 50 µg siRNA (N/P 12), Behandlung zweimal pro Woche und 5 Anwendungen insgesamt, konnte eine signifikante Regression des Tumorwachstums in der mit Polymer **386**/Ran siRNA behandelten Gruppe ab Tag 14 nachgewiesen werden. Innerhalb der anderen Gruppen konnte kein signifikanter Unterschied festgestellt werden. Dennoch konnte eine deutliche Hemmung des Tumorwachstums in der mit Polymer **332** und therapeutischer siRNA behandelten Gruppe gezeigt werden, wobei leider eine große Varianz innerhalb der Behandlungsgruppe eine Signifikanz verhinderte. Im gesamten Experiment wurde weder lokale noch systemische Toxizität festgestellt, was auf die gute Verträglichkeit

der hier getesteten Vektoren hinweist. Diese Arbeit zeigt innerhalb des etablierten und optimierten *in vivo* Modells, dass diese neue Polymerriege, die in unserem Labor entwickelt wurde, fähig ist, siRNAs *in vivo* in Neuro2A Zellen in therapeutisch wirksamer Form zu transferieren.

VII Appendices

1 Abbreviations

bPEI	branched polyethylenimine
BSA	bovine serum albumine
CCD	charge-coupled device
cDNA	complementary desoxyribonucleic acid
CMV	cytomegalovirus
CT	computer tomography
DAPI	4’,6-diamidino-2-phenylindole, dihydrochloride
DNA	desoxyribonucleic acid
DOPC	dioleoylphosphatidylcholine
DOPE	dioleoylphosphatidylethanolamine
DPPC	dipalmitoylphosphatidylcholine
EGF	epidermal growth factor
eGFP	enhanced green fluorescent protein
EPO	erythropoietin
GFP	green fluorescent protein
GTP	guanosine triphosphate
HBG	HEPES buffered glucose
HBS	HEPES buffered saline
HE	hematoxylin-eosin
HEPES	2-[4-(2-Hydroxyethyl)-1-piperazinyl]ethanesulfonic acid
HSV	herpes simplex virus
min	minute
MRI	magnetic resonance imaging
mRNA	messenger ribonucleic acid
MW	mean value
Mw	molecular weight
NIR	near infrared
Nu/nu	NMRI nude
N/P	nitrogen / phosphate

NA	nucleic acid
OEI	oligoethylenimine
PCR	polymerase chain reaction
pDNA	plasmid desoxyribonucleic acid
PEG	polyethylenglycol
PEI	polyethylenimine
PET	positron emission tomography
RFP	red fluorescent protein
RISC	ribonucleic acid induced silencing complex
RLU	relative light units
RNA	ribonucleic acid
rtQPCR	real time quantitative polymerase chain reaction
SCID	severe combined immunodeficiency
SD	standard deviation
sec	second
siRNA	short interfering ribonucleic acid
shRNA	short hairpin ribonucleic acid
SPECT	single photon emission computed tomography
SV	simian virus
TNF α	tumor necrosis factor alpha
TUNEL	TdT-mediated dUTP-biotin nick end labeling
QD	quantum dot
VEGF	vascular endothelial growth factor
w	weight

2 References

1. http://www.wiley.co.uk/genmed/clinical/.
2. Rosenecker, J., S. Huth, and C. Rudolph, *Gene therapy for cystic fibrosis lung disease: current status and future perspectives.* Curr Opin Mol Ther, 2006. **8**(5): p. 439-45.
3. Scott, D.W. and J.N. Lozier, *Gene therapy for haemophilia: prospects and challenges to prevent or reverse inhibitor formation.* Br J Haematol, 2012. **156**(3): p. 295-302.
4. Blaese, R.M., et al., *T lymphocyte-directed gene therapy for ADA- SCID: initial trial results after 4 years.* Science, 1995. **270**(5235): p. 475-80.
5. Strayer, D.S., et al., *Current status of gene therapy strategies to treat HIV/AIDS.* Mol Ther, 2005. **11**(6): p. 823-42.
6. Scherer, L.J. and J.J. Rossi, *Ex vivo gene therapy for HIV-1 treatment.* Hum Mol Genet, 2011. **20**(R1): p. 19.
7. Ferraro, B., et al., *Clinical applications of DNA vaccines: current progress.* Clin Infect Dis, 2011. **53**(3): p. 296-302.
8. Kircheis, R., et al., *Tumor-targeted gene delivery of tumor necrosis factor-alpha induces tumor necrosis and tumor regression without systemic toxicity.* Cancer Gene Ther, 2002. **9**(8): p. 673-80.
9. Raty, J.K., et al., *Gene therapy: the first approved gene-based medicines, molecular mechanisms and clinical indications.* Curr Mol Pharmacol, 2008. **1**(1): p. 13-23.
10. Fire, A., et al., *Potent and specific genetic interference by double-stranded RNA in Caenorhabditis elegans.* Nature, 1998. **391**(6669): p. 806-11.
11. Elbashir, S.M., et al., *Duplexes of 21-nucleotide RNAs mediate RNA interference in cultured mammalian cells.* Nature, 2001. **411**(6836): p. 494-8.
12. Bernstein, E., et al., *Role for a bidentate ribonuclease in the initiation step of RNA interference.* Nature, 2001. **409**(6818): p. 363-6.
13. Rand, T.A., et al., *Biochemical identification of Argonaute 2 as the sole protein required for RNA-induced silencing complex activity.* Proc Natl Acad Sci U S A, 2004. **101**(40): p. 14385-9.
14. Hammond, S.M., et al., *Argonaute2, a link between genetic and biochemical analyses of RNAi.* Science, 2001. **293**(5532): p. 1146-50.
15. Wang, Y., et al., *Structure of the guide-strand-containing argonaute silencing complex.* Nature, 2008. **456**(7219): p. 209-13.
16. Reich, S.J., et al., *Small interfering RNA (siRNA) targeting VEGF effectively inhibits ocular neovascularization in a mouse model.* Mol Vis, 2003. **9**: p. 210-6.
17. Tolentino, M.J., et al., *Intravitreal injection of vascular endothelial growth factor small interfering RNA inhibits growth and leakage in a nonhuman primate, laser-induced model of choroidal neovascularization.* Retina, 2004. **24**(1): p. 132-8.
18. Isaka, Y. and E. Imai, *Electroporation-mediated gene therapy.* Expert Opin Drug Deliv, 2007. **4**(5): p. 561-71.
19. Nishitani, M., et al., *Cytokine gene therapy for cancer with naked DNA.* Mol Urol, 2000. **4**(2): p. 47-50.
20. Wolff, J.A. and V. Budker, *The mechanism of naked DNA uptake and expression.* Adv Genet, 2005. **54**: p. 3-20.

21. Hagstrom, J.E., *Plasmid-based gene delivery to target tissues in vivo: the intravascular approach.* Curr Opin Mol Ther, 2003. **5**(4): p. 338-44.
22. Mahato, R.I., et al., *In vivo disposition characteristics of plasmid DNA complexed with cationic liposomes.* J Drug Target, 1995. **3**(2): p. 149-57.
23. Kawabata, K., Y. Takakura, and M. Hashida, *The fate of plasmid DNA after intravenous injection in mice: involvement of scavenger receptors in its hepatic uptake.* Pharm Res, 1995. **12**(6): p. 825-30.
24. Houk, B.E., et al., *Pharmacokinetics of plasmid DNA in the rat.* Pharm Res, 2001. **18**(1): p. 67-74.
25. Gao, S., et al., *The effect of chemical modification and nanoparticle formulation on stability and biodistribution of siRNA in mice.* Mol Ther, 2009. **17**(7): p. 1225-33.
26. Sato, Y., et al., *Resolution of liver cirrhosis using vitamin A-coupled liposomes to deliver siRNA against a collagen-specific chaperone.* Nat Biotechnol, 2008. **26**(4): p. 431-42.
27. Zimmermann, T.S., et al., *RNAi-mediated gene silencing in non-human primates.* Nature, 2006. **441**(7089): p. 111-4.
28. Wang, X.L., et al., *Novel polymerizable surfactants with pH-sensitive amphiphilicity and cell membrane disruption for efficient siRNA delivery.* Bioconjug Chem, 2007. **18**(6): p. 2169-77.
29. Kim, H.J., et al., *Introduction of stearoyl moieties into a biocompatible cationic polyaspartamide derivative, PAsp(DET), with endosomal escaping function for enhanced siRNA-mediated gene knockdown.* J Control Release, 2010. **145**(2): p. 141-8.
30. Philipp, A., et al., *Hydrophobically modified oligoethylenimines as highly efficient transfection agents for siRNA delivery.* Bioconjug Chem, 2009. **20**(11): p. 2055-61.
31. Love, K.T., et al., *Lipid-like materials for low-dose, in vivo gene silencing.* Proc Natl Acad Sci U S A, 2010. **107**(5): p. 1864-9.
32. Soutschek, J., et al., *Therapeutic silencing of an endogenous gene by systemic administration of modified siRNAs.* Nature, 2004. **432**(7014): p. 173-8.
33. Davis, M.E., et al., *Evidence of RNAi in humans from systemically administered siRNA via targeted nanoparticles.* Nature, 2010. **464**(7291): p. 1067-70.
34. Wagner, E., *Polymers for siRNA Delivery: Inspired by Viruses to be Targeted, Dynamic, and Precise.* Acc Chem Res, 2012. **45**(7): p. 1005-13.
35. Schiffelers, R.M., et al., *Cancer siRNA therapy by tumor selective delivery with ligand-targeted sterically stabilized nanoparticle.* Nucleic Acids Res, 2004. **32**(19): p. e149.
36. Merkel, O.M., et al., *Stability of siRNA polyplexes from poly(ethylenimine) and poly(ethylenimine)-g-poly(ethylene glycol) under in vivo conditions: effects on pharmacokinetics and biodistribution measured by Fluorescence Fluctuation Spectroscopy and Single Photon Emission Computed Tomography (SPECT) imaging.* J Control Release, 2009. **138**(2): p. 148-59.
37. Varkouhi, A.K., et al., *Polyplexes based on cationic polymers with strong nucleic acid binding properties.* Eur J Pharm Sci, 2012. **45**(4): p. 459-66.
38. Khare, R., et al., *Advances and future challenges in adenoviral vector pharmacology and targeting.* Curr Gene Ther, 2011. **11**(4): p. 241-58.

39. Prill, J.M., et al., *Modifications of adenovirus hexon allow for either hepatocyte detargeting or targeting with potential evasion from Kupffer cells.* Mol Ther, 2011. **19**(1): p. 83-92.
40. Green, N.K., et al., *Retargeting polymer-coated adenovirus to the FGF receptor allows productive infection and mediates efficacy in a peritoneal model of human ovarian cancer.* J Gene Med, 2008. **10**(3): p. 280-9.
41. Merten, O.W., *State-of-the-art of the production of retroviral vectors.* J Gene Med, 2004. **6 Suppl 1**: p. S105-24.
42. McIntyre, G.J. and G.C. Fanning, *Design and cloning strategies for constructing shRNA expression vectors.* BMC Biotechnol, 2006. **6**: p. 1.
43. Nishina, K., et al., *Efficient in vivo delivery of siRNA to the liver by conjugation of alpha-tocopherol.* Mol Ther, 2008. **16**(4): p. 734-40.
44. Xu, Y., et al., *Physicochemical characterization and purification of cationic lipoplexes.* Biophys J, 1999. **77**(1): p. 341-53.
45. Pedroso de Lima, M.C., et al., *Cationic lipid-DNA complexes in gene delivery: from biophysics to biological applications.* Adv Drug Deliv Rev, 2001. **47**(2-3): p. 277-94.
46. Aleku, M., et al., *Atu027, a liposomal small interfering RNA formulation targeting protein kinase N3, inhibits cancer progression.* Cancer Res, 2008. **68**(23): p. 9788-98.
47. Santel, A., et al., *RNA interference in the mouse vascular endothelium by systemic administration of siRNA-lipoplexes for cancer therapy.* Gene Ther, 2006. **13**(18): p. 1360-70.
48. Hean, J., et al., *Inhibition of hepatitis B virus replication in vivo using lipoplexes containing altritol-modified antiviral siRNAs.* Artif DNA PNA XNA, 2010. **1**(1): p. 17-26.
49. Podesta, J.E. and K. Kostarelos, *Chapter 17 - Engineering cationic liposome siRNA complexes for in vitro and in vivo delivery.* Methods Enzymol, 2009. **464**: p. 343-54.
50. Wagner, E., et al., *Transferrin-polycation-DNA complexes: the effect of polycations on the structure of the complex and DNA delivery to cells.* Proc Natl Acad Sci U S A, 1991. **88**(10): p. 4255-9.
51. Meyer, M., et al., *Synthesis and biological evaluation of a bioresponsive and endosomolytic siRNA-polymer conjugate.* Mol Pharm, 2009. **6**(3): p. 752-62.
52. Oskuee, R.K., et al., *The impact of carboxyalkylation of branched polyethylenimine on effectiveness in small interfering RNA delivery.* J Gene Med, 2010. **12**(9): p. 729-38.
53. Navarro, G., et al., *Low generation PAMAM dendrimer and CpG free plasmids allow targeted and extended transgene expression in tumors after systemic delivery.* J Control Release, 2010. **146**(1): p. 99-105.
54. Zintchenko, A., et al., *Simple modifications of branched PEI lead to highly efficient siRNA carriers with low toxicity.* Bioconjug Chem, 2008. **19**(7): p. 1448-55.
55. Russ, V., et al., *Oligoethylenimine-grafted polypropylenimine dendrimers as degradable and biocompatible synthetic vectors for gene delivery.* J Control Release, 2008. **132**(2): p. 131-40.
56. Godbey, W.T., K.K. Wu, and A.G. Mikos, *Poly(ethylenimine) and its role in gene delivery.* J Control Release, 1999. **60**(2-3): p. 149-60.
57. Lungwitz, U., et al., *Polyethylenimine-based non-viral gene delivery systems.* Eur J Pharm Biopharm, 2005. **60**(2): p. 247-66.

58. Behr, J.P., *The Proton Sponge: a Trick to Enter Cells the Viruses Did Not Exploit.* CHIMIA International Journal for Chemistry 1997. **51**: p. 34-36.
59. Sonawane, N.D., F.C. Szoka, Jr., and A.S. Verkman, *Chloride accumulation and swelling in endosomes enhances DNA transfer by polyamine-DNA polyplexes.* J Biol Chem, 2003. **278**(45): p. 44826-31.
60. Grayson, A.C., A.M. Doody, and D. Putnam, *Biophysical and structural characterization of polyethylenimine-mediated siRNA delivery in vitro.* Pharm Res, 2006. **23**(8): p. 1868-76.
61. Urban-Klein, B., et al., *RNAi-mediated gene-targeting through systemic application of polyethylenimine (PEI)-complexed siRNA in vivo.* Gene Ther, 2005. **12**(5): p. 461-6.
62. Fischer, D., et al., *In vitro cytotoxicity testing of polycations: influence of polymer structure on cell viability and hemolysis.* Biomaterials, 2003. **24**(7): p. 1121-31.
63. Ogris, M., et al., *Novel biocompatible cationic copolymers based on polyaspartylhydrazide being potent as gene vector on tumor cells.* Pharm Res, 2007. **24**(12): p. 2213-22.
64. Ogris, M., et al., *PEGylated DNA/transferrin-PEI complexes: reduced interaction with blood components, extended circulation in blood and potential for systemic gene delivery.* Gene Ther, 1999. **6**(4): p. 595-605.
65. Brownlie, A., I.F. Uchegbu, and A.G. Schatzlein, *PEI-based vesicle-polymer hybrid gene delivery system with improved biocompatibility.* Int J Pharm, 2004. **274**(1-2): p. 41-52.
66. Plank, C., et al., *Activation of the complement system by synthetic DNA complexes: a potential barrier for intravenous gene delivery.* Hum Gene Ther, 1996. **7**(12): p. 1437-46.
67. Chollet, P., et al., *Side-effects of a systemic injection of linear polyethylenimine-DNA complexes.* J Gene Med, 2002. **4**(1): p. 84-91.
68. Ogris, M., et al., *Tumor-targeted gene therapy: strategies for the preparation of ligand-polyethylene glycol-polyethylenimine/DNA complexes.* J Control Release, 2003. **91**(1-2): p. 173-81.
69. Russ, V., et al., *Novel degradable oligoethylenimine acrylate ester-based pseudodendrimers for in vitro and in vivo gene transfer.* Gene Ther, 2008. **15**(1): p. 18-29.
70. Wagner, E., *Application of membrane-active peptides for nonviral gene delivery.* Adv Drug Deliv Rev, 1999. **38**(3): p. 279-289.
71. Wagner, E., et al., *Influenza virus hemagglutinin HA-2 N-terminal fusogenic peptides augment gene transfer by transferrin-polylysine-DNA complexes: toward a synthetic virus-like gene-transfer vehicle.* Proc Natl Acad Sci U S A, 1992. **89**(17): p. 7934-8.
72. Plank, C., et al., *The influence of endosome-disruptive peptides on gene transfer using synthetic virus-like gene transfer systems.* J Biol Chem, 1994. **269**(17): p. 12918-24.
73. Wang, S., et al., *Synthesis, purification, and tumor cell uptake of 67Ga-deferoxamine--folate, a potential radiopharmaceutical for tumor imaging.* Bioconjug Chem, 1996. **7**(1): p. 56-62.
74. Chen, C.P., et al., *Gene transfer with poly-melittin peptides.* Bioconjug Chem, 2006. **17**(4): p. 1057-62.
75. Tosteson, M.T. and D.C. Tosteson, *The sting. Melittin forms channels in lipid bilayers.* Biophys J, 1981. **36**(1): p. 109-16.

76. Ogris, M., et al., *Melittin enables efficient vesicular escape and enhanced nuclear access of nonviral gene delivery vectors.* J Biol Chem, 2001. **276**(50): p. 47550-5.
77. Boeckle, S., E. Wagner, and M. Ogris, *C- versus N-terminally linked melittin-polyethylenimine conjugates: the site of linkage strongly influences activity of DNA polyplexes.* J Gene Med, 2005. **7**(10): p. 1335-47.
78. Wyman, T.B., et al., *Design, synthesis, and characterization of a cationic peptide that binds to nucleic acids and permeabilizes bilayers.* Biochemistry, 1997. **36**(10): p. 3008-17.
79. Li, W., F. Nicol, and F.C. Szoka, Jr., *GALA: a designed synthetic pH-responsive amphipathic peptide with applications in drug and gene delivery.* Adv Drug Deliv Rev, 2004. **56**(7): p. 967-85.
80. Simoes, S., et al., *Transfection of human macrophages by lipoplexes via the combined use of transferrin and pH-sensitive peptides.* J Leukoc Biol, 1999. **65**(2): p. 270-9.
81. Sasaki, K., et al., *An artificial virus-like nano carrier system: enhanced endosomal escape of nanoparticles via synergistic action of pH-sensitive fusogenic peptide derivatives.* Anal Bioanal Chem, 2008. **391**(8): p. 2717-27.
82. Akita, H., et al., *Nanoparticles for ex vivo siRNA delivery to dendritic cells for cancer vaccines: programmed endosomal escape and dissociation.* J Control Release, 2010. **143**(3): p. 311-7.
83. Lee, S.H., S.H. Kim, and T.G. Park, *Intracellular siRNA delivery system using polyelectrolyte complex micelles prepared from VEGF siRNA-PEG conjugate and cationic fusogenic peptide.* Biochem Biophys Res Commun, 2007. **357**(2): p. 511-6.
84. Schaffert, D., et al., *Solid-phase synthesis of sequence-defined T-, i-, and U-shape polymers for pDNA and siRNA delivery.* Angew Chem Int Ed Engl, 2011. **50**(38): p. 8986-9.
85. Buyens, K., et al., *A fast and sensitive method for measuring the integrity of siRNA-carrier complexes in full human serum.* J Control Release, 2008. **126**(1): p. 67-76.
86. Ming, X., *Cellular delivery of siRNA and antisense oligonucleotides via receptor-mediated endocytosis.* Expert Opin Drug Deliv, 2011. **8**(4): p. 435-49.
87. Davis, M.E., *The first targeted delivery of siRNA in humans via a self-assembling, cyclodextrin polymer-based nanoparticle: from concept to clinic.* Mol Pharm, 2009. **6**(3): p. 659-68.
88. Tietze, N., et al., *Induction of apoptosis in murine neuroblastoma by systemic delivery of transferrin-shielded siRNA polyplexes for downregulation of Ran.* Oligonucleotides, 2008. **18**(2): p. 161-74.
89. Oba, M., et al., *Cyclic RGD peptide-conjugated polyplex micelles as a targetable gene delivery system directed to cells possessing alphavbeta3 and alphavbeta5 integrins.* Bioconjug Chem, 2007. **18**(5): p. 1415-23.
90. Shir, A., et al., *EGF receptor-targeted synthetic double-stranded RNA eliminates glioblastoma, breast cancer, and adenocarcinoma tumors in mice.* PLoS Med, 2006. **3**(1): p. e6.
91. Biswal, B.K., N.B. Debata, and R.S. Verma, *Development of a targeted siRNA delivery system using FOL-PEG-PEI conjugate.* Mol Biol Rep, 2010. **37**(6): p. 2919-26.
92. Lee, R.J., S. Wang, and P.S. Low, *Measurement of endosome pH following folate receptor-mediated endocytosis.* Biochim Biophys Acta, 1996. **1312**(3): p. 237-42.

93. Schneider, Y.J., et al., *The role of receptor-mediated endocytosis in iron metabolism.* Prog Clin Biol Res, 1982. **91**: p. 495-521.
94. Sorkin, A. and L.K. Goh, *Endocytosis and intracellular trafficking of ErbBs.* Exp Cell Res, 2009. **315**(4): p. 683-96.
95. Cressman, S., et al., - *Binding and Uptake of RGD-Containing Ligands to Cellular.* **- 15**(- 1573-3904 (Electronic)).
96. Maeda, H., *The enhanced permeability and retention (EPR) effect in tumor vasculature: the key role of tumor-selective macromolecular drug targeting.* Adv Enzyme Regul, 2001. **41**: p. 189-207.
97. Folkman, J., *Angiogenesis in cancer, vascular, rheumatoid and other disease.* Nat Med, 1995. **1**(1): p. 27-31.
98. Maeda, H., *Tumor-selective delivery of macromolecular drugs via the EPR effect: background and future prospects.* Bioconjug Chem, 2010. **21**(5): p. 797-802.
99. Makeieff, M., et al., *Positron emission tomography-computed tomography evaluation for recurrent differentiated thyroid carcinoma.* Eur Ann Otorhinolaryngol Head Neck Dis, 2012.
100. Tung, C.H., et al., *A receptor-targeted near-infrared fluorescence probe for in vivo tumor imaging.* Chembiochem, 2002. **3**(8): p. 784-6.
101. Ntziachristos, V., et al., *In vivo tomographic imaging of near-infrared fluorescent probes.* Mol Imaging, 2002. **1**(2): p. 82-8.
102. Bogdanov, A., Jr. and R. Weissleder, *The development of in vivo imaging systems to study gene expression.* Trends Biotechnol, 1998. **16**(1): p. 5-10.
103. Paula Marques Alves, M.J.T.C., *Animal Cell Technology: From Biopharmaceuticals to Gene Therapy*, ed. A.M.M. Leda R. Castilho, Elisabeth F. P. Augusto, Michael Butler2008, London: Taylor & Francis.
104. Frohlich, T., et al., *Structure-activity relationships of siRNA carriers based on sequence-defined oligo (ethane amino) amides.* J Control Release, 2012. **160**(3): p. 532-41.
105. Koo, V., P.W. Hamilton, and K. Williamson, *Non-invasive in vivo imaging in small animal research.* Cell Oncol, 2006. **28**(4): p. 127-39.
106. Bogdanov, A.A., Jr., *Merging molecular imaging and RNA interference: early experience in live animals.* J Cell Biochem, 2008. **104**(4): p. 1113-23.
107. Berger, F., et al., *Whole-body skeletal imaging in mice utilizing microPET: optimization of reproducibility and applications in animal models of bone disease.* Eur J Nucl Med Mol Imaging, 2002. **29**(9): p. 1225-36.
108. Paulus, M.J., et al., *A review of high-resolution X-ray computed tomography and other imaging modalities for small animal research.* Lab Anim (NY), 2001. **30**(3): p. 36-45.
109. Pickhardt, P.J., et al., *Microcomputed tomography colonography for polyp detection in an in vivo mouse tumor model.* Proc Natl Acad Sci U S A, 2005. **102**(9): p. 3419-22.
110. Kauppinen, R.A., *Monitoring cytotoxic tumour treatment response by diffusion magnetic resonance imaging and proton spectroscopy.* NMR Biomed, 2002. **15**(1): p. 6-17.
111. Crich, S.G., et al., *Visualization through magnetic resonance imaging of DNA internalized following "in vivo" electroporation.* Mol Imaging, 2005. **4**(1): p. 7-17.
112. Takikawa, R., *[In-vivo visualization of gene expression using magnetic resonance imaging].* Tanpakushitsu Kakusan Koso, 2007. **52**(13 Suppl): p. 1776-7.

113. Ichikawa, T., et al., *MRI of transgene expression: correlation to therapeutic gene expression.* Neoplasia, 2002. **4**(6): p. 523-30.
114. Delikatny, E.J. and H. Poptani, *MR techniques for in vivo molecular and cellular imaging.* Radiol Clin North Am, 2005. **43**(1): p. 205-20.
115. Genove, G., et al., *A new transgene reporter for in vivo magnetic resonance imaging.* Nat Med, 2005. **11**(4): p. 450-4.
116. Weber, S.M., et al., *Imaging of murine liver tumor using microCT with a hepatocyte-selective contrast agent: accuracy is dependent on adequate contrast enhancement.* J Surg Res, 2004. **119**(1): p. 41-5.
117. Massoud, T.F. and S.S. Gambhir, *Molecular imaging in living subjects: seeing fundamental biological processes in a new light.* Genes Dev, 2003. **17**(5): p. 545-80.
118. Tjuvajev, J.G., et al., *Imaging herpes virus thymidine kinase gene transfer and expression by positron emission tomography.* Cancer Res, 1998. **58**(19): p. 4333-41.
119. Tarantal, A.F., et al., *Fetal gene transfer using lentiviral vectors: in vivo detection of gene expression by microPET and optical imaging in fetal and infant monkeys.* Hum Gene Ther, 2006. **17**(12): p. 1254-61.
120. Auricchio, A., et al., *In vivo quantitative noninvasive imaging of gene transfer by single-photon emission computerized tomography.* Hum Gene Ther, 2003. **14**(3): p. 255-61.
121. Haberkorn, U., et al., *Monitoring gene therapy with cytosine deaminase: in vitro studies using tritiated-5-fluorocytosine.* J Nucl Med, 1996. **37**(1): p. 87-94.
122. Stegman, L.D., et al., *Noninvasive quantitation of cytosine deaminase transgene expression in human tumor xenografts with in vivo magnetic resonance spectroscopy.* Proc Natl Acad Sci U S A, 1999. **96**(17): p. 9821-6.
123. Buursma, A.R., et al., *The human norepinephrine transporter in combination with 11C-m-hydroxyephedrine as a reporter gene/reporter probe for PET of gene therapy.* J Nucl Med, 2005. **46**(12): p. 2068-75.
124. Dwyer, R.M., et al., *Sodium iodide symporter-mediated radioiodide imaging and therapy of ovarian tumor xenografts in mice.* Gene Ther, 2006. **13**(1): p. 60-6.
125. Miyagawa, M., et al., *Non-invasive imaging of cardiac transgene expression with PET: comparison of the human sodium/iodide symporter gene and HSV1-tk as the reporter gene.* Eur J Nucl Med Mol Imaging, 2005. **32**(9): p. 1108-14.
126. Chudakov, D.M., S. Lukyanov, and K.A. Lukyanov, *Fluorescent proteins as a toolkit for in vivo imaging.* Trends Biotechnol, 2005. **23**(12): p. 605-13.
127. Kaneko, K., et al., *Detection of peritoneal micrometastases of gastric carcinoma with green fluorescent protein and carcinoembryonic antigen promoter.* Cancer Res, 2001. **61**(14): p. 5570-4.
128. Giepmans, B.N., et al., *The fluorescent toolbox for assessing protein location and function.* Science, 2006. **312**(5771): p. 217-24.
129. Shaner, N.C., P.A. Steinbach, and R.Y. Tsien, *A guide to choosing fluorescent proteins.* Nat Methods, 2005. **2**(12): p. 905-9.
130. Ke, S., et al., *Near-infrared optical imaging of epidermal growth factor receptor in breast cancer xenografts.* Cancer Res, 2003. **63**(22): p. 7870-5.
131. Lin, Y., R. Weissleder, and C.H. Tung, *Novel near-infrared cyanine fluorochromes: synthesis, properties, and bioconjugation.* Bioconjug Chem, 2002. **13**(3): p. 605-10.
132. Contag, C.H., et al., *Photonic detection of bacterial pathogens in living hosts.* Mol Microbiol, 1995. **18**(4): p. 593-603.

133. Zhao, H., et al., *Emission spectra of bioluminescent reporters and interaction with mammalian tissue determine the sensitivity of detection in vivo.* J Biomed Opt, 2005. **10**(4): p. 41210.
134. Tannous, B.A., et al., *Codon-optimized Gaussia luciferase cDNA for mammalian gene expression in culture and in vivo.* Mol Ther, 2005. **11**(3): p. 435-43.
135. Bhaumik, S. and S.S. Gambhir, *Optical imaging of Renilla luciferase reporter gene expression in living mice.* Proc Natl Acad Sci U S A, 2002. **99**(1): p. 377-82.
136. Bhaumik, S., X.Z. Lewis, and S.S. Gambhir, *Optical imaging of Renilla luciferase, synthetic Renilla luciferase, and firefly luciferase reporter gene expression in living mice.* J Biomed Opt, 2004. **9**(3): p. 578-86.
137. Venisnik, K.M., et al., *Fusion of Gaussia luciferase to an engineered anti-carcinoembryonic antigen (CEA) antibody for in vivo optical imaging.* Mol Imaging Biol, 2007. **9**(5): p. 267-77.
138. Loening, A.M., A.M. Wu, and S.S. Gambhir, *Red-shifted Renilla reniformis luciferase variants for imaging in living subjects.* Nat Methods, 2007. **4**(8): p. 641-3.
139. Zhao, H., et al., *Characterization of coelenterazine analogs for measurements of Renilla luciferase activity in live cells and living animals.* Mol Imaging, 2004. **3**(1): p. 43-54.
140. Pichler, A., J.L. Prior, and D. Piwnica-Worms, *Imaging reversal of multidrug resistance in living mice with bioluminescence: MDR1 P-glycoprotein transports coelenterazine.* Proc Natl Acad Sci U S A, 2004. **101**(6): p. 1702-7.
141. Wood, K.V., Y.A. Lam, and W.D. McElroy, *Introduction to beetle luciferases and their applications.* J Biolumin Chemilumin, 1989. **4**(1): p. 289-301.
142. Miloud, T., C. Henrich, and G.J. Hammerling, *Quantitative comparison of click beetle and firefly luciferases for in vivo bioluminescence imaging.* J Biomed Opt, 2007. **12**(5): p. 054018.
143. Paroo, Z., et al., *Validating bioluminescence imaging as a high-throughput, quantitative modality for assessing tumor burden.* Mol Imaging, 2004. **3**(2): p. 117-24.
144. Heidel, J.D., et al., *Potent siRNA inhibitors of ribonucleotide reductase subunit RRM2 reduce cell proliferation in vitro and in vivo.* Clin Cancer Res, 2007. **13**(7): p. 2207-15.
145. Bisanz, K., et al., *Targeting ECM-integrin interaction with liposome-encapsulated small interfering RNAs inhibits the growth of human prostate cancer in a bone xenograft imaging model.* Mol Ther, 2005. **12**(4): p. 634-43.
146. Judge, A.D., et al., *Confirming the RNAi-mediated mechanism of action of siRNA-based cancer therapeutics in mice.* J Clin Invest, 2009. **119**(3): p. 661-73.
147. http://www.pdb.org.
148. Wittmann, T., A. Hyman, and A. Desai, *The spindle: a dynamic assembly of microtubules and motors.* Nat Cell Biol, 2001. **3**(1): p. E28-34.
149. Valentine, M.T., P.M. Fordyce, and S.M. Block, *Eg5 steps it up!* Cell Div, 2006. **1**: p. 31.
150. Castillo, A., et al., *Overexpression of Eg5 causes genomic instability and tumor formation in mice.* Cancer Res, 2007. **67**(21): p. 10138-47.
151. Sazer, S. and M. Dasso, *The ran decathlon: multiple roles of Ran.* J Cell Sci, 2000. **113 (Pt 7)**: p. 1111-8.

152. Gruss, O.J. and I. Vernos, *The mechanism of spindle assembly: functions of Ran and its target TPX2.* J Cell Biol, 2004. **166**(7): p. 949-55.
153. Feng, Y., et al., *Polo-like kinase 1-mediated phosphorylation of the GTP-binding protein Ran is important for bipolar spindle formation.* Biochem Biophys Res Commun, 2006. **349**(1): p. 144-52.
154. Garuti, L., M. Roberti, and G. Bottegoni, *Polo-like kinases inhibitors.* Curr Med Chem, 2012. **19**(23): p. 3937-48.
155. Abe, H., et al., *High expression of Ran GTPase is associated with local invasion and metastasis of human clear cell renal cell carcinoma.* Int J Cancer, 2008. **122**(10): p. 2391-7.
156. Xia, F., C.W. Lee, and D.C. Altieri, *Tumor cell dependence on Ran-GTP-directed mitosis.* Cancer Res, 2008. **68**(6): p. 1826-33.
157. Morgan-Lappe, S.E., et al., *Identification of Ras-related nuclear protein, targeting protein for xenopus kinesin-like protein 2, and stearoyl-CoA desaturase 1 as promising cancer targets from an RNAi-based screen.* Cancer Res, 2007. **67**(9): p. 4390-8.
158. Russell, S.E. and P.T. Walsh, *Sterile inflammation - do innate lymphoid cell subsets play a role?* Front Immunol, 2012. **3**: p. 246.
159. Jeon, Y.H., et al., *Immune response to firefly luciferase as a naked DNA.* Cancer Biol Ther, 2007. **6**(5): p. 781-6.
160. Judge, A.D., et al., *Sequence-dependent stimulation of the mammalian innate immune response by synthetic siRNA.* Nat Biotechnol, 2005. **23**(4): p. 457-62.
161. http://www.harlan.com.
162. Festing, M.F., *Inbred mice in research.* Nature, 1969. **221**(5182): p. 716.
163. http://www.jax.org.
164. Bogdanov Jr, A. and R. Weissleder, *In vivo imaging of gene delivery and expression.* Trends Biotechnol, 2002. **20**(8): p. S11-S18.
165. Raty, J.K., et al., *Non-invasive Imaging in Gene Therapy.* Mol Ther, 2007. **15**(9): p. 1579-86.
166. Keyaerts, M., et al., *Dynamic bioluminescence imaging for quantitative tumour burden assessment using IV or IP administration of D: -luciferin: effect on intensity, time kinetics and repeatability of photon emission.* Eur J Nucl Med Mol Imaging, 2008. **35**(5): p. 999-1007.
167. Hildebrandt, I.J., et al., *Optical imaging of transferrin targeted PEI/DNA complexes in living subjects.* Gene Ther, 2003. **10**(9): p. 758-64.
168. Bartlett, D.W. and M.E. Davis, *Insights into the kinetics of siRNA-mediated gene silencing from live-cell and live-animal bioluminescent imaging.* Nucleic Acids Res, 2006. **34**(1): p. 322-33.
169. Avram, M.J., et al., *Isoflurane alters the recirculatory pharmacokinetics of physiologic markers.* Anesthesiology, 2000. **92**(6): p. 1757-68.

3 List of Publications

3.1 Articles

2012: Thomas Fröhlich, Daniel Edinger, Raphaela Kläger, Christina Troiber, Edith Salcher, Naresh Badgujar, Irene Martin, David Schaffert, Arzu Cengizeroglu, Philipp Hadwiger, Hans-Peter Vornlocher, Ernst Wagner. Structure-activity relationships of siRNA carriers based on sequence-defined oligo (ethane amino) amides. **Journal of Controlled Release,** 160(3):532-41

2012: Christina Troiber, Daniel Edinger, Petra Kos, Laura Schreiner, Raphaela Kläger, Annika Herrmann, Ernst Wagner. Stabilizing effect of oligotyrosine motif on synthetic polyplexes for oligonucleotide delivery, manuscript in preparation.

2011: David Schaffert, Christina Troiber, Eveline E. Salcher, Thomas Fröhlich, Irene Martin, Naresh Badguja, Christian Dohmen, Daniel Edinger, Raphaela Kläger, Gelja Maiwald, Katarina Farkasova, Silke Seeber, Kerstin Jahn-Hofmann, Philipp Hadwiger, Ernst Wagner. Solid-phase synthesis of sequence-defined T-, i- and U-shape polymers for pDNA and siRNA delivery. **Angewandte Chemie International Edition,** 50(38):8986-9.

3.2 Poster Presentations

2012: Raphaela Kläger, Daniel Edinger, Thomas Fröhlich, Christina Troiber, Ernst Wagner. Development of oligo (aminoethane) amides for *in vivo* delivery of siRNA. **Perspectives in Cell- and Gene-Based Medicines,** Deutsche Gesellschaft für Gentherapie, Frankfurt.

4 Acknowledgements

First of all I would like to thank Prof. Dr. Eckhard Wolf for the acceptance of this thesis at the veterinary faculty of the Ludwig-Maximilian-University Munich.

I am very grateful to Prof. Dr. Ernst Wagner for giving me the opportunity to become a member of his research group and to perform this work in his laboratories. Thanks for the scientific guidance over the last years, helpful discussions, the excellent working atmosphere and also individual freedom.

A special thank goes to the Axiolabs GmbH (former Roche Kulmbach GmbH) and the Nanosystems Initiative Munich.

I am deeply grateful to my “mouse house colleagues” Laura, Daniel, Markus and Gelja for their professional and also personal support.
Thanks to the members of the “siRNA group”, Christina, Irene, Uli, Thomas, Petra, Claudia, Christian, Daniel, Edith and Naresh.
Furthermore I really want to thank my roommates from the PhD room for putting a smile upon my face every day, the brilliant social events and also for the extraordinary gifts.
Thanks to Wolfgang Rödl for his patience and constant support.
Thanks to Ursula Biebl and Anna Kulinyak for taking care of all the laboratory consumables, lovely chit-chats and Eierlikör-cake.
Thanks to Melinda Kiss and Miriam Höhn for the nice scientific advice in molecular biology and cell culture but also for nice discussions in the coffee kitchen.

A big thanks goes to my friends SUE, Tanja, Lisi and Kathi, you are awesome!!!

Finally, I want to thank most of all my parents for their trust, appreciation, everlasting love and support during my whole life; without you this work would have never been possible!